Early–Middle Triassic fluvial ecosystems of Mallorca (Balearic Islands): biotic communities and environmental evolution in the equatorial western peri-Tethys

Rafel Matamales-Andreu[a,b]*, Enrique Peñalver[c], Eudald Mujal[a,d], Oriol Oms[e], Frank Scholze[f], Josep Juárez[b], Àngel Galobart[a,g] & Josep Fortuny[a]

[a] Institut Català de Paleontologia Miquel Crusafont, Universitat Autònoma de Barcelona, Edifici ICTA-ICP, c/ Columnes s/n, Campus de la UAB, 08193 Cerdanyola del Vallès, Barcelona, Spain.

[b] Museu Balear de Ciències Naturals, ctra. Palma-Port de Sóller km 30, 07100 Sóller, Mallorca, Illes Balears, Spain.

[c] Instituto Geológico y Minero de España (Museo Geominero), CSIC, c/ Cirilo Amorós 42, 46004 València, València, Spain.

[d] Staatliches Museum für Naturkunde Stuttgart, Rosenstein 1, 70191 Stuttgart, Germany.

[e] Departament de Geologia, Universitat Autònoma de Barcelona, av. de l'Eix Central s/n, Campus de la UAB, 08193 Cerdanyola del Vallès, Barcelona, Spain.

[f] Institut für Geowissenschaften, Friedrich-Schiller-Universität Jena, Burgweg 11, 07749 Jena, Germany.

[g] Museu de la Conca Dellà, c/ del Museu 4, 25650 Isona i Conca Dellà, Lleida, Spain.

*Corresponding author: rafel.matamales@icp.cat

Abstract

During the Early–Middle Triassic, the biosphere was recovering from the most severe mass extinction event of multicellular life, in the Permian–Triassic transition. Continental basins corresponding to present-day Mallorca (Balearic Islands, western Mediterranean) were located in the equatorial region of the supercontinent Pangaea, in the western peri-Tethys. Its recorded stratigraphic succession can be divided in four alluvial/fluvial formations, formally described here: Punta Roja Formation, Estellencs Formation, Pedra Alta Formation and Son Serralta Formation. Based on an exhaustive review of all available literature and new stratigraphic and palaeontological data, an upper Olenekian–lower Anisian interval is proposed for the whole succession. The richest fossil assemblage is that of Estellencs Formation, with abundant invertebrate and vertebrate trace fossils, and remains of plants, arthropods and rare fishes, which together represent a lotic/riverine ecosystem with a relatively complex food web. Plants and insects show strong biogeographical affinities with those of the Vosges, in central Europe; clam shrimps are similar to those of central Europe and Asia; and tetrapod tracks are also reminiscent to those of Eurasia and North America. Ultimately, integration of all these data provides a comprehensive and multidisciplinary characterisation of one of the oldest Triassic ecosystems of equatorial Pangaea, providing new insights to understand the evolution of palaeoenvironments of Iberian Plate, an area that has historically suffered from severe undersampling.

Key-words: Olenekian, Anisian, clam shrimps, insects, tetrapod tracks, central Pangaea

1. Introduction

The Triassic is a key period in the history of life, as its ecosystems were recovering from the most critical mass extinction event in the Phanerozoic, in the Permian–Triassic transition (Erwin, 1994; Benton, 2008; Romano *et al.*, 2020). Although the former complexity of the ecosystems was eventually restored, its floras and, especially, its faunas, had experienced profound turnovers (still not fully understood in the terrestrial realm), leading to more typically Mesozoic assemblages (Retallack *et al.*, 1996; Labandeira, 2005; Benton & Newell, 2014; Romano *et al.*, 2020). Those organisms lived and evolved under a megamonsoonal regime caused by the Pangaean supercontinental configuration, characterised by a marked seasonality, with alternating arid seasons and heavy rainfalls (Parrish, 1993; Zeng *et al.*, 2019).

In the western peri-Tethys, initial Triassic sedimentation resulted in the *Buntsandstein* continental red-bed facies, usually overlaying a hiatus in the form of an unconformity, and representing semi-arid to arid climates (Durand, 2006; Bourquin *et al.*, 2011; Mujal *et al.*, 2016,

2017a, 2017b; López-Gómez *et al.*, 2019a). In the case of Iberia, those sediments were deposited into half-graben basins that opened as a result of the relaxation of the Variscan orogen and subsequent fragmentation of the supercontinent (Bourquin *et al.*, 2011; Frizon de Lamotte *et al.*, 2015) in the intra-Pangaean dextral megashear zone (*e.g.*, Irving, 2004). During the Olenekian, semi-arid climates have been inferred in most of the sections because of the development of wadi and erg systems in the central part of Iberia (Marzo, 1986; Soria *et al*., 2011; López-Gómez *et al*., 2012, 2019a; Galán-Abellán *et al.*, 2013a). Conversely, during the early Anisian, the ecosystems flourished under more humid climates, recognised because of the meandering style of the rivers and other geochemical and palaeopedological proxies (Borruel-Abadía *et al*., 2014, 2015), with a biotic diversity that evidences the richness of the ecosystems of palaeoequatorial Pangaea. Typical of this stage are plant assemblages composed of horsetails, ferns, conifers, spores and pollen (*e.g.*, Diez *et al.*, 2005, 2010 and references therein). In some cases, arthropod fossils, including both traces (*e.g.*, Mujal *et al.*, 2018a) and body fossils (Aristov & Zessin, 2009; Béthoux *et al.*, 2009), are also locally abundant. Tetrapod fossils usually appear in the form of ichnites (*e.g.*, Fortuny *et al.*, 2011a and references therein; Mujal *et al.*, 2016, 2017b), but bone remains have been occasionally reported as well (Fortuny *et al.*, 2011a, 2011b, 2014; Ezcurra *et al.*, 2017).

The present work focuses on the Lower–Middle Triassic *Buntsandstein* facies of Mallorca, with outcrops located in a limited coastal area between Cala d'Estellencs and Punta de son Serralta (Estellencs, Mallorca, western Mediterranean). Its aim is to provide an accurate palaeoecological reconstruction integrating environmental, botanical, entomological and ichnological data. For that reason, the stratigraphy and sedimentology of all the outcrops are revised, formally defining lithostratigraphic units, namely, formations, in order to clear previous inaccuracies and misconceptions. This also makes it possible to infer the specific depositional palaeoenvironments represented in their rocks, as well as their evolution through time. Moreover, all the previous works on fossil plants and spores/pollen are reviewed, and the arthropod assemblages and invertebrate and vertebrate ichnoassemblages are studied in detail for the first time. These data are useful for the study of the palaeoenvironmental and palaeobiogeographical developments of ecosystems recorded in the formations of Mallorca in the context of the western peri-Tethys, and, therefore, the importance of the present work lies not only in the improvement of the regional knowledge on the continental Triassic lithostratigraphic units and palaeoecosystems, but also in contextualising these data in a broader framework for palaeoequatorial Pangaea.

2. Geographical and geological context

Mallorca, the largest of the Balearic Islands (western Mediterranean) (Figure 1A), is a northeast extension of the Betic orogen, tectonically structured in a series of grabens and horsts by northeast-southwest faults of late Miocene age (Vera *et al*., 2004). The oldest rocks that crop out on the island, as part of the lowermost unit of the Serra de Tramuntana, have been assigned to the Carboniferous marine *Culm* facies (Rodríguez-Perea & Ramos, 1984; Ramos & Rodríguez-Perea, 1985; Calafat, 1988). Above them and by means of a mechanical contact, Permian rocks appear, recording the sedimentation in continental environments such as alluvial fans, rivers and floodplains. Those palaeoenvironments persist in the Lower–Middle Triassic, with red-beds that appear in a group of very localised and precipitous outcrops along the northern coast of the island (Figure 1A–B), which are the object of the present study.

In the Early–Middle Triassic, Mallorca was part of a continental basin located in the western Tethyan domain of central Pangaea (Scotese, 2014; Scotese & Schettino, 2017), where the Variscan belt, uplifted during the Palaeozoic (*e.g.*, Edel *et al.*, 2018), still constituted a major geographical feature. The sediments resulting from its erosion ended up in the grabens of rifts that had started to open all over the western peri-Tethys (present-day western Europe and northern Africa), due to the extensional tectonic regime that prevailed until the late Mesozoic (Arche & López-Gómez, 1996; Hounslow & Ruffell, 2006; McCann *et al.*, 2006; Stampfli & Hochard, 2009; Frizon de Lamotte *et al.*, 2015). In the case of Iberia, which was right in the midst of the intra-Pangaean dextral megashear zone (*e.g.*, Irving, 2004), such basins followed a general northwest-southeast trend, and contained river systems flowing towards the southeast (Borruel-Abadía *et al*., 2015; López-Gómez *et al.*, 2019a). The Basque-Cantabrian and Pyrenean basins were an exception, as there the rivers had variable palaeocurrent directions (Nagtegaal, 1969; Robles & Llompart, 1987; Borruel-Abadía *et al*., 2015; Gretter *et al.*, 2015; López-Gómez *et al.*, 2019b), probably pointing to the endorheic character of those basins. Six main basins (each with several sub-basins) were opened in the Iberian area: the Basque-Cantabrian Basin, the Pyrenean Basin, the Catalan Basin, the Iberian Basin (with the Castilian and Aragonese branches) and the basins of Mallorca and Menorca. Those of the present-day Balearic Islands record the most distal deposits of the Iberian area and, specifically on Mallorca, the successions are well exposed and are very rich in fossil plants and animals.

The inaccessibility of the sections of Mallorca had so far precluded their correct characterisation. Over time, several informal lithostratigraphic divisions had been proposed (Supplementary Text 1; Supplementary Table 1), resulting in a plethora of disagreeing approaches that had never been properly collated. The present work provides a detailed study of all the sections of the island (Figure 1C) and formal definitions for each of the lithostratigraphic units to avoid ambiguity in future studies.

3. Material and methods

3.1. Stratigraphy and sedimentology

For the stratigraphic and sedimentological study, four stratigraphic sections have been measured bed by bed to a minimum resolution of 1 cm of bed thickness. Covered and semi-covered intervals have been measured using a Jacobs staff. Most zones of complicate access due to the steepness of the outcrops have been reached using climbing gear. They all have been logged in detail (in 1:25 scale) (presented in Supplementary Logs in 1:40 scale). Those have been named, from southwest to northeast: 'Pedra Alta' (18.5 m), 'Punta Negra' (103.5 m), 'Punta Roja' (126.5 m, including a repeated stretch of 14 m) and 'Tenassa de sa Tanca' (47.5 m) (Figure 1B). The logs have been synthesised (1:1160 scale) and correlated in Figure 1C. The datum to correlate Pedra Alta (PI) and Punta Negra (PN) logs is the top of the green/pink interval in the upper part of Estellencs Formation. The datum to correlate Punta Negra and Punta Roja (PR) logs is the boundary between Estellencs Formation and Pedra Alta Formation, that is, the change of colour from dominant red to dominant white/blue/green. The datum to correlate Punta Negra and Tenassa de sa Tanca (TT) logs is the boundary between Son Serralta Formation and the *Muschelkalk* marine facies. The recognised sedimentary lithofacies have been classified according to Miall (1977, 1985, 2006) and Postma (1990), with additional support of more specific works such as Shanley *et al*. (1992), Mack *et al*. (1993), Gómez-Gras & Alonso-Zarza (2003) and Shiers *et al*. (2018) (Table 1). Architectural elements have been classified according to Miall (1985, 2006) (Table 2).

3.2. Tetrapod tracks

The specimens of tetrapod tracks, which were left in the field, were assigned numbers depending on their position in the stratigraphic logs. The ones under the code PN-7.6?-[slab number]-[ichnite number] were found *ex situ* near the metre 7.6 of Punta Negra log and may belong to that bed. PN-7.6-[slab number]-[ichnite number] were the only ones found *in situ* there. PN-14.6-[slab number]-[ichnite number] and PN-14.7-[slab number]-[ichnite number] were found *in situ* in an unequivocal lateral equivalent of the metres 14.6 and 14.7, respectively, of Punta Negra log but at Platja de sa Marina, where no log was confected. All studied tetrapod tracks are preserved as concave epireliefs. In some cases, the natural cast is also preserved as a convex hyporelief (providing the same information as the studied epireliefs), although it is usually eroded because it is proportionally finer-grained.

In order to study the tetrapod footprints, the layers of rock covering them were removed, and the exposed surface was recorded in a digital 3D model. Photogrammetry was made mostly following the procedure explained by Mujal *et al*. (2020), using Agisoft Photoscan standard version 1.1.4. (http://www.agisoft.com) to create the mesh and the texture, MeshLab version 2016.12 (http://meshlab.sourceforge.net) to align, scale and measure the mesh, and ParaView version 4.1.0 64-bit (http://www.paraview.org) to create the false colour-coded depth maps with contours. The main descriptive parameters of each footprint (Leonardi, 1987; Hasiotis *et al.*, 2007) were measured on schematic diagrams, using the software ImageJ version 1.52d (https://imagej.nih.gov/ij), and are here presented in Supplementary Table 2. No trackway measurements were taken given the fragmentary nature of all the specimens.

3.3. Fossil arthropods and fishes

The present research is based on three different collections. The most important one is the historical Tomeu Sáez collection (Binissalem, Mallorca, Balearic Islands, Spain), which had been studied by Calafat & Sáez (1987) and Calafat (1988). It contains over 60 compression fossils of animals (30 insects, about 30 clam shrimps and a fish) in 10 slabs (A–J). All these specimens have been identified using the acronym TS-[slab letter]-[specimen number] and were obtained in the early 1980s from a single lutitic horizon rich in arthropods of Pedra Alta section (ca. metre 4.75 of the log presented in Supplementary Logs; T. Sáez, pers. comm., 2020). Specimens of a same slab have been correlatively numbered.

The second collection is that of Museu Balear de Ciències Naturals (Sóller, Mallorca, Balearic Islands, Spain). It includes one insect specimen under the acronym MBCN[specimen number] from a lutitic horizon of Pedra Alta section (ca. metre 7.55 of the log presented in Supplementary Logs).

The third collection of ca. 100 slabs with clam shrimps ("conchostracans") and insects has been sampled for the present work with permission of Consell de Mallorca (file numbers 305/2019 and 52/2021), and are deposited in Museu de Mallorca (Palma, Mallorca, Balearic Islands, Spain) with the acronym DA21/[campaign number]-[horizon number]-[specimen number]. Those were collected from four different stratigraphic levels: a few clam shrimps are from a lutitic horizon of Punta Roja section (metre 86.5 of Punta Roja log presented in Supplementary Logs); all insects (n = 120) and most clam shrimps were sampled from a lutitic bed of Pedra Alta section (ca. metre 7.20–7.30 of Pedra Alta log presented in Supplementary Logs); and several more clam shrimps were collected from lutitic horizons of Punta Negra section (metre 39.5 and 82.0 of Punta Negra log presented in Supplementary Logs). Parts/counterparts are

identified with a number “1”/“2” following the museum collection number. Different specimens on a same rock slab have been identified with correlative letters.

Photographs of clam shrimps were taken using a LEICA MZ12 stereo-microscope with a WILD drawing mirror tube, and a BRESSER MikroCamII digital camera. Insects from Tomeu Sáez collection were photographed using a single-lens reflex camera Canon EOS 40D and a digital camera Olympus SC30 attached to an Olympus SZ61-TR stereomicroscope; some of its specimens were wet with alcohol to be photographed enhancing the contrast of the carbonaceous parts. Specimens housed at Museu de Sóller and at Museu de Mallorca were photographed using a digital camera Olympus Camedia MODEL N.C5050 ZOOM attached to an Olympus SZX9 stereomicroscope.

Clam shrimp measurements and terminology follow Scholze & Schneider (2015). Mayfly morphological terminology follows that of Sinitshenkova *et al.* (2005) and Bashkuev *et al.* (2012); body lengths of the mayfly nymphs were measured up to the base of cerci and paracercus. Abbreviations for the wing venation are as follows: CuA: anterior cubitus, CuP: posterior cubitus, M: media, MA: media anterior, R: radius, Rs: radial sector, Sc: subcosta.

4. Stratigraphy and sedimentology

Formal units have hitherto never been defined for the Lower–Middle Triassic red-beds of Mallorca. Several works (Cuevas-López, 1958a, 1958b; Pomar-Gomà, 1979; Martí *et al*., 1985; Ramos *et al*., 1985; Calafat, 1986, 1987, 1988; Rodríguez-Perea *et al*., 1987; Barnolas, 1991a, 1991b; Gómez-Gras, 1992, 1993; Ramos, 1995) provided informal classifications of the different units (Supplementary Table 1), and other reviews upgraded them to formations without any formal description (Arche *et al*., 2002; López-Gómez *et al*., 2002, 2019a; Vera *et al*., 2004; Bourquin *et al*., 2007, 2011; Cassinis *et al*., 2012). This situation, as well as some miscorrelations between units (see Supplementary Text 1 and Supplementary Table 1), required a formal description of the lithostratigraphic units of the *Buntsandstein* facies of Mallorca. Whenever possible, however, the first name used for each of the units has been preserved. Descriptions and interpretations of all the lithofacies and architectural elements are here presented in Table 1 and Table 2.

4.1. Punta Roja Formation

This formation (Figure 2A) can be identified in the field because of the abundance of medium-grained sandstone beds, which are often tabular and show abundant planar cross-bedding. Those sandstones are white or pink in colour, and near the base of the unit they show a very distinct alternation of white and pink laminae. Red lutites are extremely rare in the lower part of the formation, and they become progressively more abundant towards the top.

4.1.1. Location and boundaries

A small part of Punta Roja Formation crops out at Cala d'Estellencs and southwest of Pedra Alta (Figure 1B). The most complete outcrop is at Punta Roja and, although it lacks its base, up to 53 m have been measured until its boundary with Estellencs Formation. The Punta Roja outcrop (Figure 1B) is herein formally designated as the stratotype of Punta Roja Formation. Its lower boundary cannot be observed, and its upper boundary with Estellencs Formation is transitional, characterised by the change of colour from pink to red, the presence of thick lutitic beds and a switch from dominant planar cross-bedding to dominant trough cross-bedding and ripple lamination.

4.1.2. Lithological features and palaeontological content

The lithofacies (Figure 3, Table 1) and architectural elements (Table 2) present in Punta Roja Formation are reduced to a few dominant types, the rest being quantitatively less important. Breccias (lithofacies type *Gt*) are rare, and are composed of intraformational clasts and carbonate nodules, appearing as isolated beds among sandstone deposits in the uppermost part of the formation, both in the base of sandstone packs and intercalated between lutites. Sandstones are clearly dominant, especially in the lower part. The lower half of the formation is essentially made up of medium-grained sandstones of lithofacies type *Sp*, whereas lithofacies type *St* (Figure 3I) appears more frequently towards the top of the formation. Lithofacies of types *Sl* and *Sh* also appear abundantly in the upper part of the formation, together with lithofacies type *Sr*, *Ss*, *Sm* and *Sb*, which are rarer. Lutite lithofacies (types *Fl* and *Fm*) are more frequent towards the upper part of the formation and they are often associated with lithofacies type *P*, which displays abundant carbonate nodules (diameter between 0.5–3 cm) and rhizocretions. The dominant architectural element is *SB*, with sporadic intercalations of the elements *LS* and *FF* towards the upper part.

4.1.3. Interpretation

In this formation, lithofacies type *Gt* represents reworked floodplain deposits (as the clasts are always soft pebbles and carbonate nodules) in the basal lag of some channels and in the floodplain, similarly to the cases described by Gómez-Gras & Alonso-Zarza (2003). Regarding sandstone deposits, lithofacies type *Sp* corresponds to transverse fluvial bar deposits, *St*

represents megaripple deposits formed under lower flow regime conditions, *Sl* and *Sh* correspond to events of sediment deposition under higher flow regimes, *Sr* was formed by waning flows, and *Ss* corresponds to the infill of scours. Moreover, lithofacies type *Sm* probably corresponds to events of rapid deposition or to beds reworked by bioturbation, similarly to *Sb*, which possesses abundant burrowing. Lutite lithofacies (types *Fl* and *Fm*) correspond to overbank and floodplain fine-grained deposition, and lithofacies type *P* can be interpreted as palaeosols, which in this case would correspond to Calcisols given the abundance of carbonate nodules and lack of gleyed patches (Mack *et al.*, 1993). Architectural element *SB* represents shallow channel-fill assemblages, whereas *LS* and *FF* correspond to sheetflood deposits and floodplain fines, respectively.

This formation represents a shallow perennial braided river in the sense of Miall (2006), because of the dominance of architectural element *SB*, made up of lithofacies type *Sp*, corresponding to transverse bar deposits. Calafat (1988) suggested an aeolian origin for this unit, because of the overall lack of fine sediments and the well-sorted sands. Indeed, in thin sections, those sandstones do have a relatively consistent grain size distribution (medium-grained sands), yet mica flakes are very abundant. In aeolian contexts, such minerals are usually blown away by the wind (*e.g.*, Glennie, 1970), thus making it more probable for Punta Roja Formation to be of mixed aeolian–fluvial origin. Specifically, it would correspond to river deposits that reworked aeolian dune fields, hence the well-sorted sand grains. The palaeocurrent direction, based on field measurements (n = 20), had a dominant direction towards the southwest, with little dispersion (see '7. Discussion'). Towards the top of the formation, the transition towards meandering rivers with associated floodplain deposits can be observed because of the overall increase of the relative abundance of lutites. This formation has not been confidently dated because of its lack of fossil content, however, here it is assumed to be of upper Olenekian (Spathian) age, based on the age of the overlying units and correlation with lithologically similar formations of Iberia (see '7. Discussion' and Supplementary Table 3), altough a younger age, *i.e.*, lower Anisian (lowermost Aegean), cannot be completely ruled out for its upper part.

4.2. Estellencs Formation

This formation (Figure 2B–C) can be identified in the field because of the abundance of very fine- and fine-grained sandstones with dominant trough cross-bedding and ripple lamination, interbedded with abundant lutites. Both the sandstones and the lutites are of a bright red colour.

In the upper part of the formation, there is an intercalation of coarser deposits (breccias and medium-grained sandstones) that are pink, white or green.

4.2.1. Location and boundaries

Estellencs Formation crops out completely at Cala d'Estellencs and at Punta Roja. Smaller outcrops can be observed in a roadcut near Cala d'Estellencs, between Pedra Alta and Punta Negra and at Platja de sa Marina (Figure 1B). At Punta Roja, where this formation is well accessible and crops out completely, 55 m have been measured. The Punta Roja outcrop is herein formally designated as the stratotype of Estellencs Formation. Its lower boundary is gradual and its upper boundary is sharp. Its upper boundary with Pedra Alta Formation is characterised by the change of dominant colour from red to green/blue/white, the almost complete absence of red lutites and the dominant planar cross-bedding.

4.2.2. Lithological features and palaeontological content

The lithofacies (Figure 3, Table 1) and architectural elements (Table 2) present in this formation are quite varied, consisting mostly of lutite and sandstone types. Breccias (lithofacies type *Gt*) are not frequent, and they appear as isolated events scouring underlying lutites or sandstones, both in the base of sandstone packs or as isolated beds in the lutite intervals. They show crude trough lamination, and are composed of intraformational clasts (mudstones, sandstones) and reworked calcretes. The sandstone lithofacies of types *Sh*, *Sp*, *Ss*, *St* and *Sm* (Figure 3D, H) are also rare except for the stretch between metres 18–27 of Punta Negra log and its lateral equivalent: Pedra Alta log (Figure 1C). The sandstone lithofacies of types *Sl* and *Sr* (Figure 3G) are by far the most abundant, usually in the form of thin, very fine- to fine-grained, tabular beds, although they can also be part of sequences showing clear lateral accretion, especially at the base of the formation. On the top of the beds, wrinkle structures (Porada & Bouougri, 2007) are sometimes well visible. Lithofacies type *Sb* is characterised by profuse burrowing and is usually found associated to lithofacies of types *Sl* and *Sr*. Lithofacies type *P* (Figure 3O) contains abundant carbonate nodules (diameter between 0.5 and 3 cm) and often root traces and gleyed patches as well. Lutite lithofacies (types *Fl* and *Fm*, Figure 3M, N) often appear over lithofacies of types *Sl*/*Sr* and form relatively thick packs. The dominant architectural elements are *LV/CS* and *FF*, and sporadically *LA* can also be observed.

4.2.3. Interpretation

In this formation, lithofacies type *Gt* represents high-energy deposits reworking floodplains, produced by occasional events of heavy rains or as the basal lags of channels, similarly to the case described in the Permian of Menorca (Gómez-Gras & Alonso-Zarza, 2003). Sandstone lithofacies of types *Sh*, *Sp*, *Ss*, *St* and *Sm* correspond to bedforms of major river channels under

different flow regimes (see ‘4.3. Pedra Alta Formation’). Lithofacies of types *Sl* and *Sr* are interpreted as the result of the waning flows in major sheetfloods, as overbank deposits over the floodplains or as point bar deposits of meandering channels. The wrinkle structures that appear on the top of some beds of these lithofacies types were probably formed by microbial mats (Porada & Bouougri, 2007), which favour the preservation of small tetrapod ichnites (Carmona *et al.*, 2011). Lithofacies of types *Sb* and *P* are nothing but the reworking of the other types mentioned above and, specifically, lithofacies type *P* can be interpreted to correspond to vertic Calcisols when small carbonate nodules and gleyed patches are present, whereas Calcisols can be inferred when there are only carbonate nodules, generally larger (Mack *et al.*, 1993). Lithofacies of types *Fl* and *Fm* correspond to deposition of low-energetic to still waters in environments such as the uppermost part of crevasse splays and playa lakes (in the sense of Briere, 2000). Architectural elements *LV/CS* and *FF* represent the floodplain palaeoenvironment, whereas *LA* corresponds to point bars of meandering channel deposits.

The lower half of this formation corresponds to meandering river channels with conspicuous lateral accretion. Towards the upper part, interbedded floodplain deposits, including crevasse splays, start to appear more frequently. However, the stretch between metres 18–27 of Punta Negra log, metres 103–112 of Punta Roja log and the whole Pedra Alta log represent a relatively higher energy pulse with sedimentary environments comparable to those of Pedra Alta Formation (see ‘4.3. Pedra Alta Formation’). The palaeocurrents measured in this formation (n = 13) show a wide dispersion but with a general trend towards the southeast (see ‘7. Discussion’). The palynoassemblages of this formation made it possible to date it as lower Anisian, probably lower Aegean, because the base of the overlying formation is of upper? Aegean age (see ‘4.3. Pedra Alta Formation’, ‘7. Discussion’ and Supplementary Table 3).

4.3. Pedra Alta Formation

This formation (Figure 2B–C) can be identified in the field because of the abundance of medium-grained sandstone beds, which are of a clear colour (white, yellowish, bluish, pink), intercalated with intervals of blue or green lutites. The dominant sedimentary structures in the sandstones are planar or trough cross-bedding, whereas the lutites frequently have planoparallel lamination.

4.3.1. Location and boundaries

Pedra Alta Formation crops out completely between Pedra Alta and Punta Negra, and at Platja de sa Marina. It can also partially be observed at a roadcut near Cala d’Estellencs, at Cala d’Estellencs and at Tenassa de sa Tanca (Figure 1B). The outcrop located in the precipitous

ravine between Pedra Alta and Punta Negra (Punta Negra log) is herein formally designated as the stratotype for Pedra Alta Formation, where 44 m have been measured. Both its lower and upper boundaries are sharp but apparently not erosive. Its upper boundary with Son Serralta Formation is characterised by the change of dominant colour from green/blue/white to red and the appearance of thick beds of red lutites.

4.3.2. Lithological features and palaeontological content

The lithofacies (Figure 3, Table 1) and architectural elements (Table 2) present in this formation are somewhat constant, with sequences with a lower part made up of sandstones (sometimes with basal breccias as well) and an upper part made by lutites. Breccias (lithofacies type *Gt*, Figure 3A) are exclusively composed of intraformational clasts (sandstones and lutites, sometimes also with carbonised remains of large woody debris), and possess crude trough cross-bedding. The sandstone lithofacies of types *Sp* and *St* (Figure 3F) are rather abundant and are usually constituted by medium-grained sandstones with planar or through cross-bedding, respectively. Over them, lithofacies of types *Sl* or *Sr* (Figure 3E) appear, usually in very fine- to fine-grained sandstones grading to the lutite lithofacies. Very fine-grained sandstone lithofacies type *Sh* and horizontally laminated lithofacies type *Fl* with abundant remains of plants, arthropods and, rarely, fishes constitute the top of the sequences, sometimes with lithofacies type *Fm* as well. The dominant architectural element is *SB*, but *FF* also appears between the sandy bedforms.

4.3.3. Interpretation

In this formation, lithofacies type *Gt* represents the basal lags of major channel deposits. Lithofacies of types *Sp* and *St* correspond to linguoid and/or transverse bars and sand dunes migrating on the channel floor, and those of types *Sl*/*Sr* were deposited during waning currents in channel top sequences. Lithofacies of types *Sh* (very fine-grained) and *Fl* have been interpreted as fine sediments deposited during intervals of low energy flow, and lithofacies type *Fm* corresponds to deposition in periods of still waters in abandoned channels or backswamps. Architectural element *SB* represents channel-floor dune fields and top-bar assemblages, whereas element *FF* was formed by the deposition of fine sediments in abandoned channels or backswamps.

This formation represents several sequences of a sheetflood distal braided river (as defined by Miall, 2006), consisting in superimposed flood cycles with abundant bedforms without associated floodplain deposits (the element *FF* corresponds to the infill of the channels during low water stage). Linguoid and transverse bars amount to more than half of sandstone elements, deposited during flood stage. Over them and fining upwards, low angle cross-bedded and ripple-laminated beds appear, as a result of the waning of the flow after the main flood events. The

sequences often end with greenish or red lutite deposits, either laminated or apparently massive. They represent pools with still to very low energetic flows (Coleman, 1969; Williams & Rust, 1969; Miall, 1977, 2006), isolated in abandoned channels among the remnants of megaripples (similar to those described in the Upper Cretaceous of the southern Pyrenees by Vila *et al.*, 2013) or backswamps (similar to those described for the Lower Triassic of the Central European Basin by Kustatscher *et al.*, 2014). The variety of colours of the lutites can result from pedogenetic alteration or water circulation during diagenetic processes, but in some specific beds it can also be explained by the height of the water table in the time of sediment deposition, since the fossil content varies greatly from red lutites to green lutites, being by far more abundant in the latter. Thus, lutites that were sedimented in well-drained areas underwent oxidation and became red, whereas the green/grey/blue lutites were deposited below the water table. Similar environments were inferred for the clay levels of the Middle Triassic *Grès à Voltzia* of the Vosges (Gall, 1971) and the Solling Formation (Kustatscher *et al.*, 2014), both in the Central European Basin. This accounts for the very high preservation potential of plant remains, clam shrimps, insects and, rarely, scales and very small fishes in the fossiliferous horizons of the studied sections. The palaeocurrents measured in this formation (n = 23) show a wide dispersion but with a general trend towards the southeast (see '7. Discussion'). This formation was dated as Aegean (lower Anisian), probably upper Aegean, by Diez (2000) and Diez *et al.* (2005, 2010) based on the study of spores and pollen (see '7. Discussion' and Supplementary Table 3).

4.4. Son Serralta Formation

This formation (Figure 2C–D) can be identified in the field because of the absolute dominance of fine sediments and lack of thick sandstone elements. The most abundant lithologies are red very fine- to fine-grained sandstones and red lutites. Sporadically and especially towards the top, intercalations of greenish lutites become progressively more abundant.

4.4.1. Location and boundaries

Son Serralta Formation crops out completely at Tenassa de sa Tanca, between Pedra Alta and Punta Negra, and at Platja de sa Marina (Figura 1B). Of those three, the most accessible outcrop is at Tenassa de sa Tanca, which is herein formally designated as the stratotype of this formation, with a measured thickness of 22 m. Both its lower and upper boundaries are sharp. Its upper boundary is characterised by the onset of carbonate shallow marine sedimentation (M-1 unit of the *Muschelkalk* facies; *e.g.*, Matamales-Andreu *et al.*, in press).

4.4.2. Lithological features and palaeontological content

The lithofacies (Figure 3, Table 1) and architectural elements (Table 2) present in this formation are few and quite constant throughout, with very fine to fine-grained sandstone lithofacies representing about a half of the whole sequence. At its base, the most abundant lithofacies is type *Sr* that, together with type *Sl*, form tabular deposits of very fine- to fine-grained sandstones. The lithofacies of types *St* and *Sp* are also constituted by very fine- to fine-grained sandstones, and are relatively less abundant and have usually less lateral continuity. The lutite lithofacies (types *Fl*, *Fm*) appear over the sandstone beds and form intervals that are thicker towards the top of the unit. Very typical of this formation are the yellowish massive sandstones (herein classified in lithofacies type *Sm*, Figure 3I) that appear as channelled or irregular beds isolated among the lutites, and the presence of interlayered sand/mud bedding (lithofacies type *Si*, Figure 3L), forming packs of up to 60 cm of thickness, which are usually deformed and affected by desiccation cracks. The dominant architectural elements are *LV/CS* and *FF*, whereas the element *LA* appears in the middle part of the formation.

4.4.3. Interpretation

In this formation, lithofacies of types *Sr* and *Sl* represent crevasse splay deposits, and lithofacies of types *St* and *Sp* correspond to small fluvial channel deposits. Lutite lithofacies such as type *Fl* and type *Fm* have been interpreted as the result of deposition of suspended fine sediments on the floodplain. Moreover, there are two lithofacies that are typical of this formation and common in tidal environments. In the middle part, there appear irregular or channelled beds of yellowish, massive sandstones isolated among the lutites (herein classified as a particular kind of lithofacies type *Sm*). Some of them show clear lateral accretion sets separated by lutite drapes (Figure 3I), corresponding to inclined heterolithic point bars of tidal creeks (*e.g.*, Ghinassi *et al.*, 2021). In the middle and upper part of the formation, sandstone beds are arranged in very thin layers alternating with lutites (lithofacies type *Si*), which is another typical (albeit not exclusive) trait of tidally-influenced environments, especially mixed-flats and mud-flats (*e.g.*, Nio & Yang, 1991; Davis, 2012; Shiers *et al*., 2018). Architectural elements *LV/CS* and *FF* represent the floodplain palaeoenvironment, whereas element *LA* corresponds to small tidal creek deposits.

This formation represents the transition between the continental environments of the three underlying units to a marine environment such as the overlying *Muschelkalk* facies shallow platform carbonates (Calafat, 1988; Gómez-Gras, 1993; Ramos, 1995; Matamales-Andreu *et al.*, in press), and thus representing a local expression of the so-called *Röt* facies. The lower part of Son Serralta Formation still shows a great amount of fluvial influence, with relatively thin sandstone beds with ripples representing crevasse splay deposits over the lutitic floodplain, similarly to the lower and middle parts of Estellencs Formation (see '4.2. Estellencs Formation'). In the middle and upper parts of Son Serralta Formation, there appear inclined

heterolithic point bars that conform tidal-influence criterion for red-bed successions (see Ghinassi *et al.*, 2021). Some intervals of this portion of the formation also display interlayered sand/mud bedding, which is very typical (albeit not exclusive) of tidal environments (*e.g.*, Nio & Yang, 1991; Davis, 2012; Shiers *et al*., 2018). Moreover, from this formation, Ramos (1995) reported the presence of tepee/pseudo-anticline structures, which are indicative of marine influence, appearing together with other structures such as wave ripples, flaser bedding and evaporite solution breccias, which are also common in such settings. The few palaeocurrents measured (n = 2) have not been considered representative, and therefore no palaeocurrent data are available, although the same trend towards the southeast is probably followed, similarly to the underlying units. This formation was dated as Anisian by Calafat (1988), just 12 m below the boundary with the *Muschelkalk* facies, which was confirmed by subsequent works such as Diez (2000) and Diez *et al*. (2005, 2010) (see Supplementary Table 3). Given that the base of the underlying Pedra Alta Formation is of upper? Aegean age (see '4.3. Pedra Alta Formation'), this formation could belong to either the uppermost Aegean (lower Anisian) or even the Bithynian (lower part of the middle Anisian) (see '7. Discussion' and Supplementary Table 3).

5. Systematic palaeoichnology

5.1. Invertebrate ichnofossils

Ichnogenus *Gordia* Emmons, 1844

Gordia isp.

Figure 4A

Studied material: One specimen, left in the field. From Punta Negra section (metre 9.00), middle part of Estellencs Formation, Aegean.

Description: Horizontal trace preserved in convex hyporelief, consisting in a loosely winding, unbranched burrow, thin and with a somewhat irregular wall. The preserved trace appears to make a loop that would cross over itself. The fill is the same as the surrounding matrix (very fine-grained sandstone).

Remarks: The studied ichnofossil differs from similar unspecialised freshwater grazing traces of the *Mermia* ichnofacies (Buatois & Mángano, 1998) such as *Cochlichnus*, *Helminthoidichnites*, *Helminthopsis* or *Mermia*, because of its irregular winding course and the fact that the trace crosses over itself (Hofmann & Patel, 1989; Han & Pickerill, 1995; Gaigalas & Uchman, 2004; Uchman *et al*., 2009; Getty *et al*., 2017). The ichnogenus *Gordia* occurs in marine and

continental facies from the Precambrian to the Holocene (Pickerill & Peel, 1991), and, in the case of freshwater environments, the probable trackmakers were insect larvae (Gaigalas & Uchman, 2004; Minter *et al*., 2007).

Ichnogenus *Skolithos* Haldeman, 1840

Skolithos isp.

Figure 4B

Studied material: Many specimens, left in the field. From Punta Negra (metre 8.00) and Punta Roja (metre 81.00) sections, among others, middle part of Estellencs Formation, Aegean.

Description: Subvertical, straight to slightly curved, unbranched burrows of circular section. The fill is massive; it usually corresponds to the sediment of the overlying bed (very fine-grained sandstone).

Remarks: The ichnogenus *Skolithos* occurs in marine and continental facies from the Precambrian to the Holocene (Fillion & Pickerill, 1990), and, in the case of freshwater environments, the probable trackmakers were insect larvae (Bromley & Asgaard, 1979; Ratcliffe & Fagerstrom, 1980; Fitzgerald & Barrett, 1986). In continental deposits, it usually appears in the *Scoyenia* ichnofacies (Buatois & Mángano, 1998).

Ichnogenus *Taenidium* Heer, 1877

Taenidium barretti (Bradshaw, 1981)

Taenidium isp. cf. *T. barretti*

Figure 4C

Studied material: Many specimens, left in the field. From Punta Roja section (metre 81.00), among others, middle part of Estellencs Formation, Aegean.

Description: Variably oriented (usually horizontal but vertical sections also observed), unwalled, sinuous to winding, unbranched burrows of circular section. They have a meniscate backfill with a similar sediment to that of the surrounding matrix (fine-grained sandstone). Menisci are short, arcuate and closely spaced.

Remarks: Ichnotaxonomy of meinscate backfilled traces is somewhat contentious (*e.g*., Minter *et al.*, 2007; Smith *et al*., 2008; Díez-Canseco *et al*., 2016) and it is beyond the scope of the

present work to provide a systematic review of such ichnotaxa. The specimens studied herein are comparable to those illustrated by Minter *et al*. (2007) under the identification of *T. barretti*. Those traces have been interpreted to be produced by arthropods, probably coleopterans (Baucon *et al.*, 2014), which would aestivate in the moist sediment during the dry season (Minter *et al.*, 2007). In continental deposits, this ichnogenus usually appears in the *Scoyenia* ichnofacies (Buatois & Mángano, 1998).

Ichnogenera *Rusophycus* Hall, 1852, *Cruziana* d'Orbigny, 1842, and *Diplichnites* Dawson, 1873

Diplichnites gouldi (Gevers *in* Gevers, Frakes, Edwards *et* Marzolf, 1971)

Rusophycus isp. - *Cruziana* isp. - *Diplichnites* isp. cf. *D. gouldi*

Figure 4D

Studied material: Two specimens, left in the field. From Punta Negra section (on an *ex situ* block, probably from metre 6.00), middle part of Estellencs Formation, Aegean.

Description: Positive hyporelief of a compound trace with three different ichnotaxa in fine-grained sandstone. The part corresponding to *Rusophycus* is a weakly bilobate mound, with a longitudinal, very smoothed ridge. The part corresponding to *Cruziana* originates from the central part of the anterior margin of the *Rusophycus*, and corresponds to a chevronate (V-shaped) trace with more or less symmetric lobes on each side of its longitudinal axis. Finally, *Diplichnites* isp. cf. *D. gouldi* appears connected to the open part of the V of the chevrons. The parts corresponding to *Diplichnites* isp. cf. *D. gouldi* consist of two parallel trace series of circular to tear-shaped, regularly spaced impressions. In the more completely preserved areas, the impressions form a V shape with two smaller imprints located outwards and anteriorly, and two larger imprints located inwards and posteriorly.

Remarks: The studied specimens represent the traces left by three different behaviours of a same organism, recording its movement from a resting position in the sediment (*Rusophycus*), to crawling to get out of it (*Cruziana*), to walking over it (*Diplichnites* isp. cf. *D. gouldi*). Such behaviour, expressed in the same ichnotaxa, is well known from Palaeozoic trilobites (*e.g.*, Crimes, 1970), but it has also been reported in younger deposits (*e.g.*, Bromley & Asgaard, 1979; Minter *et al.*, 2007; Hminna *et al.*, 2020), meaning that the potential producers of these ichnofossil are disparate (see Hammersburg *et al.*, 2018, for a review of the possible producers of these three ichnogenera). In the case of the traces studied here, the most likely producer was a notostracan crustacean, similarly to the cases described by Bromley & Asgaard (1979), Minter

et al. (2007) and Gand *et al.* (2008). In continental deposits, these traces usually appear in the *Scoyenia* ichnofacies (Buatois & Mángano, 1998).

5.2. Tetrapod tracks

Ichnogenus *Rhynchosauroides* Maidwell, 1911

Rhynchosauroides isp. 1

Figure 5A–B; Supplementary Table 2

Studied material: PN-7.6?-01 (gypsum cast made in the 1980s of a right manus undertrack). PN-14.7-01 (left manus undertrack and a partially preserved probable left pes undertrack, left in the field). From Punta Negra section and its lateral equivalent at Platja de sa Marina, middle part of Estellencs Formation, Aegean.

Description: Manus track semiplantigrade to plantigrade, pentadactyl, with the base of the digits III–IV being the deepest imprinted zone. The imprints of the digits I–IV end in pointed tips and can be slightly curved inwards. The imprint of digit V also possesses a pointed tip and is slightly curved outwards. The length of the digit impressions can be ordered as follows: I<V<II<III≈IV. Pes track located behind and exteriorly to the manus in the case of PN-14.7-01. The palm impression is anteroposteriorly short, with a concave distal outline.

Remarks: This morphotype is preserved in very fine-grained sandstones and agrees with the ichnogenus *Rhynchosauroides*, for which a revision is much needed (Klein & Niedźwiedzki, 2012; Mujal *et al*., 2018b). Regardless, the specimens here described show strong similarities in terms of size, shape and digit divergence with *Rhynchosauroides brevidigitatus*, *Rhynchosauroides peabodyi*, *Rhynchosauroides rdzaneki*, *Rhynchosauroides schochardti* and *Rhynchosauroides tirolicus* (Haubold, 1971; Avanzini & Renesto, 2002; Klein & Lucas, 2010a; Klein & Niedźwiedzki, 2012). Most of the diagnostic features of the aforementioned ichnospecies are in the pes imprint and in the trackway pattern, which are unavailable in the case of the specimens from Mallorca. Therefore, we prefer to use open nomenclature.

In Triassic beds, this ichnogenus has been reported from Europe, north Africa, south and north America and Asia (*e.g*., Haubold, 1971; Melchor & De Valais, 2006; Gand *et al*., 2007; Klein & Lucas, 2010a; Lucas *et al*., 2010; Avanzini *et al*., 2011; Klein *et al*., 2011; Klein & Niedźwiedzki, 2012; Mujal *et al*., 2016, 2017a, 2018b; De Jaime Soguero *et al.*, 2021; Xing & Klein, 2021). Distantly related clades have been suggested as possible *Rhynchosauroides* trackmackers, from archosauromorphs (Avanzini & Renesto, 2002; Mujal *et al*., 2017a, 2018b) to non-archosaurian neodiapsids (Lucas, 2019).

Rhynchosauroides isp. 2

Figure 5C; Supplementary Table 2

Studied material: PN-7.6?-03 (left manus-pes set (undertracks), left in the field). From Punta Negra section, middle part of Estellencs Formation, Aegean.

Description: Manus track digitigrade, probably pentadactyl, with deeply imprinted straight digits II–IV ending in pointed tips. Of digit I, only the tip is impressed. The length of the digit impressions can be ordered as follows: I<II<III<IV. Pes track digitigrade, pentadactyl, with deeply imprinted straight digits II–IV and tips of digits I and V. The distal portion of the digits III and IV are the deepest imprinted parts. The length of the digit impressions can be ordered as follows: I<?V<II<III<IV. Although no clear track midline can be established, it can be said that the manus is smaller than the pes and is located internally and behind it, denoting a complete anterolateral overstepping. The manus track is slightly rotated inwards with respect to the pes track.

Remarks: The fact that the only studied specimen (preserved in very fine-grained sandstone) is an isolated manus-pes set and that only some digits are partially imprinted makes ichnospecies-level identification difficult. The traits that make it possible to distinguish PN-7.6?-03 from the other specimens from Mallorca are that the manus digit IV imprint is clearly longer than the digit III imprint, that the manus track is located clearly behind the pes track and that the manus and pes are distinctly digitigrade/unguligrade, with digit V impression present only in the case of the pes. However, all these traits are common in several ichnospecies of *Rhynchosauroides* (*e.g.*, Haubold, 1971) and might in part respond to extramorphological variability. Therefore, the specimen studied here is left in open nomenclature.

Ichnogenus *Prorotodactylus* Ptaszyński, 2000

Prorotodactylus mesaxonichnus Mujal, Fortuny, Bolet, Oms *et* López, 2017

Prorotodactylus mesaxonichnus

Figure 5D–F; Supplementary Table 2

Studied material: PN-14.6-03 (left manus-pes set (undertracks), left in the field) and perhaps PN-14.6-01 (left manus undertrack, left in the field) and PN-14.6-02 (left manus-pes set (undertracks), left in the field). From the lateral equivalent of Punta Negra section at Platja de sa Marina, middle part of Estellencs Formation, Aegean.

Description: Manus track digitigrade, pentadactyl, with digits II–III being the deepest imprinted zones, especially in its basal phalangeal impressions. The digit I–IV imprints are thin, straight to slightly curved inwards, and end in distinctly pointed claw traces. The imprint of digit I is shallower than those of digits II and III. The basal phalangeal impressions of digits II and III are oval-shaped (anteriorly elongated) and somewhat connected. The proximal parts of digits IV and V are not very deeply imprinted, and only its distal portion may appear. Although the length cannot be confidently measured on all the digit imprints, they seem to be ordered as: V≈I<II≈IV<III.

Pes track digitigrade, pentadactyl, with digits I–II being the deepest imprinted zones. The digits I–IV are straight to very slightly curved inwards, and end in pointed tips corresponding to claw traces. Digits I and II have expanded distal portions, which correspond to deformation of the sediment during the kick-off phase. Digit III is weakly imprinted proximally, whereas the clawed tip is deeper. The imprint of digit IV is only very shallowly preserved in its distal part, but the tip is not well defined. Digit V is not very well defined either, and only the tip can be observed. Although the length cannot be confidently measured on all the digit imprints, they seem to be ordered as: V<I<II<IV<III. The divergence angles between digits I, II, III and IV are very low, always smaller than 10º.

Trackway pattern not visible in any of the studied specimens. However, from the manus/pes sets, it can be said that the manus imprints are located approximately at the same height than those of the pedes, and the pes tracks are slightly rotated outwards and laterally positioned regarding those of the manus.

Remarks: The tracks here considered (preserved in very fine-grained sandstone) have a somewhat ‘lacertoid’ morphology, but a combination of characters such as that the manus digit III is longer than IV and that the divergence angle between digits IV–V is very low allows to exclude the ichnogenus *Rhynchosauroides*. The specimens from Mallorca are also different from *Gwyneddichnium* (see Lucas *et al*., 2014) because, in the latter, the digit III is not much longer than IV, and digit IV is longer than II. All these traits listed above, together with a relatively short digit V and the pes imprints rotated outwards with respect to the manus, agree with the ichnospecies *P. mesaxonichnus* described by Mujal *et al.* (2017a) from the upper Lower Triassic–lower Middle Triassic of the Pyrenean Basin (Mujal *et al*., 2016, 2017a), and thus of a very similar age and palaeogeographic position than the material from Mallorca. Their potential trackmakers are non-archosaurian archosauromorphs (Mujal *et al*., 2017a).

Indeterminate morphotype

Figure 5G–H; Supplementary Table 2

Studied material: PN-7.6?-02 (left ?manus and right ichnite (undertracks) of the same trackway, left in the field), PN-7.6-01 (partial left and right manus-pes sets (undertracks) of the same trackway, and traces of other ichnites (undertracks), left in the field). From Punta Negra section, middle part of Estellencs Formation, Aegean.

Description: Manus imprint plantigrade to semiplantigrade, pentadactyl, with the palm being the most deeply impressed region, followed by the distal region of the digits II–IV (excluding the claw impressions). The length of the digits of the manus imprint can be ordered as follows: V<I<II<III<IV. They are relatively straight and end in pointed tips, corresponding to claw impressions. The palm has a somewhat diffuse proximal end and a less impressed zone in the union with the digits. Pes imprint apparently plantigrade, probably pentadactyl, with the sole and the digit tips being the deepest impressed parts. The digits are not clearly impressed in any of the studied specimens and measurement is complicated, but it can be said that the digit impressions of the pedes are somewhat straight and with pointed to somewhat rounded tips. No clear midline has been established, however the manus imprints are rotated slightly inwards (lines drawn following the angle of digit III impressions of both manus end up converging), and are located slightly in front of and internal to the pes imprints. The pes imprints slightly overstep the manus imprints and the pace length is very short, with the manus-pes sets almost at the same height in the trackway, in the case of PN-7.6-01.

Remarks: The paucity of material and the fact that almost all the studied specimens correspond to manus undertracks (preserved in very fine-grained sandstones) has hindered its ichnogenus-level identification. Small manus tracks that are almost as long as wide and with a relatively short palm, median functional prevalence, with short and stout digits ended in pointed tips (claw impressions) and with digit III longer than IV, point to archosauromorph trackmakers, or more generally diapsid reptiles (*e.g*., Haubold, 1971; Mujal *et al.*, 2020). Chirotheriids, however, may be excluded because their manus tracks possess a very weakly imprinted palm and there is no manus-pes overstepping (Haubold, 1971; Klein & Haubold, 2007; Klein & Lucas, 2010b; Reolid *et al*., 2020). Other ichnogenera attributed to archosauromorphs, such as *Gwyneddichnium*, *Prorotodactylus* and *Rhynchosauroides* (as already mentioned above) show slightly different digit proportions and divarication angles, the digits are not as stout as in the specimens from Mallorca, and the manus is slightly less wide (Klein & Niedźwiedzki, 2012; Niedźwiedzki *et al*., 2013; Lucas *et al*., 2014; Mujal *et al*., 2017a). Some tracks included in 'Morphotype A' by Mujal *et al*. (2016) are similar to those studied here, with relatively stout and short manus digit imprints and the divarication angle between digits II–III being greater than that of digits III–IV (Supplementary Table 2). However, the lack of trackway data and the

small number of specimens available for study make it impossible to confidently identify them, thus leaving them under 'Indeterminate morphotype', waiting for future specimens that may shed light on their ichnospecies-level identification.

Additionally, from the middle part of Pedra Alta Formation, Calafat *et al.* (1986, 1986–1987) and Calafat (1988) reported the presence of several circular, concave structures of 30–40 cm of diameter, which were thought to correspond to very large tetrapod ichnites (Supplementary Text 1, Supplementary Figure 1A). However, after examining them *in situ* for the present work (Supplementary Figure 1B), it has been concluded that they are not ichnites, given their very large size and the lack of expulsion rims, any distinct pes or manus-like shape and trackway arrangement.

Almost all the ichnofossils mentioned above (*Skolithos*, *Taenidium*, *Rusophycus*-*Cruziana*-*Diplichnites* and tetrapod tracks) are typical of the *Scoyenia* ichnofacies, corresponding to areas with recurrent flooding and desiccation (Buatois & Mángano, 1998). This is consistent with the inferred palaeoenvironment from the middle part of Estellencs Formation, that is, a floodplain setting with sporadic overbank flows that produced crevasse splays. Nevertheless, the ichnogenus *Gordia* is typical of the *Mermia* ichnofacies, corresponding to relatively more stable water bodies (Buatois & Mángano, 1998). Indeed, the presence of symmetrical wave ripples in some beds also suggests the development of seasonal playa lakes (in the sense of Briere, 2000). Although the specimens of *Gordia* do not appear in the exact same bed as the wave ripples, both structures are separate pieces of evidence for the presence of stable bodies of water, at least seasonally.

6. Systematic palaeontology

6.1. Clam shrimps ("conchostracans")

Diplostraca Gerstaecker, 1866

Superfamily Lioestheriacea Raymond, 1946

Family Xiangxiellidae Shen (*in* Chang, Chen *et* Shen, 1976)

Genus *Hornestheria* Kozur *et* Lepper (*in* Kozur *et* Weems, 2010)

Hornestheria sollingensis Kozur *et* Lepper (*in* Kozur *et* Weems, 2010)

Hornestheria sp. aff. *Ho. sollingensis*

Figure 6A–B

Studied material: Eight specimens, DA21/03-02-58, DA21/03-02-68, DA21/03-02-72, DA21/03-02-75, DA21/03-02-77, DA21/03-02-78, DA21/03-02-80, DA21/03-02-81. From Pedra Alta section (metre 7.2–7.3), upper part of Estellencs Formation, Aegean.

Description: Carapace valves of medium to large size (carapace valve length between 2.5–3.9 mm), oval to elongated oval in shape (carapace valve height/length ratio values between 0.57–0.70). Its dorsal margin is straight, of a length between 1.8–2.3 mm. The height of the larval carapace valve varies between 0.1–0.5 mm. The umbo is in submedially and marginal to inframarginal position. The points of maximum curvature along the anterior and posterior margins are located in the median-dorsal to median-ventral region, and along the ventral margin they are located in the median to median-posterior region. On the external side of the shells, the studied specimens show either indistinct or finely reticulated ornamentation.

Remarks: The specimens from Pedra Alta section differ from *Hornestheria sollingensis* because of its very small larval carapace valve and the fact that the characteristic radial element on it is not clearly recognizable in most of the specimens from Mallorca (except for the specimen illustrated in Figure 6B), due to a variable degree of deformation in the umbonal area. Therefore, an affinity-based, open nomenclature is preferred. Occurrences of the genus *Hornestheria* are known to range biostratigraphically from the uppermost Olenekian (uppermost Spathian) to the Anisian (Kozur & Weems, 2010; Scholze & Matamales-Andreu, 2021).

Hornestheria? sp. indet. morphotype 1

Figure 6E

Studied material: Nine specimens, DA21/03-04-01, DA21/03-04-02, DA21/03-04-07-1a, DA21/03-04-07-2a (counterpart), DA21/03-04-07-1c, DA21/03-04-07-2c (counterpart), DA21/03-04-07-1d, DA21/03-04-10, DA21/03-04-11, DA21/03-04-12-1, DA21/03-04-12-2 (counterpart), DA21/03-04-13a, DA21/03-04-13b (counterpart). From Punta Negra section (metre 82), upper part of Pedra Alta Formation, Aegean.

Description: Carapace valves very large (carapace valve length between 4.9–7.8 mm) and round in shape (carapace valve height/length ratio values between 0.76–0.87). The dorsal margin is straight, of a length between 2.7–4.6 mm. The height of the larval carapace valve ranges between 0.3–0.9 mm. The umbo is in anterior to slightly submedial and inframarginal to slightly marginal position. The points of maximum curvature along the anterior margin are located median-dorsal to median-ventral, in the posterior margin they are located median-ventral, and in

the ventral margin they are located median-anterior. The ventral margin is often indented in its median-posterior area.

Remarks: Instead of using formal genus and species names, an open nomenclature is applied here due to both a limited number of studied individuals and the generally needed taxonomic revision of clam shrimp records of the uppermost *Buntsandstein* deposits of Europe (*i.e.*, "*Euestheria albertii albertii*" in the sense of Kozur *et al.*, 1993; Kozur & Weems, 2010). Carapace valves of *Hornestheria*? sp. indet. morphotype 1 show irregular remnants of brownish shell substance, whereas neither radial sculptures on the larval carapace valve nor microstructures (ornamentation) are preserved. In comparison, similarly sized carapace valves of *Dictyonatella* have been described from the upper *Buntsandstein* central European deposits of the Vosges (*e.g.*, Kozur, 1982) and from the Holy Cross Mountains (Żyła *et al.*, 2013), but they differ from *Hornestheria*? sp. indet. morphotype 1 either because of their larger-sized reticulated ornamentation or by a concavely recurved posterior margin directly below the dorsal margin (Scholze & Matamales-Andreu, 2021).

Hornestheria? sp. indet. morphotype 2

Figure 6F

Studied material: Five specimens, DA21/03-04-04a, DA21/03-04-06, DA21/03-04-07-1b, DA21/03-04-07-2b (counterpart), DA21/03-04-08, DA21/03-04-09. From Punta Negra section (metre 82), upper part of Pedra Alta Formation, Aegean.

Description: Carapace valves very large (carapace valve length between 3.2–4.9 mm) and oval to very elongated-oval in shape (carapace valve height/length ratio values between 0.57–0.71). Dorsal margin slightly to moderately curved, with a length ranging between 3.0–4.0 mm. The larval carapace valve height is between 0.2–0.9 mm. The umbo is located in submedial and marginal to supramarginal position. The points of maximum curvature are located median or slightly median-dorsal in the anterior and posterior margins, and in the ventral margin they are located median-anterior. The ventral margin is often concavely indented in the median-posterior area of the carapace valve.

Remarks: *Hornestheria*? sp. indet. morphotype 2 occurs in the same stratigraphic level than *Hornestheria*? sp. indet. morphotype 1, and can be differenced because the former has a smaller total carapace valve size and a more oval shape than the latter. Both morphotypes might reflect a stout and a slender form of a same species; however, this cannot be confirmed with the present material. *Hornestheria*? sp. indet. morphotype 2 is also very similar to the specimens here

considered as *Hornestheria* sp. aff. *Ho. sollingensis*, but the latter are usually smaller and their umbo is less intensely curved (Scholze & Matamales-Andreu, 2021).

"Conchostraca" indet.

Figure 6C–D

Studied material: Three specimens, DA21/03-01-01a, DA21/03-01-01b, DA21/03-01-02. From Punta Roja section (metre 86.5), middle part of Estellencs Formation, Aegean. Two specimens, DA21/03-03-01, DA21/03-03-02. From Punta Negra section (metre 39.5), lower part of Pedra Alta Formation, Aegean.

Description: Individuals are either fragmented or deformed (*i.e.*, diagenetically compacted); their total carapace valve length is up to 3.5 mm, and their height is up to 2.6 mm.

Remarks: Based on preliminary observations, the most completely preserved specimen (Figure 6D) from Punta Negra section is morphologically reminiscent of *Hornestheria* sp. aff. *Ho. sollingensis* (Figure 6A) from Pedra Alta section (Scholze & Matamales-Andreu, 2021). The study of further material seems necessary in order to fully understand both their intraspecific and preservational variability.

6.2. Insects

Ephemeroptera Hyatt *et* Arms, 1891

Family Sharephemeridae Sinitshenkova, 2002

Genus *Hammephemera* Sinitshenkova (*in* Bashkuev, Sell, Aristov, Ponomarenko, Sinitshenkova *et* Mahler, 2012)

Hammephemera pulchra Sinitshenkova (*in* Bashkuev, Sell, Aristov, Ponomarenko, Sinitshenkova *et* Mahler, 2012)

Hammephemera sp. cf. *Ha. pulchra*

Figure 7A–E, N

Studied material: Four specimens, TS-A-1, TS-A-2, TS-D-1, TS-F-1. From Pedra Alta section (metre 4.75), upper part of Estellencs Formation, Aegean. One specimen, DA21/03-02-88. From Pedra Alta section (metre 7.20–7.30), upper part of Estellencs Formation, Aegean. The specimen TS-D-1 (see Figure 7B) is virtually complete and with a well-exposed forewing

venation (the description below is mainly from this specimen, which Calafat (1988) figured as a lepidopteran in his photo 22).

Description: Body length ca. 7.5 mm. Forewing length 7.25 mm, maximum width ca. 3.00 mm. Forewing two times as long as wide (but slight deformation in some of the specimens), with base broad and with anal area narrowed, and cubital area narrow. Anterior margin of the forewing slightly convex and its top rounded. Tornus in a distal position, close to the middle of wing. Rs with seven longitudinal veins. Forks of MA and CuA relatively short. Long CuA fork with intercalary vein, CuP long and simple, anal veins simple and long.

Remarks: The extinct family Sharephemeridae contains two genera based on isolated forewings, *Sharephemera* and *Hammephemera*, from the Upper Jurassic of Mongolia and Middle Triassic (lower Anisian) of Germany (Bashkuev *et al.*, 2012), respectively. The new specimens from Mallorca are the first articulate, but details of the body remain obscure. General forewing venation and the forewing size are coincident with the German species. Despite the five articulated adult specimens from the same level with well-exposed forewing venations, the slight deformation of the wings and some not well-resolved venation details prevent an accurate comparison with the exceptionally preserved holotype of *Hammephemera pulchra*. Therefore, we consider the specimens from Mallorca as *Hammephemera* sp. cf. *Ha. pulchra*. This taxon is relatively abundant in Pedra Alta section (two additional specimens could correspond to this form: TS-E-2 and TS-H-1), so more specimens will probably be discovered and will inform if it corresponds to this previously described species or to a new one. An enigmatic adult specimen (TS-B-1; Supplementary Figure 2A–B), only showing a few anatomical details and apparently without head due to disarticulation, was figured by Calafat (1988) as an indeterminate winged form. That specimen was later suggested to be an indeterminate dipteran by Shcherbakov *et al.* (1995), based on the not very detailed photograph in the study by Calafat (1988), in which the habitus strongly suggests a dipteran. However, it actually corresponds to a mayfly that may have died during emersion from the nymphal stage, because the aspect of its wings is similar to unexpanded wings (note that the length of thorax plus abdomen is 5.5 mm in this specimen, being 5.9 mm in the best *Hammephemera* sp. cf. *Ha. pulchra* specimen, and thus their sizes are very similar).

Family indet.

Adult morphotype 1

Supplementary Figure 2C–G

Studied material: Two specimens, TS-G-1a, TS-G-1b (counterpart), TS-G-2, the slab with the part is 5×3.5 cm. From Pedra Alta section (metre 4.75), upper part of Estellencs Formation, Aegean.

Description: Body length ca. 3 mm. Only a few features of the forewings can be described, as most of the anatomical details are not preserved. Distal margins of the four studied forewings are not preserved or are obscure, and therefore a suitable measure of the forewing length is not available. Longitudinal veins in the costal margin and some of other longitudinal veins (Rs and MA) are well preserved, but this only indicates that these adult specimens are mayflies.

Remarks: These two adult mayfly specimens preserved one next to the other exhibit a very few anatomical details due to their poor preservation, but they are clearly conspecific. It is not possible to classify them at family level, and they certainly correspond to a morphotype different from the other adults reported in the present work, based on their different size compared to the *Hammephemera* sp. cf. *Ha. pulchra* specimens (ca. 3.0 mm vs. ca. 7.5 mm of body length). They occur in the same slab surface together with a clam shrimp (TS-G-7) and four mayfly nymphs (TS-G-3, TS-G-4, TS-G5 and TS-G-6; three of them virtually complete), notably much larger (Supplementary Figure 2C), and thus not conspecific; the counterside contains two clam shrimps (TS-G-9 and TS-G-10) and a small mayfly nymph (TS-G-8).

Family indet.

Detritivore nymph type

Figure 7F–H

Studied material: Over 50 specimens in the two collections studied. From Pedra Alta section (metres 4.75 and 7.20–7.30), upper part of Estellencs Formation, Aegean.

Description: This group of forms is very abundant in Pedra Alta section but only a few specimens are virtually complete and well preserved. There are diverse stages of development, from specimens of 3–4 mm of body length (specimens DA21/03-02-05 and DA21/03-02-30) to more developed specimens, with body lengths of ca. 6.6–7.0 mm. Body flattened or not clearly cylindrical (only a few specimens preserved in lateral position). Wing pads not conspicuous. Legs simple, short and slender. Tergaliae large, rounded, slightly fringed on the borders, slightly overlapped, present in the abdominal segments I–VII. Except for a few specimens that show the digestive preserved as a carbonaceous tube, these nymphs exhibit 3D cololites (see Figure 7F–H). Cerci and paracercus (= terminal filament) not very long (ca. 3/5 the abdominal length in a specimen without 3D cololite) and covered with hairs.

Remarks: The digestive contents in these nymphs did not collapse during stratigraphic compression, as revealed by their 3D cololites, indicating that they contained detritic particles, apparently including abundant fine sedimentary grains. This indicates that this group of mayflies was detritivore during aquatic, preimaginal stages, most likely obtaining organic particles present in the fine sediment of the pools. Taphonomy of the outcrop suggests that this extremely abundant group of detritivore nymphs could be conspecific with the adults identified as *Hammephemera* sp. cf. *Ha. pulchra*. The taphonomic observations are: (1) the abundant mayfly nymph record is virtually constituted by this type; (2) there are different stages of development; (3) all these specimens are articulated (in all the cases in which this circumstance could be observed); (4) adults of *Hammephemera* sp. cf. *Ha. pulchra* are abundant in the deposit of Mallorca, considering that the family Sharephemeridae was known previously by only two isolated forewings; (5) all these adults are articulated; (6) these adults occur together with this nymph type in the slabs (for example, slab D, 7×5.5 cm in size, see Figure 7A, contains the adult TS-D-1 and remains of 10 nymphs); and (7) the largest detritivore nymphs have sizes that could match with the adult body sizes. However, in the studied fossil assemblage there are also two small-sized mayfly adults (adult morphotype 1; see above), and therefore some of the small detritivorous nymphs may be conspecific with these adults. Further research and new specimens with exceptional preservation could elucidate this topic and complete the description herein provided.

Family Triassoephemeridae Sinitshenkova *et* Papier (*in* Sinitshenkova, Marchal-Papier, Grauvogel-Stamm *et* Gall, 2005)

Genus *Triassoephemera* Sinitshenkova *et* Papier (*in* Sinitshenkova, Marchal-Papier, Grauvogel-Stamm *et* Gall, 2005)

Triassoephemera punctata Sinitshenkova *et* Papier (*in* Sinitshenkova, Marchal-Papier, Grauvogel-Stamm *et* Gall, 2005)

Triassoephemera punctata

Figure 7I–J

Studied material: A single, articulate specimen, MBCN23697a, MBCN23697b (counterpart). From Pedra Alta section (metre 7.55), upper part of Estellencs Formation, Aegean. One clam shrimp is close the thorax in ventral position.

Description: Large nymph. Head not preserved (likely not due disaticulation, but preservational) and thorax partially preserved (wing pads not observed). Body length is ca. 18 mm as preserved

(estimated 20 mm), and the greater width of the abdomen is 4 mm. Legs not preserved, and therefore claw features unknown. Body not flattened (clearly cylindrical), and abdomen with short segments and without side protrusions. All the 10 abdominal segments preserved. Gills in latero-ventral position at least in the abdominal segments I–V, as plates rounded in shape, densely fringed on the borders. Dense punctuated ornamentation of the abdominal tergal cuticle (Figure 7J). Absence of a 3D cololite preserved. Base of cerci and paracercus preserved.

Remarks: This genus and species were described based on 9 specimens from the Vosges (Sinitshenkova *et al.*, 2005), with body lengths of 15, 20 and 30 mm depending on the nymphal stages represented (the preserved body portion of the specimen from Mallorca is ca. 18 mm, with an estimated body length of about 20 mm). The deposit of Mallorca is the second with the presence of this Anisian species, implying a faunal similitude with the Vosges at species level. In the Vosges, *Te. punctata* is rare, as it only represents the 2.5 % of the mayflies (Sinitshenkova *et al.*, 2005), but it is even rarer in the deposit of Mallorca (0.7 %). The absence of a 3D cololite in the specimen studied herein (and not described in the Vosges specimens), suggests that this mayfly species was not detritivore, contrarily to the "detritivore nymph type" described above.

Family Siphlonuridae Ulmer, 1920 (*sensu lato*)

Genus *Triassonurus* Sinitshenkova *et* Papier (*in* Sinitshenkova, Marchal-Papier, Grauvogel-Stamm *et* Gand, 2005)

Triassonurus doliiformis Sinitshenkova *et* Papier (*in* Sinitshenkova, Marchal-Papier, Grauvogel-Stamm *et* Gand, 2005)

Triassonurus doliiformis

Figure 7K–M

Studied material: A single, articulate specimen, TS-C-1. From Pedra Alta section (metre 4.75), upper part of Estellencs Formation, Aegean. Four clam shrimps are present in the same surface having the nymph.

Description: Large nymph exceptionally preserved. Body length is ca. 11 mm, and the greater width of the abdomen in lateral position excluding tergaliae is ca. 2 mm. Body cylindrical (not flattened). Head triangular, wider than long, narrowing towards the anterior margin; it is longer than the prothorax, which is short. Mesothorax large. Wing pads apparently not preserved. Legs simple, short and slender; femora shorter than tibiae and tarsi slightly shorter than tibiae.

Abdominal segments short, 2.5 times wider than long, with short denticles in their posterior margins. Tergaliae very large, rounded, with thickened anterior margin, and overlapped between them forming a close surface (their dimensions in respect to the abdominal segments as described for this species by Sinitshenkova *et al.*, 2005). Cerci and paracercus incomplete, but based on their preserved basal portions they were long; they are segmented and densely covered with hairs (the posterior margin of the segments show a line of small, short spines). Absence of a 3D cololite preserved, but the digestive is strongly marked as a carbonaceous tube.

Remarks: This specimen shows an excellent preservation and is virtually complete. It was figured in Calafat (1988) and Martínez *in* Gallemí *et al.* (1988) as an indeterminate mayfly nymph. The specimen matches all the features described for *Tn. doliiformis*, but the forewing pads, which are large in this species, are apparently not preserved in the specimen from Mallorca. Its body length (ca. 11 mm) is close to the estimated for the holotype of *Tn. doliiformis* (ca. 12 mm; see Sinitshenkova *et al.*, 2005). The deposit of Mallorca is the second with the presence of this Anisian species, implying a second faunal similitude with the Vosges at species level. The fossils of this genus are the oldest of the family Siphlonuridae (Sinitshenkova *et al.*, 2005). In the Vosges, *Tn. doliiformis* is relatively abundant (13% of the Grauvogel and Gall collection, as indicated in Sinitshenkova *et al.*, 2005), but it is very rare in the deposit studied here (0.7%). This species was not detritivore, similarly to *Te. punctata* described above and unlike the "detritivore nymph type".

Family Voltziaephemeridae Sinitshenkova *et* Papier (*in* Sinitshenkova, Marchal-Papier, Grauvogel-Stamm *et* Gand, 2005)

Genus *Voltziaephemera* Sinitshenkova *et* Papier (*in* Sinitshenkova, Marchal-Papier, Grauvogel-Stamm *et* Gand, 2005)

Voltziaephemera fossoria Sinitshenkova *et* Papier (*in* Sinitshenkova, Marchal-Papier, Grauvogel-Stamm *et* Gand, 2005)

cf. *Voltziaephemera fossoria*

Figure 8

Studied material: A single, virtually complete nymph, TS-J-1a, TS-J-1b (counterpart). From Pedra Alta section (metre 4.75), upper part of Estellencs Formation, Aegean. One specimen corresponding to an incomplete exuvium, DA21/03-02-38. From Pedra Alta section (metre 7.20–7.30), upper part of Estellencs Formation, Aegean.

Description: Nymph in lateral position (Figure 8A–D). Estimated body length of 14.5 mm. Head details not clear, but antennae preserved. Head with anterior rounded protrusion (observed in lateral habitus; character not conspicuous). Large eyes, elongate in lateral view. Prothorax longer than the head. Wing pads not well discernible in this specimen. Legs well developed, with abundant hairs and with a terminal single claw, thus of burrowing type (see Sinitshenkova *et al.*, 2005). Fore and hind legs about a quarter of estimated body length. Fore legs not shorter than hind legs, but slightly longer; tibiae lacking a conspicuous protrusion. Fore and hind femora swollen; mid femur not well discernible. First seven abdominal segments with tergaliae marginally with long and slender fringes. The abdominal segments present "small black-coloured comma-shaped sclerified structures" (peculiar structures as described by Sinitshenkova *et al.*, 2005) on their lateral parts. No cololite, but digestive as a carbonaceous tube. Cerci and paracercus not preserved by slab margin.

Remarks: Sinitshenkova (2000) considered this nymph from Mallorca, figured in photo 24 of Calafat (1988), as a burrowing form. The specimen shares all its important preserved characters with the species *Voltziaephemera fossoria* from the Vosges. For example, the fore legs are identical to those of this fossil burrowing species (Sinitshenkova *et al.*, 2005; fig. 6B, D, E in p. 386). That species was described based on specimens preserved in dorso-ventral position, not lateral. The specimen from Mallorca apparently lacks convergent tusks in its head and protruding anterior eye margins, but surely this is due to preservation and/or lateral position (these features were only observed in a few specimens from the Vosges and, in fact, the head features of the specimen from Mallorca are similar to those of the specimen paratype 9229 in Sinitshenkova *et al.*, 2005). The relative leg lengths of the specimen from Mallorca are not identical to the Vosges specimens, but its body length has been based on an estimation, and the legs of the Vosges specimens apparently are not well preserved to allow accurate descriptions. Unfortunately, the wing pads of the specimen from Mallorca are not well discernible and its cerci and paracercus cannot be compared as they are not preserved. Most likely, this new specimen belongs to *Voltziaephemera fossoria*, but new material will be necessary to confirm that identification. Another specimen from Mallorca, corresponding to an incomplete exuvium (Figure 8E–G), is from a younger stage and only shows a few structures, but it can be considered conspecific with the other specimen found in this locality because it has the same abdominal "small black-coloured comma-shaped sclerified structures" and same fore leg of burrowing type.

Blattodea Brunner von Wattenwyl, 1882

Blattodea indet.

Figure 7O

Studied material: One isolated tegmina (= forewing), DA21/03-02-85. From Pedra Alta section (metre 7.20), upper part of Estellencs Formation, Aegean. One isolated tegmina, DA21/14-02-03a, DA21/14-02-03b (counterpart). From Pedra Alta section (metre 7.55), upper part of the Estellencs Formation, Aegean.

Description: Specimen DA21/14-02-03 shows few details. Specimen DA21/03-02-85 is partial but exceptionally preserved as a carbonaceous film lacking slight relief. The incomplete wing (proximal portion) shows a well-marked venation (but its intricate, dichotomous venation has not been completely resolved), with slightly marked intercalary veins in R, M, CuA systems, and possibly in Sc as well.

Remarks: Ansorge (1997) cited three wings of cockroaches from this deposit, but without description. Wings of cockroaches are difficult to interpret, and they show vein variation even in the same individual. The partial wing DA21/03-02-85 has been compared to other known Mesozoic species with intercalary veins, but identification has been unsuccessful. Nevertheless, that portion is similar to the wings of the species *Voltziablatta intercalata* from the Anisian of the Vosges (Papier & Grauvogel-Stamm, 1995), a deposit that yielded over 5,000 specimens, the 40 % of the individuals being cockroaches. Cockroaches are very polyphagous, mainly saprophagous, and thus not very informative for the reconstruction of the palaeoecosystem.

6.3. Fishes

Osteichthyes Huxley, 1880

Osteichthyes indet.

Figure 9

Studied material: One specimen, virtually complete, TS-E-1. From Pedra Alta section (metre 4.75), upper part of Estellencs Formation, Aegean. The same slab surface contains a mayfly adult (TS-E-2) at a distance of 2.5 cm from the fish.

Description: The specimen is preserved in a dorso-ventral position, except for the posterior third of the body, which is in lateral position. Its estimated length is 16 mm (the preserved portion is 13 mm long). The right pectoral, the dorsal (perhaps a second dorsal fin as well) and the anal fins are preserved, all with well-marked radii. The caudal fin is distally missing due to its being on the edge of the slab. No remains of the vertebral column or ribs are preserved, neither as carbonaceous films nor as their impressions.

Remarks: The poor preservation of this specimen has precluded any precise identification. It had been figured by Calafat (1988), who identified it as an indeterminate fish, and here it is identified as an osteichthyan based on the presence of opercles and fins with radii. Its very small size and lack of ossification makes it possible to consider it as a juvenile specimen.

The aquatic palaeocommunity described above (clam shrimps, mayfly nymphs and fishes) developed in ponds near the channels or among sand bars. Some horizons lacking bioturbation show abundant specimens of mayfly nymphs in complete articulation, without a preferred orientation and sharing the same or a very similar stage of development (slab TS-A, 5.0×3.5 cm in size, contains 4 nymphs; slab TS-D, 7.0×5.5 cm, contains 10 nymphs; and slab DA21/14-02-01, 6.5×6.0 cm, contains 14 nymphs, but in this case they are not in a clear, single surface). These records do not indicate accumulations caused by currents, but high mortality in a short time, in a population with individuals of very similar age. These features are indicative of mass mortality, implying the presence of many carcasses covering an anoxic bottom, most likely due to a low transport in the water column before their final sinking. Such evidences suggest sudden variations of the environmental conditions, probably related with desiccation and/or depletion of oxygen in those water bodies.

Other terrestrial insect material from unspecified beds of Estellencs Formation and/or Pedra Alta Formation was reported by Zessin (2008a, 2008b), who illustrated some of the specimens and preliminarily identified remains of the orders “Blattaria”, Coleoptera, Diptera, Heteroptera, (?)Megaloptera, Homoptera and (?)Orthopteroidea. From the same beds, Aristov & Zessin (2009) described a new grylloblattid species: *Mallorcagryllus hispanicus*. Despite the intensive fieldwork campaigns carried out during the present work, beds bearing such a rich terrestrial palaeoassemblage have not been found again.

7. Discussion

7.1. Palaeoenvironmental evolution and palaeogeography

The sedimentary palaeoenvironments in the Iberian area during the Triassic were likely strongly influenced by the climate (Borruel-Abadía *et al.*, 2015). Previous works have shown that subsidence rates were irregular among the different sub-basins of each of the main basins, and yet similar sedimentary successions were recorded, varying mostly in the thickness of each of the lithostratigraphic units (*e.g.*, Arche & López-Gómez, 1996; Borruel-Abadía *et al.*, 2015; Mujal *et al.*, 2017a, 2017b; López-Gómez *et al.*, 2019a). In the case of Mallorca, even though

the Triassic continental succession echoes those of the southeastern Iberian Basin (located in the central-eastern zone of the Iberian area; see below) in the succession of the different palaeoenvironments through time, the lack of detailed studies on palaeoclimate indicators (clay mineralogy, palaeosols, etc.) in the former prevents extrapolating the climatic conditions inferred for each of the units of the latter. Therefore, in this section, the changes in palaeoenvironments are not attributed directly to cimate but, more broadly, to shifts in the energy conditions, which may be caused by the climate but also by tectonics and geomorphology (*e.g.*, Miall, 2006).

The lowermost lithostratigraphic unit of the Triassic of Mallorca, Punta Roja Formation (Figure 10), is here considered a distal equivalent to the southeast of the fluvial units reworking aeolian sediments recognised in the central part of southwestern Europe (eastern Iberia, Menorca, Sardigna and Provençe). There, wind-transported sediments have been identified in several areas, recognising fluvial systems with aeolian reworking in the Catalan Basin (Marzo, 1986; Galán-Abellán *et al.*, 2013a), in the Castilian branch of the Iberian Basin (López-Gómez *et al*., 2012), and an erg system in the Aragonian branch of the Iberian Basin (Soria *et al*., 2011). The aforementioned units have been dated, usually by inference, as Spathian (upper Olenekian) to Aegean (lower Anisian) (reviews in Durand, 2006; López-Gómez *et al*., 2019a), coinciding with the late part of an arid period recognised in central Europe (Péron *et al.*, 2005; Durand, 2006; Bourquin *et al*., 2011; Sun *et al.*, 2012; Borruel-Abadía *et al.*, 2015; Trotter *et al.*, 2015). However, towards the northern and southern margins of eastern Iberia, Menorca, Sardigna and Provençe, those aeolian sediments were often reworked by rivers, appearing in the form of well-sorted fluvial deposits, sometimes with ventifacts (Cassinis *et al.*, 2003; Durand, 2006; Linol *et al.*, 2009; López-Gómez *et al.*, 2012; Galán-Abellán *et al.*, 2013a). As posited in '4. Stratigraphy and sedimentology', Punta Roja Formation also corresponds to a perennial shallow braided river that reworked aeolian sediments, with an increase of sinuosity towards the top, probably near the Olenekian–Anisian transition (Figure 10).

With the decrease of the system energy, the depositional environment gradually shifted to sand-bed meandering rivers that traversed lutitic floodplains, corresponding to Estellencs Formation (Figure 10). Abundant growth of vegetation under more favourable conditions may have contributed to the stabilisation of the river banks (plant roots make them more cohesive and thus more difficult to erode) and led to the development of sinuous channels, a process that has been observed in both modern and ancient examples (Ebisemiju, 1994; Rowntree & Dollar, 1999; Huisink, 2000; Michaelsen, 2002; Miall, 2006; Davies & Gibling, 2010; López-Gómez *et al*., 2012; Borruel-Abadía *et al*., 2015). Evidence of such a plant cover lies in the presence in this unit of sporadic hygrophytic plant remains such as *Equisetites* (found in living position, see Juárez-Ruiz & Wachtler, 2015) and well-developed palaeosols. The latter always present

abundant small-sized carbonate concretions, thus corresponding to Calcisols, which are indicative of climates with low precipitation regimes (semi-arid conditions), at least during part of the year (Mack *et al.*, 1993; Alonso-Zarza, 2003; Tabor & Poulsen, 2008). Moreover, almost all the ichnofossils, including the tetrapod footprints, belong to the *Scoyenia* ichnofacies (Buatois & Mángano, 1998), typical of aquatic non-marine palaeoenvironments with recurring desiccation events, such as river margins (Buatois & Mángano, 1998; Minter *et al.*, 2007; Hminna *et al.*, 2020). The *Mermia* ichnofacies, on the other hand, was developed in playa lakes (see Buatois & Mángano, 1998). All these pieces of evidence suggest the alternation of semi-arid seasons (characterised by desiccation of playa lakes) and more humid seasons (characterised by inundation and plant sprouting). Calcification of palaeosols could have taken place in either season (Alonso-Zarza, 2003). This parallels with the probably coeval lower units of the Eslida Formation of the Iberian Basin (Borruel-Abadía *et al*., 2015; Juncal *et al*., 2017), which also correspond to meandering rivers deposited under similar conditions.

In the upper part of Estellencs Formation (metres 18–27 of Punta Negra log, metres 103–112 of Punta Roja log and the whole Pedra Alta log: Figure 1C; Supplementary Logs), there is an interval characterised by high-regime flow structures, channel migration and the formation of bars (Figure 10). The fossil content is much more abundant in this interval than in the rest of the formation (see '7.2. Palaeoecosystem'), but this is probably because (1) the low preservation potential that any remains would have had in the underlying heavily oxidised red-beds and (2) the fact that the floods that deposited the sediments of this interval swept hinterland conifer forests, carrying and rapidly burying large fragments of plant material, including branches with leaves and strobyles with *in situ* pollen (Calafat, 1988; Álvarez-Ramis *et al.*, 1989, 1995; Grauvogel-Stamm & Álvarez-Ramis, 1994, 1996; Juárez-Ruiz & Wachtler, 2015). Mayfly nymphs develop well in this kind of environment of still, limpid, well-oxygenated freshwater but, similarly to the palaeoassemblages of *Grès à Voltzia* of the Central European Basin, the mayflies from Mallorca show evidence of mass mortality in some horizons, most likely due to sudden changes in the environmental aquatic conditions. In fact, recent mayfly nymphs are very sensitive to oxygen concentration, salinity variation and water turbidity (Sinitshenkova *et al.*, 2005).

The uppermost part of Estellencs Formation records a very similar palaeoenvironment to that of the lower 35 m of the formation, as evidenced by the presence of lutitic floodplains with small, sinuous channels and crevasse splay deposits (Figure 10). Therefore, it may have been deposited under similar energy conditions of the system.

After this brief interval, the higher-energy conditions were restored again, but this time it was for a thicker interval, represented by Pedra Alta Formation (Figure 10). The sand-bed braided

rivers expanded over the floodplains during seasonal heavy rains, and created new ephemeral aquatic niches in which arthropods and fish thrived. This formation has been confidently dated as Aegean (Diez, 2000; Diez *et al.*, 2005, 2010), and does not have any recognisable equivalent in the series of the southeastern Iberian Basin. It is somewhat reminiscent of the unit Ems-5 of the most distal part of the Eslida Formation, which consists of a braided interval that has been recognised in all the sections in southeastern Iberia (Borruel-Abadía *et al.*, 2014, 2015). That unit appears a few metres below the *Röt* facies, and has been interpreted as a semi-arid interval based on the local presence of aeolian sediments, xerophytic flora and the unconfinement of the fluvial systems (Borruel-Abadía *et al.*, 2014, 2015). The age of the Iberian unit, however, has been inferred to be of upper Bithynian (Borruel-Abadía *et al.*, 2015), whereas this formation in Mallorca is well dated as Aegean (Diez, 2000; Diez *et al.*, 2005, 2010; Supplementary Table 3). Therefore, they are not lateral equivalents of a same unit, but two different units deposited under comparable local conditions.

Son Serralta Formation is generally equivalent to the *Röt* facies described elsewhere in Iberia (López-Gómez & Arche, 1992; Ramos, 1995; López-Gómez *et al.*, 2019a), representing the transition from fluvial deposits to the shallow marine carbonate ramps of the *Muschelkalk* facies (Figure 10). The mud-flats were established in response to the rise of the base level during the *Muschelkalk* transgression (Franzel *et al.*, 2021), a phenomenon also reported in other basins of different age (*e.g.*, Miall, 2006).

As previously stated, this fluvial succession and its evolution through time is in part parallel to that of the southeastern Iberian Basin, providing clues on the possible distribution of palaeoenvironments in the most distal part of Iberia, that is, the Balearic basins, during the Early–Middle Triassic. Several works have attempted to propose a location for the Balearic Islands in the western Tethys in the early Mesozoic, leading to disparate hypotheses (*e.g.*, Lonergan & White, 1997; Diez *et al.*, 2005; Linol *et al.*, 2009; Bourquin *et al.*, 2011; Fortuny *et al.*, 2011a; Gretter *et al.*, 2015; Edel *et al.*, 2018; Borruel-Abadía *et al.*, 2019). In the present work, the palaeogeographic position of Mallorca is reconstructed using the work of Roca (1992), who studied the tectonic history of the opening of the modern Catalan-Balearic Basin in detail, and Parés *et al.* (1992), who, by means of palaeomagnetism, observed a 10º clockwise rotation in Mallorca during the opening of the València Trough (Figure 11), separating Mallorca from continental Iberia. The resulting position of Mallorca is somewhat aligned with the Iberian Basin (Figure 11) and, although this does not necessarily imply that the sediments of Mallorca were deposited in a lateral extension of that basin (a claim which is impossible to back up with surface data), it supports the idea of a similar palaeoenvironmental evolution of both regions. The palaeogeographical location of Menorca is still contentious (Sàbat *et al.*, 2018), but here it

has been included in the map of Figure 11 in its modern position relative to Mallorca in order to show its palaeocurrent directions during the Early–Middle Triassic.

Consequently, from a regional point of view, the fluvial series from the Lower–Middle Triassic of Mallorca were deposited in the most distal areas of the systems traversing Iberia towards the southeast (Figure 11A). In addition, the fact that the succession is in part comparable to that of the Iberian Basin makes it possible to infer that high-energy conditions with river systems reworking aeolian sediments were widespread in Iberia until the late Olenekian–earliest Aegean (Punta Roja Formation) and that the energy of the systems dwindled the early? Aegean (Estellencs Formation). In the late? Aegean, however, there was a local interval with slightly higher energy conditions (Pedra Alta Formation) followed by the reestablishment of lower energy conditions, probably at some point during the latest Aegean–Bithynian (Son Serralta Formation).

This proves the hypothesis that the first *Muschelkalk* transgression occurred on Mallorca, as the most distal region of Iberia towards the Tethys, approximately at the same time as in the most distal basins of the Iberian Peninsula. In the other Balearic Islands, the age of the base of the Triassic marine carbonate ramps is unknown, and previous inferences as Illyrian by means of lithological correlation with Iberia (Arche *et al.*, 2002; Escudero-Mozo *et al.*, 2014) are here considered unfounded because lateral facies variations were not taken into account. Diez *et al.* (2010) reviewed all the palynological data of the Anisian of the Iberian Peninsula known until then, concluding that in Mont-roig del Camp, in the southwest Catalan Basin, the *Röt* facies, equivalent to the Son Serralta Formation of Mallorca, were also of Aegean age (Figure 11B). However, in other deposits of the Catalan Basin located further North, equivalent *Röt* facies were dated as Bithynian, both in Els Hostalets de Balenyà and in L'Espluga de Francolí (Diez *et al.*, 2010 and references therein) (Figure 11C). The upper *Buntsandstein* lutites were dated as lower? Pelsonian in the Pyrenean Basin (in Igüerri and Sant Sebastià de Buseu) (Diez *et al.*, 2010 and references therein) (Figure 11D), whereas in the Basque-Cantabrian Basin (in Amaiur), similar units were dated as Bithynian–Pelsonian (Diez *et al.*, 2010 and references therein) (Figure 11D). In the Iberian branch of the Iberian Basin (in Almarja), the lower part of the *Muschelkalk* succession was also dated as Bithynian–Pelsonian (Ortí *et al.*, 2020) (Figure 11C).

After this first transgression, during the highstand phase, a system of mud-flats, coastal lagoons and, in some cases, alluvial sediments, developed in the margins of the Ebro High (Ortí *et al.*, 2018, 2020). These units have been dated between the Pelsonian and the Illyrian (Diez *et al.*, 2010 and references therein; Ortí *et al.*, 2020), and reached Mallorca in the form of a brief interval of red fine-grained sediments, evaporites and dolostones (Cuevas-López, 1958a, 1958b;

Rodríguez-Perea *et al.*, 1987; Matamales-Andreu *et al.*, in press) (Figure 11D). The upper part of these systems was affected by a second transgressive event, generating *Röt* facies similar to those of the uppermost part of the *Buntsandstein*. In the Iberian Basin, both in the Aragonian branch (in Fombuena) and in the Castilian branch (in Andilla, El Paraíso and Montant), those facies were considered as Pelsonian–Illyrian (Diez *et al.*, 2010 and references therein; Ortí *et al.*, 2020) (Figure 11D), and Franzel *et al.* (2021) determined that the *Muschelkalk* sea reached the northwestern, most proximal margins of the Castilian branch of the Iberian Basin (in Riba de Santiuste), in the middle Ladinian (Figure 11E). All these data agree with studies on other peri-Tethyan basins that suggested a progressive rise of the sea level during the Early–Middle Triassic (*e.g.*, Rüffer & Zühlke, 1994; Narkiewicz & Szulc, 2004), in this case in two main pulses, and show how the first areas to be drowned under the sea were Mallorca, the southern Catalan Basin and the southeastern Iberian Basin, followed by the northern Catalan Basin and then by the Basque-Cantabrian and Pyrenean basins. The last areas to be flooded by the sea were both branches of the Iberian Basin, and especially the Castilian branch, which was the one opening deeper inland (Arche *et al.*, 2004; López-Gómez *et al.*, 2019a; Figure 11E).

7.2. Palaeoecosystems

After the Permian–Triassic mass extinction event, palaeoequatorial continental environments remained quite inhospitable because of the very high temperatures and fast climate changes that affected them (Sun *et al.*, 2012; Trotter *et al.*, 2015; MacLeod *et al.*, 2017; Bernardi *et al.*, 2018). This situation became more stable towards the Middle Triassic, when those continental ecosystems started to regain their lost complexity (Chen & Benton, 2012; Benton & Newell, 2014; Romano *et al.*, 2020). In the western peri-Tethys, it has been suggested that high acidity levels delayed the recovery of its ecosystems until the Middle Triassic (Galán-Abellán *et al.*, 2013b, 2013c; Borruel-Abadía *et al.*, 2016, 2019), which coincides with the rise in abundance of palaeosols and trace fossils (Borruel-Abadía *et al.*, 2019).

In the case of Punta Roja Formation of Mallorca, biotic activity has been recorded in the form of carbonate palaeosols (vertic Calcisols or Calcisols) and invertebrate burrows only in the upper part of the unit. In its lower part, this formation is composed of transverse sand bars, in which the oxidation of the sediments and the general paucity of fine-grained beds most probably caused a preservation bias. The first trace fossils appear in Punta Roja Formation once the grain size decreases and the first floodplain deposits appear, as it is very unlikely for biogenic traces to be preserved in the medium-grained sands of an active river channel (bars of braided rivers are usually colonised only during intervals of interruption or waning of the flow: *e.g.*, Stanley & Fagerstrom, 1974). López-Gómez *et al.* (2012) suggested that such a lack of fossils in

equivalent strata of the Iberian formations was indicative of ecosystems that had not still recovered from the Permian–Triassic extinction. This, however, cannot be applied to Mallorca, because biogenic structures (palaeosols and burrows) appear as soon as the fossilisation conditions became better (finer and waterlogged sediment) towards the upper part of Punta Roja Formation. This is similar to what happens in the Pyrenean sections, where the first biotic traces appear abundantly just above the basal Triassic conglomerates (Mujal *et al.*, 2018a).

The palaeoecosystem represented in Estellencs Formation is certainly the richest of the ones of the continental Lower–Middle Triassic of Mallorca, with at least three recognisable trophic levels. In general terms, the heavily oxidised red-beds only preserve palaeosols, large plant fragments such as stems and logs and bioturbation traces produced by both invertebrates and vertebrates (Figures 4–5). In addition, some fine-grained beds deposited under reducing conditions enclose very well-preserved plant remains (leaves, branches, spores and pollen), clam shrimps, insects and, rarely, fishes and fish scales (Figures 6–9).

The plant remains found in Estellencs Formation suggest the presence of a hygrophitic local flora (Figure 12) and fragments from the hinterland conifer forests dragged and rapidly buried by sheetfloods. The species mentioned below are based on the review of the figures of Álvarez-Ramis *et al.* (1995) and Juárez-Ruiz & Wachtler (2015) (E. Kustatscher, pers. comm., 2021). Horsetails are represented by *Equisetites mougeotii* (*e.g.*, Álvarez-Ramis *et al.*, 1995: pl. 1, fig. 1), *Neocalamites merianii* (*e.g.*, Juárez-Ruiz & Wachtler, 2015: p. 31, fig. 6) and *Schizoneura paradoxa* (*e.g.*, Álvarez-Ramis *et al.*, 1995: pl. 1, fig. 3). Among the ferns, there are *Anomopteris mougeotii* (*e.g.*, Juárez-Ruiz & Wachtler, 2015: p. 34, fig. 1) and *Chiropteris digitata* (*e.g.*, Álvarez-Ramis *et al.*, 1995: pl. 1, fig. 8). In the case of non-arboreous conifers, *Aethophyllum stipulare* (*e.g.*, Juárez-Ruiz & Wachtler, 2015: p. 17, fig. 1), *Albertia latifolia* (*e.g.*, Juárez-Ruiz & Wachtler, 2015: p. 9, figs. 2–3) and *Pelourdea vogesiaca* (*e.g.*, Juárez-Ruiz & Wachtler, 2015: p. 34, fig. 2) have been identified. Arboreous conifers are represented by *Voltzia heterophylla* (*e.g.*, Juárez-Ruiz & Wachtler, 2015: p. 25, fig. 1) and *Voltzia walchiaeformis* (*e.g.*, Álvarez-Ramis *et al.*, 1995: pl. 2, fig. 4). Finally, among the different types of reproductive organs, there is one specimen assignable putatively to *Cycadocarpidium* sp. (*e.g.*, Álvarez-Ramis *et al.*, 1995: pl. 2, fig. 3) and numerous conifer cones of the species *Willsiostrobus acuminatus* (*e.g.*, Álvarez-Ramis *et al.*, 1995: pl. 2, fig. 1), *Willsiostrobus hexasacciphorus* (*e.g.*, Álvarez-Ramis *et al.*, 1995: pl. 2, fig. 7) and *Willsiostrobus rhomboidalis* (*e.g.*, Álvarez-Ramis *et al.*, 1995: pl. 2, fig. 8). These plant fossils are found in two different assemblages, also noted by Juárez-Ruiz & Wachtler (2015): green sandstones with *Equisetites mougeotii*, *Schizoneura paradoxa*, *Chiropteris digitata*, *Aethophyllum stipulare*, *Pelourdea vogesiaca*, *Voltzia* spp., *Willsiostrobus acuminatus* and *Willsiostrobus hexasacciphorus*, and white sandstones with abundant *Albertia latifolia*, accompanied by *Anomopteris mougeotii*,

Pelourdea vogesiaca, *Voltzia* spp., *Willsiostrobus rhomboidalis* and, rarely, *Neocalamites merianii*. Although both are located in the upper part of Estellencs Formation, the former assemblage probably corresponds to a relatively autochtonous, hygrophytic plant community developed on the river banks, whereas the latter were probably dragged by sheetfloods from further inland. Similar assemblages have been recognised in other European basins of a similar age (*e.g.*, Gall, 1971; Grauvogel-Stamm, 1978; Grauvogel-Stamm & Grauvogel, 1980; Kustatscher *et al.*, 2014; Borruel-Abadía *et al.*, 2015).

Decaying plant fragments that had fallen into the water bodies, together with algae, were probably consumed by the various arthropods found in Estellencs Formation. Modern clam shrimps are usually filter feeders, consuming plankton and organic detritus suspended in the water (*e.g.*, Dodson & Frey, 2001). Larger crustaceans, such as the notostracans, which probably produced the *Rusophycus-Cruziana-Diplichnites* traces, are nowadays grazers, detritivores, scavengers, and can also hunt small prey such as other arthropods and small vertebrates (*e.g.*, Dodson & Frey, 2001). Other bioturbation traces such as *Gordia* and *Skolithos* were made by indeterminate insect larvae, and thus will not be considered further in this discussion. Mayfly nymphs, recorded as body fossils in Estellencs Formation (Figure 12), can be assigned to different feeding guilds in aquatic environments such as detritivores, grazers and filter-feeders (Sinitshenkova *et al.*, 2005). Their abundance indicates that they were important components of the aquatic trophic net together with clam shrimps, similarly to the palaeoassemblages of the Triassic of the Vosges (Sinitshenkova *et al.*, 2005). Representatives of the terrestrial insect community, such as coleopterans (which are the purported producers of *Taenidium*) and cockroaches are either herbivorous or omnivorous. Other entomological remains found in this palaeoenvironment (Ansorge, 1997; Zessin, 2008a, 2008b; Aristov & Zessin, 2009) suggest a richer terrestrial insect community, but since no more specimens have been found for the present study and previous authors have generally offered only preliminary determinations, those will not be further assessed here.

In the aquatic environments, fishes were probably the main predators on invertebrates, although they could also feed on the terrestrial insects that reached the water surface, since the few terrestrial specimens (most likely para-autochthonous) are represented in the studied deposit by isolated wings. On land, small-sized diapsid reptiles (Figure 12), such as the ones that made the tracks studied herein, possibly preyed on the adult insects and other small animals. The trackmakers of *Rhynchosauroides* and *Prorotodactylus mesaxonichnus* are thought to have been small archosauromorphs such as tanystropheids or euparkeriids (Avanzini & Renesto, 2002; Mujal *et al.*, 2017b, 2018b), and some coeval body fossil genera such as *Macrocnemus* and *Euparkeria* have been inferred to have an insectivorous diet based on anatomical features (*e.g.*, Sookias & Butler, 2013; Rieppel, 2019), supporting our hypothesis. Triassic ichnoassemblages

dominated by small ichnites, such as the one studied herein, have been correlated to coastal settings and/or areas with presence of microbial mats (De Jaime-Soguero *et al.*, 2021). No structures diagnostic of marine influence have been recognised in Estellencs Formation, but wrinkle structures are indeed very common in the tetrapod footprint horizons, thus pointing to the presence of microbial mat development in the floodplain (Porada & Bouougri, 2007; Carmona *et al.*, 2011). It has been considered that under these conditions, larger tetrapods were at disadvantage when walking, as their feet would penetrate too deep in the substrate hindering their movement, and thus small footprints of lighter tetrapods are usually dominant (Mujal *et al.*, 2018b; De Jaime-Soguero *et al.*, 2021).

The palaeoecosystem recorded in Pedra Alta Formation is somewhat similar to that of the underlying Estellencs Formation, although fossil remains are much scarcer. Plant remains are usually preserved in the form of unidentifiable debris or large tree logs, although well-preserved *Neocalamites* stems were found *ex situ* (Juárez-Ruiz & Wachtler, 2015). Arthropods are represented by clam shrimps and scarce ephemeropterans, appearing together with rare fish scales. No macrofossils have been reported from Son Serralta Formation.

7.3. Palaeobiogeography

The rich palaeoecosystems preserved in the Lower–Middle Triassic formations of Mallorca show strong similarities with those of southern and central Europe, and secondarily also with North America and Asia, in the "*Voltzia* and *Pleuromeia* floras" of Dobruskina (1994) and the "N-American–Eurasian Fauna" of Romano *et al.* (2020). Plant fossils of Estellencs Formation, although comparatively poorly sampled, have the main components of fossil floras of similar age found in Iberia (*e.g.*, Diez *et al.*, 2010; Borruel-Abadía *et al.*, 2014), the Alpine region (*e.g.*, Dobruskina, 1994; Kustatscher *et al.*, 2004, 2007; Kustatscher & van Konijnenburg-van Cittert, 2005; van Konijnenburg-van Cittert *et al.*, 2006), the Vosges (*e.g.*, Gall, 1971; Grauvogel-Stamm, 1978; Dobruskina, 1994), and central Europe (*e.g.*, Dobruskina, 1994; Kustatscher *et al.*, 2014).

Clam shrimp assemblages of Estellencs and Pedra Alta formations, of carapace valve morphologies similar to *Hornestheria*, suggest a correlation to upper Olenekian–Anisian occurrences of this genus in central Europe and Asia (Kozur & Weems, 2010) and are different from those of the Vosges, dated as Bithynian (Gall, 1971; Kozur & Weems, 2010). Insect assemblages of Estellencs Formation are the second in importance based on mayfly abundance, just after those of the Vosges (Sinitshenkova *et al.*, 2005), with which they share at least two species of mayfly nymphs, *Triassoephemera punctata* and *Triassonurus doliiformis*.

Tetrapod ichnites, although scarce, are similar to those found in southern and central Europe and in southern North America, belonging to the N-American–Eurasian faunas of Romano *et al.* (2020). The ichnospecies *Prorotodactylus mesaxonichnus* had so far only been reported from the upper Olenekian–lower Anisian of the Pyrenean Basin (Mujal *et al.*, 2017b), but the morphologically similar ichnogenus *Gwynnedichnium* is known from the Anisian of central Europe and the Anisian–Rhaetian of southern North America (Lucas *et al.*, 2014; Klein & Lucas, 2018), and other ichnospecies of *Prorotodactylus* are known from the Olenekian of the Central European Basin (Niedźwiedzki *et al.*, 2013; Klein & Lucas, 2021). Conversely, the ichnogenus *Rhynchosauroides* has little palaeobiogeographic value because of its sub-cosmopolitan distribution (De Jaime-Soguero *et al.*, 2021 and references therein). These data are consistent with the abundance of archosauromorphs and lepidosauromorphs in the palaeoequatorial latitudes of Pangaea during the Early Triassic (Mujal *et al.*, 2017b; Romano *et al.*, 2020).

In summary, these facts indicate that, during the Early–Middle Triassic, the Iberian area was biogeographically well connected to central Europe (Vosges, Central European Basin) and therefore they suggest that there were no important barriers or strong climatic gradients between the two areas, especially in the distribution of floras and invertebrates. This implies that the Variscan orogen had little impact in the distribution of species or that there were corridors that made migration possible, and that Iberia (including Mallorca) and central Europe were under similar semi-arid climatic conditions, as suggested by Romano *et al.* (2020).

8. Conclusions

The present work provides, for the first time, a comprehensive and interdisciplinary characterisation of the palaeoecosystems of the Lower–Middle Triassic of Mallorca (Balearic Islands, western Mediterranean). Four lithostratigraphic units have been formally described, and are named, from lower to upper: Punta Roja Formation (shallow perennial braided rivers), Estellencs Formation (meandering rivers with a braided interval in the upper part), Pedra Alta Formation (braided rivers) and Son Serralta Formation (mud-flats with tidal influence). For all of them and based on a review of all the previous literature and new data, detailed stratigraphic, sedimentological and palaeoentological interpretations have been provided in order to reconstruct their ecosystems and their evolution over time.

The Lower–Middle Triassic sequence of Mallorca is reminiscent of those of eastern Iberian Peninsula, which represent more proximal deposits of the river systems that developed in the

different basins, and that flowed from the Iberian Massif (and Ebro High) towards the Tethys. The macroflora is comparable to those of other Anisian localities of the western peri-Tethys, and a review of the palynofloras makes it possible to date Estellencs and Pedra Alta formations in the Aegean (lower Anisian). The clam shrimp fauna from Estellencs Formation can be dated in the upper Olenekian–Anisian, and is biogeographically similar to other Eurasian palaeoassemblages. The insect fauna shows a diverse aquatic community, very similar to that of the Vosges, which is slightly younger (Bithynian) but palaeogeographically close (central Europe). Tetrapod ichnofaunas are also comparable to coeval assemblages of North America and Eurasia, and are especially similar to those of the Pyrenees and central Europe. Nevertheless, both the insect and vertebrate faunas seem to be not very diverse compared to other sites of similar age. In fact, the insect assemblage shows an overrepresentation of mayflies, both in number of specimens and different forms, and a notable paucity of terrestrial forms. In the case of tetrapod footprints, there is clear dominance of small-sized tracks, but more data is needed to elucidate whether it is just a product of sampling bias or is actually related to the palaeoenvironment.

In any case, the results of the present work indicate that ecosystems of palaeoequatorial Pangaea, such as Mallorca, showed strong signs of recovery from the Permian–Triassic mass extinction by the earliest Middle Triassic, presenting diverse and complex aquatic and terrestrial communities. Moreover, this work also suggests that although the biota of the continental Triassic of Mallorca was quite similar to that of nearby basins of similar age, the stratigraphic succession does not appear to reflect global patterns, but local particularities instead. This stresses the need for caution when interpreting global trends from regional successions, as the imprint of more geographically-limited causes may mask that of more widespread changes.

9. Acknowledgements

To Tomeu Sáez, Feliu Calafat, David Gómez-Gras and Antoni Rodríguez-Perea for their valuable insights and data on the outcrops they discovered and studied, and for providing bibliographic references. To Bernadí Gelabert for information and literature on the possible palaeogeographic position of Mallorca during the Triassic. To Sebastià Matamalas, Francesc Baiget, Eduardo Barrón, Ana Rodrigo and Enric Pedrón for aid in fieldwork. To Pedro Agustín Robledo, Ana Sevillano and José María López García, who facilitated the field and laboratory palaeontological research on Mallorca, and to Tomeu Sáez, who kindly travelled to Palma with his collection to allow that research. To Evelyn Kustatscher for the revision of the identifications of plant fossils figured by previous authors. To Fran Poyato for comments on the

indeterminate osteichthyan. To Llorenç Homar and Onofre Rullan for offering an insight into local toponymy. To Hendrik Klein and an anonymous reviewer for their insightful comments, that considerably improved the initial version of the manuscript, and to Christopher Fielding, editor, for handling the manuscript. To the Comissió Insular de Patrimoni Històric (Consell Insular de Mallorca, Spain) for granting us the excavation permits (file numbers 305/2019 and 52/2021). We acknowledge support from the CERCA program (Generalitat de Catalunya, Spain). R.M.A. was supported by the predoctoral grant FPU17/01922 (Ministerio de Ciencia, Innovación y Universidades, Spain). O.O. and À.G. are members of the consolidated research group 2017 SGR 1666 GRC (Generalitat de Catalunya, Spain). J.F. was supported by the Agencia Estatal de Investigación (Spain) and the European Regional Development Fund AEI/FEDER EU, project CGL2017-82654-P (European Union). J.F. is member of the consolidated research group 2017 SGR 086 GRC (Generalitat de Catalunya, Spain). We acknowledge support from the project "Mallorca abans dels dinosaures: estudi dels ecosistemes continentals del Permià i Triàsic amb especial èmfasi en les restes de vertebrats" (ref. 15 - 619/2020), based at the Institut Català de Paleontologia Miquel Crusafont and funded by the Departament de Cultura, Patrimoni i Política Lingüística (Consell Insular de Mallorca, Spain).

10. References

Alonso-Zarza, A.M. (2003). Palaeoenvironmental significance of palustrine carbonates and calcretes in the geological record. *Earth-Science Reviews*, 60: 261–298.

Álvarez-Ramis, C.; Solé, N. & Calafat, F. (1989). Paleoflora del Triásico inferior de Mallorca. *In*: *Abstracts of the II European Paleobotanical Conference*. Madrid: p. 12.

Álvarez-Ramis, C.; Fernández-Marrón, T. & Calafat, F. (1995). Avance sobre la megaflora triásica, en facies germánica, de Estellencs (sector noroccidental de la sierra de Tramontana, Mallorca). *Revista Española de Paleontología*, nº homenaje al Dr. Guillermo Colom: 55–58.

Ansorge, J. (1997). Insekten aus dem Buntsandstein (Untere Trias) von Mallorca (Spanien). *In*: *Abstracts für 4 Fachgespröch "Fossile Insekten"*. Clausthal-Zellerfeld, 28–29 Juni: 1 pp.

Arche, A. & López-Gómez, J. (1996). Origin of the Permian-Triassic Iberian Basin, central-eastern Spain. *Tectonophysics*, 266: 443–464.

Arche, A.; López-Gómez, J. & Vargas, H. (2002). Propuesta de correlación entre los sedimentos Pérmicos y Triásicos de la Cordillera Ibérica Este y de las Islas Baleares. *Geogaceta*, 32: 275–278.

Arche, A.; López-Gómez, J.; Marzo, M. & Vargas, H. (2004). The siliciclastic Permian-Triassic deposits in Central and Northeastern Iberian Peninsula (Iberian, Ebro and Catalan Basins): A proposal for correlation. *Geologica Acta*, 2(4): 306–320.

Aristov, D. & Zessin, W. (2009). *Mallorcagryllus hispanicus* n. get. et sp. - eine neue Grylloblattide (Insecta: Grylloblattida: Blattogryllidae) aus dem Buntsadstein der Insel Mallorca, Spanien. *Virgo, Mitteilungsblatt des Entomologischen Vereins Mecklenburg*, 12(1): 30–34.

Avanzini, M. & Renesto, S. (2002). A review of *Rhynchosauroides tirolicus* Abel, 1926 ichnospecies (Middle Triassic: Anisian-Ladinian) and some inference on *Rhynchosauroides* trackmaker. *Rivista Italiana di Paleontologia e Stratigrafia*, 108(1): 51–66.

Avanzini, M.; Bernardi, M. & Nicosia, U. (2011). The Permo-Triassic tetrapod faunal diversity in the Italian southern Alps. *In*: Ahmad Dar, I. (Ed.). *Earth and Environmental Sciences*: 591–608.

Barnolas, A. (1991a). *Mapa Geológico de España. Escala 1:50.000. Andraitx.* Segunda serie, primera edición. Instituto Tecnológico GeoMinero de España, Madrid. 56 pp. + 1 map + 5 stratigraphic logs.

Barnolas, A. (1991b). *Mapa Geológico de España. Escala 1:50.000. Sóller.* Segunda serie, primera edición. Instituto Tecnológico GeoMinero de España, Madrid. 62 pp. + 1 map + 8 stratigraphic logs.

Bashkuev, A.; Sell, J.; Aristov, D.; Ponomarenko, A.; Sinitshenkova, N. & Mahler, H. (2012). Insects from Buntsandstein of Lower Franconia and Thuringia. *Paläontologische Zeitschrift*, 86: 175–185.

Baucon, A.; Ronchi, A.; Felletti, F. & Neto de Carvalho, C. (2014). Evolution of Crustaceans at the edge of the end-Permian crisis: Ichnonetwork analysis of the fluvial succession of Nurra (Permian–Triassic, Sardinia, Italy). *Palaeogeography, Palaeoclimatology, Palaeoecology*, 410: 74–103.

Benton, M.J. (2008). *When life nearly died. The greatest mass extinction of all time*. Thames & Hudson, London. 336 pp.

Benton M.J. & Newell, A.J. (2014). Impacts of global warming on Permo-Triassic terrestrial ecosystems. *Gondwana Research*, 25: 1308–1337.

Bernardi, M.; Petti, F.M. & Benton, M.J. (2018). Tetrapod distribution and temperature rise during the Permian–Triassic mass extinction. *Proceedings of the Royal Society B*, 285: 20172331.

Béthoux, O.; De la Horra, R.; Benito, M.I.; Barrenechea, J.F.; Galán, A.B. & López-Gómez, J. (2009). A new triadotypomorphan insect from the Anisian (Middle Triassic), Buntsandstein facies, Spain. *Journal of Iberian Geology*, 35(2): 179–184.

Borruel-Abadía, V.; Galán-Abellán, A.B.; Kustatscher, E.; Diéguez, C.; López-Gómez, J.; De la Horra, R.; Barrenechea, J.F. & Arche, A. (2014). Palaeoenvironmental reconstruction of the early Anisian from sedimentology and plant remains in the SE Iberian Range (E Spain). *Palaeogeography, Palaeoclimatology, Palaeoecology*, 414: 352–369.

Borruel-Abadía, V.; López-Gómez, J.; De la Horra, R.; Galán-Abellán, B.; Barrenechea, J.F.; Arche, A.; Ronchi, A.; Gretter, N. & Marzo, M. (2015). Climate changes during the Early–Middle Triassic transition in the E. Iberian plate and their palaeogeographic significance in the western Tethys continental domain. *Palaeogeography, Palaeoclimatology, Palaeoecology*, 440: 671–689.

Borruel-Abadía, V.; Barrenechea, J.F.; Galán-Abellán, A.B.; Alonso-Azcárate, J.; De la Horra, R.; Luque, F.J. & López-Gómez, J. (2016). Quantifying aluminium phosphate–sulphate minerals as markers of acidic conditions during the Permian–Triassic transition in the Iberian Ranges, E Spain. *Chemical Geology*, 429: 10–20.

Borruel-Abadía, V.; Barrenechea, J.F.; Galán-Abellán, A.B.; De la Horra, R.; López-Gómez, J.; Ronchi, A.; Luque, F.J.; Alonso-Azcárate, J. & Marzo, M. (2019). Could acidity be the reason behind the Early Triassic biotic crisis on land? *Chemical Geology*, 515: 77–86.

Bourquin, S.; Durand, M.; Diez, J.B.; Broutin, J. & Fluteau, F. (2007). The Permian-Triassic boundary and Early Triassic sedimentation in Western European Basins: an overview. *Journal of Iberian Geology*, 33(2): 221–236.

Bourquin, S.; Bercovici, A.; López-Gómez, J.; Diez, J.B.; Broutin, J.; Ronchi, A.; Durand, M.; Arche, A.; Linol, B. & Amour, F. (2011). The Permian–Triassic transition and the onset of Mesozoic sedimentation at the northwestern peri-Tethyan domain scale: Palaeogeographic maps and geodynamic implications. *Palaeogeography, Palaeoclimatology, Palaeoecology*, 299: 265–280.

Bradshaw, M.A. (1981). Paleoenvironmental interpretations and systematics of Devonian trace fossils from the Taylor Group (lower Beacon Supergroup), Antarctica. *New Zealand Journal of Geology and Geophysics*, 24: 615–652.

Briere, P.R. (2000). Playa, playa lake, sabkha: proposed definitions for old terms. *Journal of Arid Environments*, 45: 1–7.

Brocklehurst, N.; Dunne, E.M.; Cashmore, D.D. & Fröbisch, J. (2018). Physical and environmental drivers of Paleozoic tetrapod dispersal across Pangaea. *Nature Communications*, 9: 5216.

Bromley, R. & Asgaard, U. (1979). Triassic freshwater ichnocoenoses from Carlsberg Fjord, East Greenland. *Palaeogeography, Palaeoclimatology, Palaeoecology*, 28: 39–80.

Buatois, L.A. & Mángano, M.G. (1998). Trace fossil analysis of lacustrine facies and basins. *Palaeogeography, Palaeoclimatology, Palaeoecology*, 140: 367–382.

Calafat, F. (1986). Estratigrafía y sedimentología de la litofacies Buntsandstein de Mallorca. *In*: Cabrera, L. (Ed.). *XI Congreso Español de Sedimentología. Libro de Resúmenes*: p. 39.

Calafat, F. (1987). Paleoambients de les facies Buntsandstein de Mallorca. *In*: *I Jornades del Medi Ambient de les Illes Balears. Llibre de Resums*: 16–17.

Calafat, F. (1988). *Estratigrafía y sedimentología de la litofacies Buntsandstein de Mallorca*. Bachelor's thesis. Universitat de Barcelona, Barcelona. 127 pp. + 31 annexed fig.

Calafat, F. & Sáez, B. (1987). Paleofauna lacustre del Triàsic Inferior de Mallorca. *In*: *I Jornades del Medi Ambient de les Illes Balears. Llibre de Resums*: 18–19.

Calafat, F.; Fornós, J.J.; Marzo, M.; Ramos, E. & Rodríguez-Perea, A. (1986). Icnología de vertebrados de las facies Buntsandstein de Mallorca. *In*: Cabrera, L. (Ed.). *XI Congreso Español de Sedimentología. Libro de Resúmenes*: p. 40.

Calafat, F.; Fornós, J.J.; Marzo, M.; Ramos-Guerrero, E. & Rodríguez-Perea, A. (1986–1987). Icnología de vertebrados de las facies Buntsandstein de Mallorca. *Acta Geològica Hispànica*, 21–22: 515–520.

Carmona, N.; Bournod, C.; Ponce, J.J. & Cuadrado, D. (2011). The role of microbial mats in the preservation of bird footprints: a case study from the mesotidal Bahía Blanca estuary (Argentina). *Society for Sedimentary Geology, Special Publication*, 101: 37–45.

Cassinis, G.; Durand, M. & Ronchi, A. (2003). Permian-Triassic continental sequences of northwest Sardinia and south Provence: stratigraphic correlations and palaeogeographical implications. *Bolletino della Società Geologica Italiana*, Volume speciale 2: 119–129.

Cassinis, G.; Perotti, C.R. & Ronchi, A. (2012). Permian continental basins in the Southern Alps (Italy) and peri-mediterranean correlations. *International Journal of Earth Sciences/GR Geologische Rundschau*, 101: 129–157.

Chang, W.-T.; Chen, P.-J. & Shen, Y.-B. (1976). *Fossil Conchostraca of China*. Science Press, Beijing. 325 pp. + 138 pls.

Chen, Z.-Q. & Benton, M.J. (2012). The timing and pattern of biotic recovery following the end-Permian mass extinction. *Nature Geoscience*, 5(6): 375–383.

Coleman, J.M. (1969). Brahmaputra river: channel processes and sedimentation. *Sedimentary Geology*, 3(2): 129–239.

Crimes, T.P. (1970). Trilobite tracks and other trace fossils from the Upper Cambrian of North Wales. *Geological Journal*, 7(1): 47–68.

Cuevas-López, F. (1958a). *Informe geológico y minero de los yacimientos de cobre de Banyalbufar y Estallenchs, Mallorca*. Barcelona. 37 pp. + 8 fig.

Cuevas-López, F. (1958b). *Informe geológico y minero de los yacimientos de cobre de Banyalbufar y Valldemosa, Mallorca*. Barcelona. 23 pp. + 7 fig.

d'Orbigny, A. (1842). *Voyage dans l'Amérique méridionale (le Brésil, la République Orientale de l'Uruguay, la République Argentine, la Patagonie, la République du Chili, la République de Bolivia, la République du Perou) exécuté pendant les années 1826, 1827, 1828, 1829, 1830, 1831, 1832 et 1833*. Pitois-Levrault, Paris & Levrault, Strasbourg, 3(4) (Paléontologie). 188 pp.

Davies, N.S. & Gibling, M.R. (2010). Paleozoic vegetation and the Siluro-Devonian rise of fluvial lateral accretion sets. *Geology*, 38(1): 51–54.

Davis, R.A., Jr. (2012). Tidal signatures and their preservation potential in stratigraphic sequences. *In*: Davis, R.A., Jr. & Dalrymple, R.W. (Eds.). *Principles of Tidal Sedimentology*. Springer, Dordrecht, Heidelberg, London, New York: 35–55.

Dawson, S.J.W. (1873). Impressions and footprints of aquatic animals and imitative markings on Carboniferous rocks. *American Journal of Science, 3rd series*, 5: 16–24.

De Jaime-Soguero, Ch.; Mujal, E.; Dinarès-Turell, J.; Oms, O.; Bolet, A.; Orlandi-Oliveras, G. & Fortuny, J. (2021). Palaeoecology of Middle Triassic tetrapod ichnoassociations (middle Muschelkalk, NE Iberian Peninsula) and their implications for palaeobiogeography in the western Tethys region. *Palaeogeography, Palaeoclimatology, Palaeoecology*, 565: 110204.

Diez, J.B. (2000). *Geología y Paleobotánica de la Facies Buntsandstein en la Rama Aragonesa de la Cordillera Ibérica. Implicaciones paleogeográficas en el Peritethys Occidental*. Ph.D. dissertation. Universidad de Zaragoza–Université Pierre & Marie Curie, Paris VI, Zaragoza & Paris. 424 pp.

Diez, J.B.; Broutin, J. & Ferrer, J. (2005). Difficulties encountered in defining the Permian–Triassic boundary in Buntsandstein facies of the western Peritethyan domain based on palynological data. *Palaeogeography, Palaeoclimatology, Palaeoecology*, 229: 40–53.

Diez, J.B.; Broutin, J.; Grauvogel-Stamm, L.; Bourquin, S.; Bercovici, A. & Ferrer, J. (2010). Anisian floras from the NE Iberian Peninsula and Balearic Islands: A synthesis. *Review of Palaeobotany and Palynology*, 162: 522–542.

Díez-Canseco, D.; Buatois, L.A.; Mángano, M.G.; Díaz-Molina, M. & Benito, M.I. (2016). Ichnofauna from coastal meandering channel systems (Upper Cretaceous Tremp Formation, South-Central Pyrenees, Spain): delineating the fluvial-tidal transition. *Journal of Paleontology*, 90(2): 250–268.

Dobruskina, I.A. (1994). Triassic floras of Eurasia. *In*: Zapfe, H. (Ed.). *Osterreichische Akademie der Wissenschaften Schriftenreihe der Erdwissenschaftlichen Kommissionen*, 10. Springer-Verlag, New York. 422 pp.

Dodson, S.I. & Frey, D.G. (2001). Cladocera and other branchiopoda. *In*: Thorp, J.H. & Covich, A.P. (Eds.). *Ecology and classification of North American freshwater invertebrates*. Academic Press, California: 849–913.

Durand, M. (2006). The problem of the transition from the Permian to the Triassic Series in southeastern France: comparison with other Peritethyan regions. *Geological Society, London, Special Publications*, 265: 281–296.

Ebisemiju, F.S. (1994). The sinuosity of alluvial river channels in the seasonally wet tropical environment: Case study of river Elemi, southwestern Nigeria. *Catena*, 21: 13–25.

Edel, J.B.; Schulmann, K.; Lexa, O. & Lardeaux, J.M. (2018). Late Palaeozoic palaeomagnetic and tectonic constraints for amalgamation of Pangea supercontinent in the European Variscan belt. *Earth-Science Reviews*, 177: 589–612.

Emmons, E. (1844). *The Taconic System: based on observations in New York, Massachusetts, Maine, Vermont, and Rhode Island*. Caroll and Cook, Albany. 68 pp.

Erwin, D.H. (1994). The Permo–Triassic extinction. *Nature*, 367: 231–236.

Escudero-Mozo, M.J.; Martín-Chivelet, J.; Goy, A. & López-Gómez, J. (2014). Middle-Upper Triassic carbonate platforms in Minorca (Balearic islands): Implications for Western Tethys correlations. *Sedimentary Geology*, 310: 41–58.

Ezcurra, M.D.; Fortuny, J.; Mujal, E. & Bolet, A. (2017). First direct archosauromorph remains from the Early-Middle Triassic transition of the Iberian Peninsula. *Palaeontologia Electronica*, 20.3.62A: 1–10.

Fillion, D. & Pickerill, R.K. (1990). Ichnology of the upper Cambrian? to Lower Ordovician Bell Island and Wabana groups of eastern Newfoundland, Canada. *Palaeontographica Canadiana*, 7: 1–119.

Fitzgerald, P.G. & Barrett, P.J. (1986). *Skolithos* in a Permian braided river deposit, southern Victoria Land, Antarctica. *Palaeogeography, Palaeoclimatology, Palaeoecology*, 52(3–4): 237–247.

Fortuny, J.; Bolet, A.; Sellés, A.G.; Cartanyà, J. & Galobart, À. (2011a). New insights on the Permian and Triassic vertebrates from the Iberian Peninsula with emphasis on the Pyrenean and Catalonian basins. *Journal of Iberian Geology*, 37(1): 65–86.

Fortuny, J.; Galobart, À. & De Santiesteban, C. (2011b). A new capitosaur from the Middle Triassic of Spain and the relationships within the Capitosauria. *Acta Palaeontologica Polonica*, 56(3): 553–566.

Fortuny, J.; Bolet, A.; Sellés, A.G. & Galobart, À. (2014). A potential record of a procolophonid parareptile from the Triassic of the Iberian Peninsula. *Geologica Acta*, 12(2): 121–126.

Franzel, M.; Jones, S.J.; Meadows, N.; Allen, M.B.; McCaffrey, K. & Morgan, T. (2021). Basin-scale fluvial correlation and response to the Tethyan marine transgression: An example from the Triassic of central Spain. *Basin Research*, 33(1): 1–25.

Frizon de Lamotte, D.; Fourdan, B.; Leleu, S.; Leparmentier, F. & de Clarens, P. (2015). Style of rifting and stages of Pangea breakup. *Tectonics*, 34: 1009–1029.

Galán-Abellán, A.B.; Barrenechea, J.F.; Benito, M.I.; De la Horra, R.; Luque, F.J.; Alonso-Azcárate, J.; Arche, A.; López-Gómez, J. & Lago, M. (2013b). Palaeoenvironmental implications of aluminium phosphate-sulphate minerals in Early–Middle Triassic continental sediments, SE Iberian Range (Spain). *Sedimentary Geology*, 289: 169–181.

Galán-Abellán, A.B.; Alonso-Azcárate, J.; Newton, R.J.; Bottrell, S.H.; Barrenechea, J.F.; Benito, M.I.; De la Horra, R.; López-Gómez, J. & Luque, J. (2013c). Sources of Sr and S in aluminum-phosphate–sulfate minerals in Early–Middle Triassic sandstones (Iberian Ranges, Spain) and paleoenvironmental implications for the West Tethys. *Journal of Sedimentary Research*, 83: 406–426.

Galán-Abellán, B.; López-Gómez, J.; Barrenechea, J.F.; Marzo, M.; De la Horra, R. & Arche, A. (2013a). The beginning of the Buntsandstein cycle (Early–Middle Triassic) in the Catalan Ranges, NE Spain: Sedimentary and palaeogeographic implications. *Sedimentary Geology*, 296: 86–102.

Gall, J.-C. (1971). Faunes et paysages du Grès à *Voltzia* du nord des Vosges. Essai paléoécologique sur le Buntsandstein supérieur. *Service de la Carte Géologique d'Alsace et de Lorraine*, 34: 1–318.

Gallemí, J.; Riba, O.; Reguant, S.; Agustí, J.; Álvarez, G.; Calzada, S.; Caus, M.; López, C.; Martinell, J.; Martínez, R.; Martínez, X.; Porta, J. de; Sanz de Siria, A.; Solé, N.; Truyols, J.; Truyols, M. & Via, Ll. (Eds.). *Història Natural dels Països Catalans, 15: Registre Fòssil.* Enciclopèdia Catalana, Barcelona. 478 pp.

Gaigalas, A. & Uchman, A. (2004). Trace fossils from Upper Pleistocene varved clays S of Kaunas, Lithuania. *Geologija*, 45: 16–26.

Gand, G.; Demathieu, G. & Montenat, C. (2007). Les traces de pas d'amphibiens, de dinosaures et autres reptiles du Mesozoïque français: inventaire et interpretations. *Palaeovertebrata*, 2007(1–4): 1–149.

Gand, G.; Garric, J.; Schneider, J.; Walter, H.; Lapeyrie, J.; Martin, C. & Thiery, A. (2008). Notostraca trackways in Permian playa environments of the Lodève basin (France). *Journal of Iberian Geology*, 34(1): 73–108.

Gerstaecker, A. (1866–1879). Die Klassen und Ordnungen der Arthropoden wissenschaftlich dargestellt in Wort und Bild. Erste Abtheilung Crustacea (Erste Hälfte). *In*: Bronn, H.G. (Ed.). *Die Klassen und Ordnungen des Thier-Reichs wissenschaftlich dargestellt in Wort und Bild. Fünfter Band Gliederfüssler (Arthropoda).* C.F. Winter, Leipzig & Heidelberg. 1320 pp.

Getty, P.R.; Sproule, R.; Stimson, M.R. & Lyons, P.C. (2017). Invertebrate trace fossils from the Pennsylvanian Rhode Island Formation of Massachusetts, USA. *Atlantic Geology*, 53: 185–206.

Gevers, T.W.; Frakes, L.A.; Edwards, L.N. & Marzolf, J.E. (1971). Trace fossils in the lower Beacon sediments (Devonian), Darwin Mountains, southern Victoria Land, Antarctica. *Journal of Paleontology*, 45(1): 81–94.

Ghinassi, M.; Oms, O.; Cosma, M.; Finotello, A. & Munari, G. (2021). Reading tidal processes where their signature is cryptic: The Maastrichtian meandering channel deposits of the Tremp Formation (Southern Pyrenees, Spain). *Sedimentology*, 68(5): 2009–2042.

Glennie, K.W. (1970). *Desert sedimentary environments*. Developments in sedimentology, 14. Elsevier, Amsterdam, London, New York. 222 pp. + 4 maps.

Gómez-Gras, D.M. (1992). *El Permotrías de las Baleares, de la Cordillera Costero Catalana y de la vertiente mediterránea de la Cordillera Ibérica: Facies y Petrología Sedimentaria*. Ph.D. dissertation. Universitat Autònoma de Barcelona, Barcelona. XIX + 242 pp. + 55 fig. + 7 tab.

Gómez-Gras, D. (1993). El Permotrías de las Baleares y de la vertiente mediterránea de la Cordillera Ibérica y del Maestrat: Facies y Petrología Sedimentaria (Parte II). *Boletín Geológico y Minero*, 104: 467–515.

Gómez-Gras, D. & Alonso-Zarza, A.M. (2003). Reworked calcretes: their significance in the reconstruction of alluvial sequences (Permian and Triassic, Minorca, Balearic Islands, Spain). *Sedimentary Geology*, 158: 299–319.

Grauvogel-Stamm, L. (1978). La flore du Grès à *Voltzia* (Buntsandstein supérieur) des Vosges du Nord (France). Morphologie, anatomie, interpretations phylogénique et paléogéographique. *Sciences Géologiques, bulletins et mémoires*, 50: 1–225 + 54 pl.

Grauvogel-Stamm, L. & Grauvogel, L. (1980). Morphologie et anatomie d'*Anomopteris mougeotii* Brongniart (synonyme : *Pecopteris sulziana* Brongniart), une fougère du Buntsandstein supérieur des Vosges (France). *Sciences Géologiques Bulletin*, 33(1): 56–66.

Grauvogel-Stamm, L. & Álvarez-Ramis, C. (1994). Macroflore et microflore in situ du Buntsandstein de l'île de Majorque (Baléares, Espagne). *In*: *III Coloquio de Estratigrafía y Paleogeografía del Pérmico y Triásico de España. Resúmenes*. Cuenca, 27–29 Junio 1994: 51–53.

Grauvogel-Stamm, L. & Álvarez-Ramis, C. (1996). Conifères et pollen in situ du Buntsandstein de l'île de Majorque (Baléares, Espagne). *Cuadernos de Geología Ibérica*, 20: 229–243.

Gretter, N.; Ronchi, A.; López-Gómez, J.; Arche, A.; De la Horra, R.; Barrenechea, J. & Lago, M. (2015). The Late Palaeozoic-Early Mesozoic from the Catalan Pyrenees (Spain): 60 Myr of environmental evolution in the frame of the western peri-Tethyan palaeogeography. *Earth-Science Reviews*, 150: 679–708.

Haldeman, S.S. (1840). *Supplement to Number one of "A monograph of the* Limniades, *or Freshwater Unicarapace valve Shells of North America," containing descriptions of*

apparently new animals in different classes, and the names and characters of the subgenera in Paludina *and* Anculosa. J. Dobson, Philadelphia. 3 pp.

Hall, J. (1852). *Palaeontology of New York. Volume II. Containing descriptions of the organic remains of the Lower Middle Division of the New York System, (Equivalent in part to the Middle Silurian rocks of Europe)*. C. van Benthuysen, Albany & New York. 362 pp.

Hammersburg, S.R.; Hasiotis, S.T. & Robison, R.A. (2018). Ichnotaxonomy of the Cambrian Spence Shale Member of the Langston Formation, Wellsville Mountains, Northern Utah, USA. *Paleontological Contributions*, 20: 1–66.

Han, Y. & Pickerill, R.K. (1995). Taxonomic review of the ichnogenus *Helminthopsis* Heer 1877 with a statistical analysis of selected ichnospecies. *Ichnos*, 4: 83–118.

Hasiotis, S.T.; Platt, B.F.; Hembree, D.I. & Everhart, M.J. (2007). The Trace-Fossil Record of Vertebrates. *In*: William Miller, III (Ed.). *Trace Fossils: Concepts, Problems, Prospects*. Elsevier: 196–218.

Haubold, H. (1971). Die Tetrapodenfährten des Buntsandsteins in der Deutschen Demokratische Republik und in Westdeutschland und ihre Äquivalente in der gesamten Trias. *Paläontologische Abhandlungen, Abteilung A*, 4(3): 395–660.

Heer, O. (1876–1877). *Flora fossilis Helvetiae. Die vorweltliche Flora der Schweiz*. Verlag J. Wurster & Co., Zürich. 182 pp. [Parts 1, 2 (1876):1–90; Parts 3, 4 (1877): 91–182]

Hminna, A.; Lagnaoui, A.; Zouheir, T.; Saber, H. & Schneider, J.W. (2020). Late Triassic ichnoassemblage from a playa-lake system of the Coastal Meseta, Morocco: Palaeoenvironmental and palaeoecological implications. *Journal of African Earth Sciences*, 172: 103995.

Hofmann, H.J. & Patel, I.M. (1989). Trace fossils from the type "Etchemnian Series" (Lower Cambrian Ratcliffe Brook Formation), Saint John area, New Brunswick, Canada. *Geological Magazine*, 126: 139–157.

Homar, Ll. (1985). *Toponímia del litoral de la costa d'Estellencs, Banyalbufar i Valldemossa: de na Foradada a sa Foradada*. 7 aerial photographs.

Hounslow, M.W. & Ruffell, A.H. (2006). Triassic: seasonal rivers, dusty deserts and saline lakes. *In*: Brenchley, P.J. & Rawson, P.F. (Eds.). *The Geology of England and Wales*. Geological Society of London, London: 295–324.

Huisink, M. (2000). Changing river styles in response to Weichselian climate changes in the Vecht valley, eastern Netherlands. *Sedimentary Geology*, 133: 115–134.

Hyatt, A. & Arms, J.M. (1891). A novel diagrammatic representation of the orders of insects. *Psyche*, 6(177): 11–13.

IDEIB (2019). *Infraestuctura de dades espacials de les Illes Balears*. Conselleria d'Agricultura, Medi Ambient i Territori. Govern de les Illes Balears. http://www.ideib.cat (last accessed on 26/07/2019).

Irving, E. (2004). The case for Pangea B, and the intra-Pangean megashear. *Geophysical Monograph*, 145: 13–27.

Juárez-Ruiz, J. & Wachtler, M. (2015). Early–middle Triassic (Anisian) fossil flora from Majorca (Spain). *Dolomythos*, 2015: 1–49.

Juncal, M.; Diez, J.B.; De la Horra, R.; Galán-Abellán, B.; Borruel-Abadía, V.; Barrenechea, J.F.; Arche, A. & López-Gómez, J. (2017). Palynostratigraphy of the Middle Triassic (Anisian) Eslida Formation, SE Iberian Ranges, Spain. *Palynology*, 42(2): 149–157.

Klein, H. & Haubold, H. (2007). Archosaur footprints – potential for biochronology of Triassic continental sequences. *New Mexico Museum of Natural History and Science Bulletin*, 41: 120–130.

Klein, H. & Lucas, S.G. (2010a). Review of the tetrapod ichnofauna of the Moenkopi Formation/Group (Early-Middle Triassic) of the American Southwest. *New Mexico Museum of Natural History and Science Bulletin*, 50: 1–67.

Klein, H. & Lucas, S.G. (2010b). Tetrapod footprints – their use in biostratigraphy and biochronology of the Triassic. *Geological Society, London, Special Publications*, 334: 419–446.

Klein, H. & Niedźwiedzki, G. (2012). Revision of the Lower Triassic tetrapod ichnofauna from Wióry, Holy Cross Mountains, Poland. *New Mexico Museum of Natural History and Science Bulletin*, 56: 1–62.

Klein, H.; Voigt, S.; Saber, H.; Schneider, J.W.; Hminna, A.; Fischer, J.; Lagnaoui, A. & Brosig, A. (2011). First occurrence of a Middle Triassic tetrapod ichnofauna from the Argana Basin (Western High Atlas, Morocco). *Palaeogeography, Palaeoclimatology, Palaeoecology*, 307: 218–231.

Klein, H. & Lucas, S.G. (2018). Diverse Middle Triassic tetrapod footprints assemblage from the Muschelkalk of Germany. *Ichnos*, 25: 162–176.

Klein, H. & Lucas, S.G. (2021). The Triassic tetrapod footprint record. *New Mexico Museum of Natural History and Science Bulletin*, 83: 1–194.

Kozur, H. (1982). Beiträge zur Taxonomie und stratigraphischen Auswertung der untertriassischen Conchostracen. *Geologisch-Paläontologische Mitteilungen Innsbruck*, 11(11): 355–398.

Kozur, H.W. & Weems, R.E. (2010). The biostratigraphic importance of conchostracans in the continental Triassic of the northern hemisphere. *Geological Society, London, Special Publications*, 334: 315–417.

Kozur, H.W.; Mahler, H. & Sell, J. (1993). Stratigraphic and paleobiologic importance of the latest Olenekian and Early Anisian conchostracans of Middle Europe. *New Mexico Museum of Natural History and Science Bulletin*, 3: 255–259.

Kustatscher, E. & van Konijnenburg-van Cittert, J.H.A. (2005). The Ladinian flora (Middle Triassic) of the Dolomites: palaeoenvironmental reconstructions and palaeoclimatic considerations. *Geo.Alp*, 2: 31–51.

Kustatscher, E.; Wachtler, M. & van Konijnenburg-van Cittert, J.H.A. (2004). A number of additional and revised taxa from the Ladinian flora of the Dolomites, northern Italy. *Geo.Alp*, 1: 57–69.

Kustatscher, E.; Wachtler, M. & van Konijnenburg-van Cittert, J.H.A. (2007). Horsetails and seed ferns from the Middle Triassic (Anisian) locality Kühwiesenkopf (Monte Prà della Vacca), Dolomites, northern Italy. *Palaeontology*, 50(5): 1277–1298.

Kustatscher, E.; Franz, M.; Heunisch, C.; Reich, M. & Wappler, T. (2014). Floodplain habitats of braided river systems: depositional environment, flora and fauna of the Solling Formation (Buntsandstein, Lower Triassic) from Bremke and Fürstenberg (Germany). *Palaeodiversity and Palaeoenvironments*, 94 (2): 237–270.

Labandeira, C.C. (2005). The fossil record of insect extinction: new approaches and future directions. *American Entomologist*, 51(1): 14–29.

Lago, M.; De la Horra, R.; Ubide, T.; Galé, C.; Galán-Abellán, B.; Barrenechea, J.F.; López-Gómez, J.; Benito, M.I.; Arche, A.; Alonso-Azcárate, J.; Luque, F.J. & Timmerman, M.J. (2012). First report of a Middle-Upper Permian magmatism in the SE Iberian Ranges: characterisation and comparison with coeval magmatisms in the western Tethys. *Journal of Iberian Geology*, 38(2): 331–348.

Leonardi, G. (1987). *Glossary and Manual of Tetrapod Footprint Palaeoichnology*. Departamento Nacional de Produção Mineral, Brasilia. 117 pp.

Linol, B.; Bercovici, A.; Bourquin, S.; Diez, J.B.; López-Gómez, J.; Broutin, J.; Durand, M. & Villanueva-Amadoz, U. (2009). Late Permian to Middle Triassic correlations and palaeogeographical reconstructions in south-western European basins: New sedimentological data from Minorca (Balearic Islands, Spain). *Sedimentary Geology*, 220: 77–94.

Lonergan, L. & White, N. (1997). Origin of the Betic-Rif mountain belt. *Tectonics*, 16(3): 504–522.

López-Gómez, J. (1985). *Sedimentología y estratigrafía de los materiales pérmicos y triásicos del sector SE. de la rama castellana de la cordillera Ibérica entre cueva de Hierro y Chelva (provincias de Cuenca y Valencia)*. Seminarios de Estratigrafía, 11. Universidad Complutense de Madrid & Consejo Superior de Investigaciones Científicas, Madrid. 344 pp.

López-Gómez, J. & Arche, A. (1992). Paleogeographical significance of the Röt (Anisian, Triassic) Facies (Marines clays, muds and marls Fm.) in the Iberian ranges, eastern Spain. *Palaeogeography, Palaeoclimatology, Palaeoecology*, 91: 347–361.

López-Gómez, J.; Arche, A. & Pérez-López, A. (2002). Permian and Triassic. *In*: Gibbons, W. & Moreno, M.T. (Eds.). *The Geology of Spain*. Geological Society, London: 185–212.

López-Gómez, J.; Galán-Abellán, B.; De la Horra, R.; Barrenechea, J.F.; Arche, A.; Bourquin, S.; Marzo, M. & Durand, M. (2012). Sedimentary evolution of the continental Early–Middle Triassic Cañizar Formation (Central Spain): Implications for life recovery after the Permian–Triassic crisis. *Sedimentary Geology*, 249–250: 26–44.

López-Gómez, J.; Alonso-Azcárate, J.; Arche, A.; Arribas, J.; Fernández-Barrenechea, J.; Borruel-Abadía, V.; Bourquin, S.; Cadenas, P.; Cuevas, J.; De la Horra, R.; Díez, J.B.; Escudero-Mozo, M.J.; Fernández-Viejo, G.; Galán-Abellán, B.; Galé, C.; Gaspar-Escribano, J.; Gisbert-Aguilar, J.; Gómez-Gras, D.; Goy, A.; Gretter, N.; Heredia-Carballo, N.; Lago, M.; Lloret, J.; Luque, J.; Márquez, L.; Márquez-Aliaga, A.; Martín-Algarra, A.; Martín-Chivelet, J.; Martín-González, F.; Marzo, M.; Mercedes-Martín, R.; Ortí, F.; Pérez-López, A.; Pérez-Valera, F.; Pérez-Valera, J.A.; Plasencia, P.; Ramos, E.; Rodríguez-Méndez, L.; Ronchi, A.; Salas, R.; Sánchez-Fernández, D.; Sánchez-Moya, Y.; Sopeña, A.; Suárez-Rodríguez, Á.; Tubía, J.M.; Ubide, T.; Valero-Garcés, B.; Vargas, H. & Viseras, C. (2019a). Permian-Triassic rifting stage. *In*: Vergés, J. & Kullberg, J.C. (Coord.). *The Geology of Iberia: A Geodynamic Approach. Volume 3: The Alpine Cycle*. Springer, Cham: 29–112.

López-Gómez, J.; Martín-González, F.; Heredia, N.; De la Horra, R.; Barrenechea, J.F.; Cadenas, P.; Juncal, M.; Diez, J.B.; Borruel-Abadía, V.; Pedreira, D.; García-Sansegundo, J.; Farias, P.; Galé, C.; Lago, M.; Ubide, T.; Fernández-Viejo, G. & Gand, G. (2019b). New lithostratigraphy for the Cantabrian Mountains: a common tectono-stratigraphic evolution for the onset of the Alpine cycle in the W Pyrenean realm, N Spain. *Earth-Science Reviews*, 188: 249–271.

Lucas, S.G. (2019). An ichnological perspective on some major events of Paleozoic tetrapod evolution. *Bollettino della Società Paleontologica Italiana*, 58(3): 223–266.

Lucas, S.G.; Spielmann, J.A.; Klein, H. & Lerner, A.J. (2010). Ichnology of the Upper Triassic (Apachean) Redonda Formation, east-central New Mexico. *New Mexico Museum of Natural History and Science Bulletin*, 47: 3–75.

Lucas, S.G.; Szajna, M.J.; Lockley, M.G.; Fillmore, D.L.; Simpson, E.L.; Klein, H.; Boyland, J. & Hartline, B.W. (2014). The Middle-Late Triassic tetrapod footprint ichnogenus *Gwyneddichnium*. *New Mexico Museum of Natural History and Science Bulletin*, 62: 135–156.

Mack, G.H.; James, W.C. & Monger, H.C. (1993). Classification of paleosols. *Geological Society of America Bulletin*, 105: 129–136.

MacLeod, K.G.; Quinton, P.C. & Bassett, D.J. (2017). Warming and increased aridity during the earliest Triassic in the Karoo Basin, South Africa. *Geology*, 45(6): 483–486.

Maidwell, F.T. (1911). Notes on footprints from the Keuper of Runcorn Hill. *Proceedings of the Liverpool Geological Society*, 11: 140–152.

Matamales-Andreu, R.; Oms, O.; Galobart, À. & Fortuny, J. (in press). Middle–Upper Triassic marine vertebrates of Mallorca (Balearic Islands, western Mediterranean). *Historical Biology*: https://doi.org/10.1080/08912963.2020.1810682

Matesanz-Yagüe, J. (1987). Estudio sedimentológico de las facies Buntsandstein en el extremo NW. de la rama castellana de la cordillera Ibérica (prov. de Soria). *Estudios Geológicos*, 43: 79–94.

Martí, J.; Paniello, X.; Pomar, L.; Ramos, E. & Rodríguez-Perea, A. (1985). El Triásico de las Baleares. *In*: Mateu Ibars, F. & Marzo, M. (Eds.). *II Coloquio de Estratigrafía y Paleogeografía del Pérmico y Triásico de España.* La Seu d'Urgell, 23–25 Septiembre 1985. Libro de Resúmenes: 84–85.

Marzo, M. (1980). *El Buntsandstein de los Catalánides: estratigrafía y procesos de sedimentación*. Ph.D. dissertation. Universitat de Barcelona, Barcelona. 317 pp. + 12 pls.

Marzo, M. (1986). Secuencias fluvio-eólicas en el Buntsandstein del macizo del Garraf (provincia de Barcelona). *Cuadernos de Geología Ibérica*, 10: 207–233.

McCann, T.; Pascal, C.; Timmerman, M.j.; Krzywiec, P.; López-Gómez, J.; Wetzel, A.; Krawczyk, C.M.; Rieke, H. & Lamarche, J. (2006). Post-Variscan (end Carboniferous–Early Permian) basin evolution in Western and Central Europe. *Geological Society, London, Memoirs*, 32: 355–388.

Melchor, R.N. & De Valais, S. (2006). A review of Triassic tetrapod track assemblages from Argentina. *Palaeontology*, 49(2): 355–379.

Miall, A.D. (1977). A review of the braided-river depositional environment. *Earth-Science Reviews*, 13: 1–62.

Miall, A.D. (1985). Architectural-Element Analysis: a new method of facies analysis applied to fluvial deposits. *Earth-Science Reviews*, 22: 261–308.

Miall, A.D. (2006). *The Geology of Fluvial Deposits: Sedimentary Facies, Basin Analysis, and Petroleum Geology*. 4th ed. Springer, Berlin, Heidelberg, New York. 582 pp.

Michaelsen, P. (2002). Mass extinction of peat-forming plants and the effect on fuvial styles across the Permian–Triassic boundary, northern Bowen Basin, Australia. *Palaeogeography, Palaeoclimatology, Palaeoecology*, 179: 173–188.

Minter, N.J.; Krainer, K.; Lucas, S.G.; Braddy, S.J. & Hunt, A.P. (2007). Palaeoecology of an Early Permian playa lake trace fossil assemblage from Castle Peak, Texas, USA. *Palaeogeography, Palaeoclimatology, Palaeoecology*, 246: 390–423.

Mujal, E.; Gretter, N.; Ronchi, A.; López-Gómez, J.; Falconnet, J.; Diez, J.B.; De la Horra, R.; Bolet, A.; Oms, O.; Arche, A.; Barrenechea, J.F.; Steyer, J.-S. & Fortuny, J. (2016).

Constraining the Permian/Triassic transition in continental environments: Stratigraphic and palaeontological record from the Catalan Pyrenees (NE Iberian Peninsula). *Palaeogeography, Palaeoclimatology, Palaeoecology*, 445: 18–37.

Mujal, E.; Fortuny, J.; Bolet, A.; Oms, O. & López, J.A. (2017a). An archosauromorph dominated ichnoassemblage in fluvial settings from the late Early Triassic of the Catalan Pyrenees (NE Iberian Peninsula). *PLoS ONE*, 12(4): e0174693.

Mujal, E.; Fortuny, J.; Pérez-Cano, J.; Dinarès-Turell, J.; Ibáñez-Insa, J.; Oms, O.; Vola, I.; Bolet, A. & Anadón, P. (2017b). Integrated multi-stratigraphic study of the Coll de Terrers late Permian–Early Triassic continental succession from the Catalan Pyrenees (NE Iberian Peninsula): A geologic reference record for equatorial Pangaea. *Global and Planetary Change*, 159: 46–60.

Mujal, E.; Belaústegui, Z.; Fortuny, J.; Bolet, A.; Oms, O. & López, J.A. (2018a). Ichnological evidence of a horseshoe crab hot-spot in the Early Triassic Buntsandstein continental deposits from the Catalan Pyrenees (NE Iberian Peninsula). *Journal of Iberian Geology*, 44: 139–153.

Mujal, E.; Iglesias, G.; Oms, O.; Fortuny, J.; Bolet, A. & Méndez, J.M. (2018b). *Rhynchosauroides* footprint variability in a Muschelkalk detrital interval (late Anisian–middle Ladinian) from the Catalan Basin (NE Iberian Peninsula). *Ichnos*, 25(2–3): 150–161.

Mujal, E.; Marchetti, L.; Schoch, R.R. & Fortuny, J. (2020). Upper Paleozoic to lower Mesozoic tetrapod ichnology revisited: photogrammetry and relative depth pattern inferences on functional prevalence of autopodia. *Frontiers in Earth Science*, 8:248.

Nagtegaal, P.J.C. (1969). Sedimentology, paleoclimatology, and diagenesis of post-Hercynian continental deposits in the south-central Pyrenees, Spain. *Leidse Geologische Mededelingen*, 42: 143–238.

Narkiewicz, K. & Szulc, J. (2004). Controls on migration of conodont fauna in peripheral oceanic areas. An example from the Middle Triassic of the Northern Peri-Tethys. *Geobios*, 37: 425–436.

Niedźwiedzki, G.; Brusatte, S.L. & Butler, R.J. (2013). *Prorotodactylus* and *Rotodactylus* tracks: an ichnological record of dinosauromorphs from the Early–Middle Triassic of Poland. *Geological Society, London, Special Publications*, 379: 319–351.

Nio, S.-D. & Yang, C.-S. (1991). Diagnostic attributes of clastic tidal deposits: a review. *Canadian Society of Petroleum Geologists*, 16: 3–28.

Ortí, F.; Salvany, J.M.; Rosell, L.; Castelltort, X.; Inglès, M. & Playà, E. (2018). Middle Triassic evaporite sedimentation in the Catalan basin: Implications for the paleogeographic evolution in the NE Iberian platform. *Sedimentary Geology*, 374: 158–178.

Ortí, F.; Guimerà, J. & Götz, A.E. (2020). Middle-Upper Triassic stratigraphy and structure of the Alt Palància (eastern Iberian Chain): A multidisciplinary approach. *Geologica Acta*, 18(4): 1–25.

Papier, F. & Grauvogel-Stamm, L. (1995). Les Blattodea du Trias: le genre *Voltziablatta* n.gen. du Buntsandstein supérieur des Vosges (France). *Palaeontographica A*, 235(4/6): 141–162.

Parés, J.M.; Freeman, R. & Roca, E. (1992). Neogene structural development in the Valencia trough margins from palaeomagnetic data. *Tectonophysics*, 203: 111–124.

Parrish, J.T. (1993). Climate of the supercontinent Pangea. *Journal of Geology*, 101: 215–233.

Péron, S.; Bourquin, S.; Fluteau, F. & Guillocheau, F. (2005). Paleoenvironment reconstructions and climate simulations of the Early Triassic: Impact of the water and sediment supply on the preservation of fluvial systems. *Geodinamica Acta*, 18(6): 431–446.

Pickerill, R.K. & Peel, J.S. (1991). *Gordia nodosa* isp. nov. and other traces from the Cass Fjord Formation (Cambrian) of North Greenland. *Rapport Grønlands Geologiske Undersøgelse*, 150: 15–28.

Pomar-Gomà, L. (1979). *The Triassic of the Balearic Islands*. Geology Department, Palma de Mallorca University, Palma. 49 pp. + 7 Petrologic Logs.

Porada, H. & Bouougri, E.H. (2007). Wrinkle structures—a critical review. *Earth-Science Reviews*, 81(3–4): 199–215.

Postma, G. (1990). Depositional architecture and facies of river and fan deltas: a synthesis. *Special Publications of the International Association of Sedimentologists*, 10: 13–27.

Ramos, A. (1979). *Estratigrafía y paleogeografía del Pérmico y Triásico al Oeste de Molina de Aragón (prov. de Guadalajara)*. Seminarios de Estratigrafía, 6. Universidad Complutense de Madrid & Consejo Superior de Investigaciones Científicas, Madrid. 313 pp.

Ramos, A. (1995). Transition from alluvial to coastal deposits (Permian–Triassic) on the Island of Mallorca, western Mediterranean. *Geological Magazine*, 132(4): 435–447.

Ramos, A.; Olmo, P. del & Alvaro, M. (1985). El Buntsandstein de la isla de Mallorca. *In*: Mateu Ibars, F. & Marzo, M. (Eds.). *II Coloquio de Estratigrafía y Paleogeografía del Pérmico y Triásico de España*. La Seu d'Urgell, 23–25 Septiembre 1985. Libro de Resúmenes: 103–104.

Ramos, E. & Rodríguez-Perea, A. (1985). Découverte d'un affleurement de terrains paléozoïques dans l'île de Majorque (Baléares, Espagne). *Comptes Rendus de l'Académie des Sciences de Paris*, 2nd series, 16, 301: 1205–1207.

Ratcliffe, B.C. & Fagerstrom, J.A. (1980). Invertebrate lebensspuren of Holocene floodplains: their morphology, origin and paleoecological significance. *Journal of Paleontology*, 54(3): 614–630.

Raymond, P.E. (1946). The genera of fossil Conchostraca – An order of bivalved crustaceans. *Bulletin of the Museum of Comparative Zoology*, 96: 217–370.

Reolid, J.; Cardenal, F.J.; Reolid, M. & Mata, E. (2020). 3D imaging of the southernmost Triassic footprints from Europe (southern Spain). *Journal of Iberian Geology*, 46: 145–161.

Retallack, G.J.; Veevers, J.J. & Morante, R. (1996). Global coal gap between Permian–Triassic extinction and Middle Triassic recovery of peat-forming plants. *Bulletin of Geological Society of America*, 108: 195–207.

Rieppel, O. (2019). *Mesozoic sea dragons: Triassic marine life from the ancient tropical lagoon of Monte San Giorgio*. Indiana University Press, Indiana. 256 pp.

Robles, S. & Llompart, C. (1987). Análisis paleogeográfico y consideraciones paleoicnológicas del Pérmico superior y Triásico Inferior en la transversal del río Segre (Alt Urgell, pirineo de Lérida). *Cuadernos de Geología Ibérica*, 11: 115–130.

Roca, E. (1992). *L'estructura de la conca Catalano-Balear: paper de la compressió i de la distensió en la seva gènesi*. Ph.D. dissertation. Universitat de Barcelona, Barcelona. 564 pp. [Volume 1: 1–330; Volume 2: 206 figs. + 5 seismic profiles].

Rodríguez-Perea, A. & Ramos, E. (1984). Presencia de Paleozoico en la Sierra de Tramuntana (Mallorca). *Bolletí de la Societat d'Història Natural de Balears*, 28: 145–148.

Rodríguez-Perea, A.; Ramos-Guerrero, E.; Pomar, L.; Paniello, X.; Obrador, A. & Martí, J. (1987). El Triásico de las Baleares. *Cuadernos de Geología Ibérica*, 11: 295–321.

Romano, M.; Bernardi, M.; Petti, F.M.; Rubidge, B.; Hancox, J. & Benton, M.J. (2020). Early Triassic terrestrial tetrapod fauna: a review. *Earth-Science Reviews*, 210: 103331.

Rowntree, K.M. & Dollar, E.S.J. (1999). Vegetation controls on channel stability in the Bell River, Eastern Cape, South Africa. *Earth Surface Processes and Landforms*, 24: 127–134.

Rüffer, T. & Zühlke, R. (1994). Sequence stratigraphy and sea-level changes in the Early to Middle Triassic of the Alps: a global comparison. *In*: Haq, B.U. (Ed.). *Sequence stratigraphy and depositional response to eustatic, tectonic and climatic forcing*. Springer: 161–207.

Sàbat, F.; Gelabert, B. & Rodríguez-Perea, A. (2018). Minorca, an exotic Balearic island (western Mediterranean). *Geologica Acta*, 16(4): 411–426.

Scholze, F. & Schneider, J.W. (2015). Improved methodology of 'conchostracan' (Crustacea: Branchiopoda) classification for biostratigraphy. *Newsletters on Stratigraphy*, 48: 287–298.

Scholze, F. & Matamales-Andreu, R. (2021). Triassic clam shrimps ("Conchostraca"; Branchiopoda: Diplostraca) from Mallorca: Taxonomic description and interregional comparisons. *Zootaxa*, 4964(3): 471–496.

Scotese, C.R. (2014). Atlas of Middle & Late Permian and Triassic Paleogeographic Maps, maps 43 – 48 from Volume 3 of the PALEOMAP Atlas for ArcGIS (Jurassic and Triassic) and maps 49 – 52 from Volume 4 of the PALEOMAP Atlas for ArcGIS (Late Paleozoic), Mollweide Projection, PALEOMAP Project, Evanston, IL.

Scotese, C.R. & Schettino, A. (2017). Late Permian-Early Jurassic paleogeography of western Tethys and the world. *In*: Soto, J.I.; Flinch, J.F. & Tari, G. (Eds.). *Permo-Triassic salt provinces of Europe, North Africa and the Atlantic margins. Tectonics and hydrocarbon potential*. Elsevier, Amsterdam, Oxford and Cambridge: 57–95.

Sevillano, A. & Barnolas, A. (2019). Mapa Geológico Digital Continuo E. 1:50.000, Zona Mallorca (Zona-2210). *In*: GEODE. Mapa Geológico Digital continuo de España. Available online at: http://info.igme.es/visorweb/ (last accessed on 26/07/2019).

Shanley, K.W.; McCabe, P.J. & Hettinger, R.D. (1992). Tidal influence in Cretaceous fluvial strata from Utah, USA: a key to sequence stratigraphic interpretation. *Sedimentology*, 39: 905–930.

Shcherbakov, D.E.; Lukashevich, E.D. & Blagoderov, V.A. (1995). Triassic Diptera and initial radiation of the order. *Journal of Dipterological Research*, 6(2): 75–115.

Shiers, M.N.; Mountney, N.P.; Hodgson, D.M. & Colombera, L. (2018). Controls on the depositional architecture of fluvial point-bar elements in a coastal-plain succesion. *International Association of Sedimentologists Special Publications*, 48: 15–46.

Sinitshenkova, N.D. (2000). A review of Triassic mayflies, with the description of new species from Western Siberia and Ukraine (Ephemerida = Ephemeroptera). *Paleontological Journal*, 34(3): S275–S283.

Sinitshenkova, N.D. (2002). New Late Mesozoic mayflies from the Shar-Teeg Locality, Mongolia (Insecta, Ephemerida=Ephemeroptera). *Paleontological Journal*, 36(3): 270–276.

Sinitshenkova, N.D.; Marchal-Papier, F.; Grauvogel-Stamm, L. & Gall, J.-C. (2005). The Ephemeridea (Insecta) from the Grès à Voltzia (early Middle Triassic) of the Vosges (NE France). *Paläontologische Zeitschrift*, 79/3: 377–397.

Smith, J.J.; Hasiotis, S.T.; Kraus, M.J. & Woody, D.T. (2008). *Naktodemasis bowni*: new ichnogenus and ichnospecies for adhesive meniscate burrows (AMB), and paleoenvironmental implications, Paleogene Willwood Formation, Bighorn Basin, Wyoming. *Journal of Paleontology*, 82(2): 267–278.

Sookias, R.B. & Butler, R.J. (2013). Euparkeriidae. *Geological Society, London, Special Publications*, 379: 35–48.

Soria, A.R.; Liesa, C.L.; Rodríguez-López, J.P.; Meléndez, N.; de Boer, P.L. & Meléndez, A. (2011). An Early Triassic evolving erg system (Iberian Chain, NE Spain): palaeoclimate implications. *Terra Nova*, 23: 76–84.

Stampfli, G.M. & Hochard, C. (2009). Plate tectonics of the Alpine realm. *Geological Society, London, Special Publications*, 327: 89–111.

Stanley, K.O. & Fagerstrom, J.A. (1974). Miocene invertebrate trace fossils from a braided river environment, western Nebraska, U.S.A. *Palaeogeography, Palaeoclimatology, Palaeoecology*, 15(1): 63–82.

Sun, Y.; Joachimski, M.M.; Wignall, P.B.; Yan, C.; Chen, Y.; Jiang, H.; Wang, L. & Lai, X. (2012). Lethally hot temperatures during the Early Triassic greenhouse. *Science*, 338(6105): 366–370.

Tabor, N.J. & Poulsen, C.J. (2008). Palaeoclimate across the Late Pennsylvanian–Early Permian tropical palaeolatitudes: a review of climate indicators, their distribution, and relation to palaeophysiographic climate factors. *Palaeogeography, Palaeoclimatology, Palaeoecology*, 268: 293–310.

Trotter, J.A.; Williams, I.S.; Nicora, A.; Mazza, M. & Rigo, M. (2015). Long-term cycles of Triassic climate change: a new δ^{18}O record from conodont apatite. *Earth and Planetary Science Letters*, 415: 165–174.

Uchman, A.; Kazakauskas, V. & Gaigalas, A. (2009). Trace fossils from Late Pleistocene varved lacustrine sediments in eastern Lithuania. *Palaeogeography, Palaeoclimatology, Palaeoecology*, 272: 199–211.

Van Konijnenburg-van Cittert, J.H.A.; Kustatscher, E. & Wachtler, M. (2006). Middle Triassic (Anisian) ferns from Kühwiesenkopf (Monte Prá Della Vacca), Dolomites, Northern Italy. *Palaeontology*, 49(5): 943–968.

Vera, J.-A.; Alonso-Chaves, F.M.; Andreo, B.; Arias, C.; Azañón, J.M.; Balanyá, J.C.; Barón, A.; Booth-Rea, G.; Castro, J.M.; Chacón, B.; Company, M.; Crespo-Blanc, A.; Delgado, F.; Díaz de Federico, A.; Esteras, M.; Estévez, A.; Fernández, J.; Fornós, J.J.; Galindo-Zaldívar, J.; García-Casco, A.; García-Dueñas, V.; García-Hernández, M.; Garrido, C.J..; Gea, G.A. de; Gelabert, B.; Gervilla, F.; González-Lodeiro, F.; Jabaloy, A.; López-Garrido, A.C.; Luján, M.; Martín-Algarra, A.; Martín-Chivelet, J.; Martín-Martín, M.; Molina, J.M.; Morata, D.; Nieto, J.M.; Obrador, A.; O'Dogherty, L.; Orozco, M.; Pérez-López, A.; Pomar, L.; Puga, E.; Ramos, E.; Rey, J.; Rivas, P.; Rodríguez-Cañero, R.; Ruiz-Cruz, M.D.; Ruiz-Ortiz, P.A.; Sàbat, F.; Sánchez-Gómez, M.; Sánchez-Navas, A.; Sandoval, J.; Sanz de Galdeano, C.; Soto, J.I.; Torres-Roldán, R.L. & Villas, L. (2004). Cordillera Bética y Baleares. *In*: Vera, J.-A. (Ed.). *Geología de España*. IGME, Madrid: 346–464.

Vila, B.; Oms, O.; Fondevilla, V.; Gaete, R.; Galobart, À.; Riera, V. & Canudo, J.I. (2013). The latest succession of dinosaur tracksites in Europe: hadrosaur ichnology, track production and palaeoenvironments. *PLoS ONE*, 8(9): e72579.

Williams, P.F. & Rust, B.R. (1969). The sedimentology of a braided river. *Journal of Sedimentary Petrology*, 39(2): 649–670.

Xing, L. & Klein, H. (2021). *Chirotherium* and first Asian *Rhynchosauroides* tetrapod trackways from the Middle Triassic of Yunnan, China. *Historical Biology*, 33(6): 791–801.

Zeng, Z.; Zhu, H.; Yang, X.; Zeng, H.; Hu, X. & Xia, C. (2019). The Pangaea megamonsoon records: evidence from the Triassic Mungaroo Formation, northwest shelf of Australia. *Gondwana Research*, 69: 1–24.

Zessin, W. (2008a). Einige neue Insekten aus der Unteren Trias (Buntsandstein) von Mallorca, Spanien (Blattaria, Coleoptera, Diptera, Heteroptera und Megaloptera). *Deutschen Gesellschaft für allgemeine und angewandte Entomologie – Nachrichten*, 22(1): 20–21.

Zessin, W. (2008b). Neue Insekten aus der Unteren Trias (Buntsadstein) von Mallorca, Spanien (Blattaria, Coleoptera, Diptera, Heteroptera, Orthopteroidea und Homoptera). *Virgo, Mitteilungsblatt des Entomologischen Vereins Mecklenburg*, 11(1): 99–101.

Żyła, D.; Wegierek, P.; Krzysztof, O. & Niedźwiedzki, G. (2013). Insects and crustaceans from the latest Early–early Middle Triassic of Poland. *Palaeogeography, Palaeoclimatology, Palaeoecology*, 371: 136–144.

Figures and tables

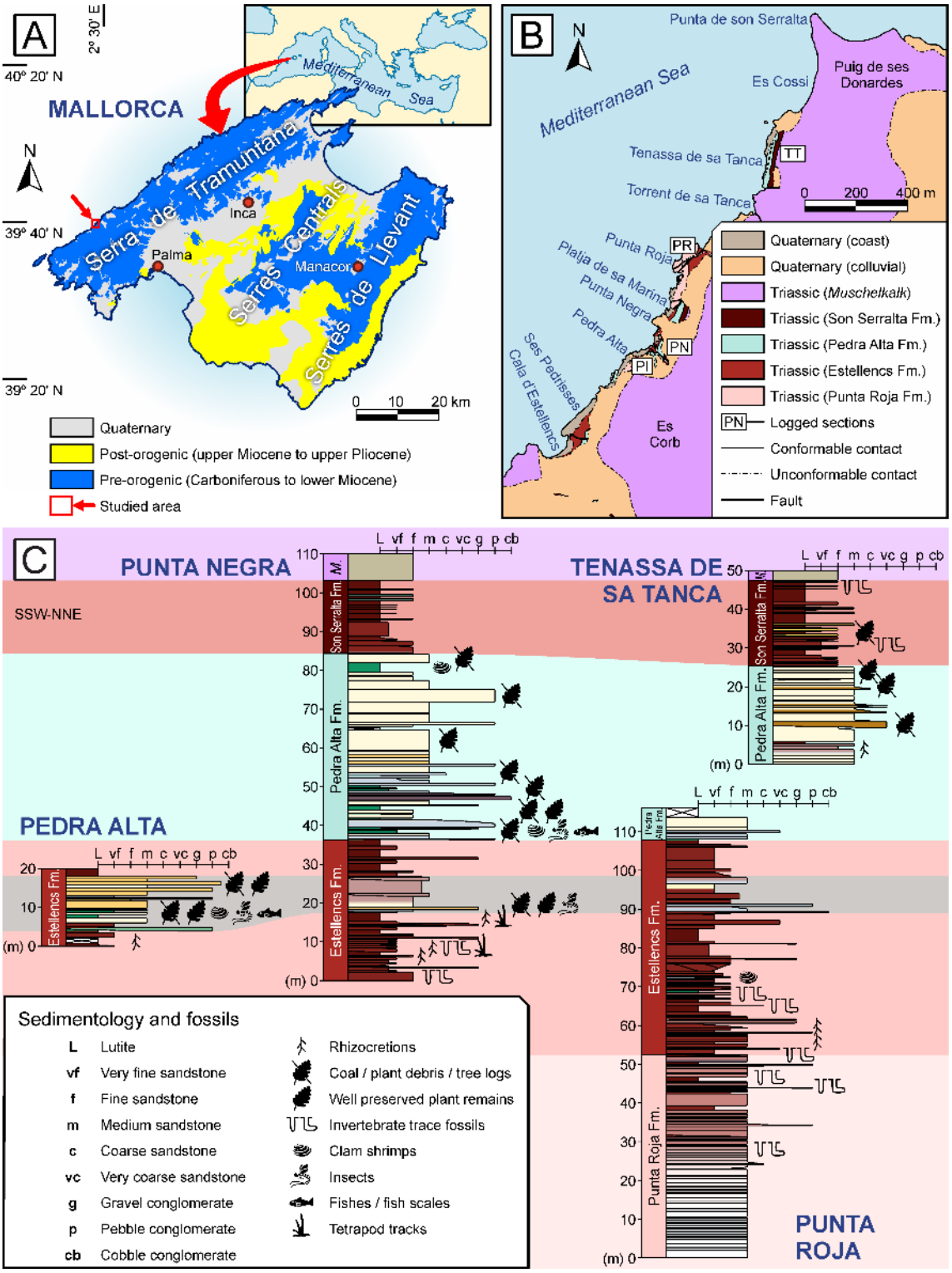

Figure 1. A: Synthetic geological map of the island of Mallorca (Balearic Islands), with position of the study area (red rectangle and arrow). Simplified from Sevillano & Barnolas (2019). **B:** Detailed geological map of the outcrops between Cala d'Estellencs and Punta de son Serralta (Estellencs, Mallorca), with indication of the location of the four confected logs (PI:

Pedra Alta; PN: Punta Negra; PR: Punta Roja; TT: Tenassa de sa Tanca). Toponyms after Homar (1985) and IDEIB (2019). **C:** Correlation of the four synthetic stratigraphic logs of the Lower–Middle Triassic red-beds of Mallorca (detailed stratigraphic logs are included in Supplementary Logs). Changes of the background colour represent boundaries between formations or particular units, which have been used as datums to correlate the logs.

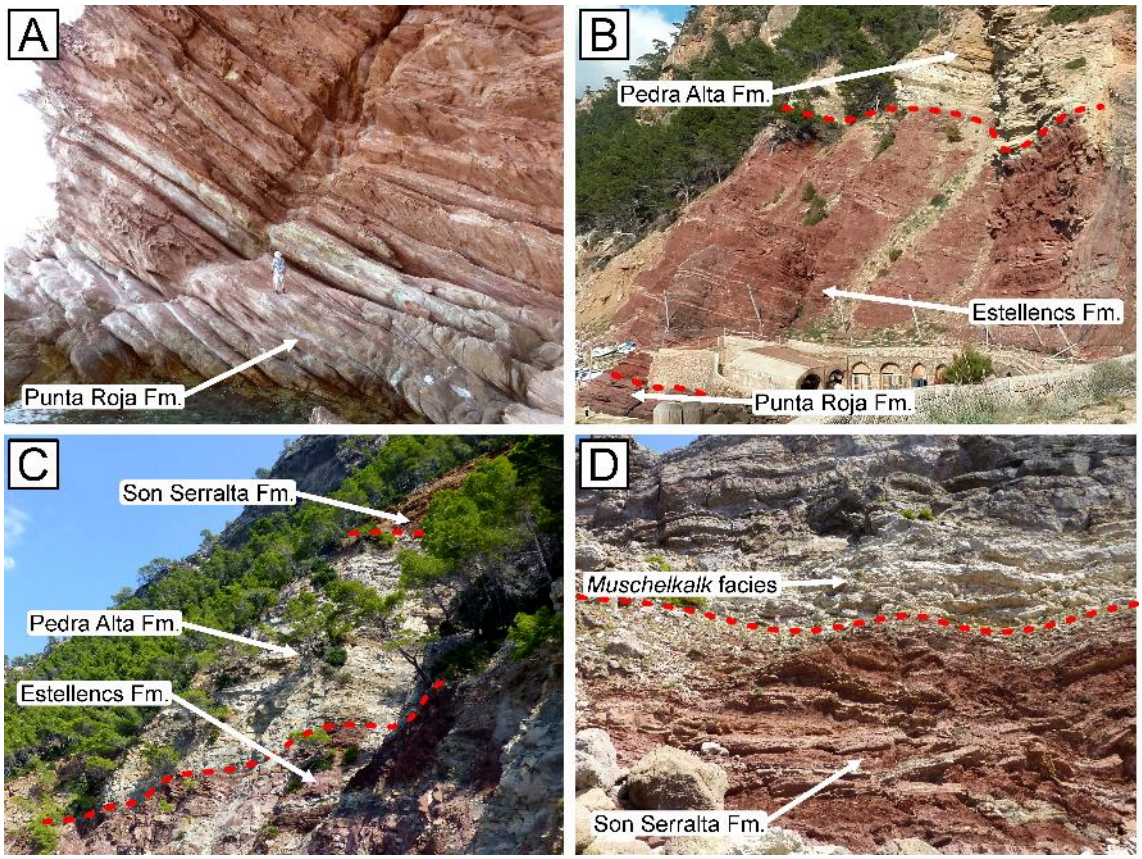

Figure 2. Representative views of the studied formations and their boundaries. **A:** Panoramic view of Punta Roja, showing the typical facies assemblage of Punta Roja Formation. **B:** Panoramic view of Cala d'Estellencs, showing the upper and lower boundaries of Estellencs Formation. **C:** Panoramic view of the ravine between Pedra Alta and Punta Negra, showing the upper and lower boundaries of Pedra Alta Formation. **D:** Panoramic view of the cliffs at Tenassa de sa Tanca, showing the upper boundary of Son Serralta Formation. Dashed red lines mark the boundaries between formations.

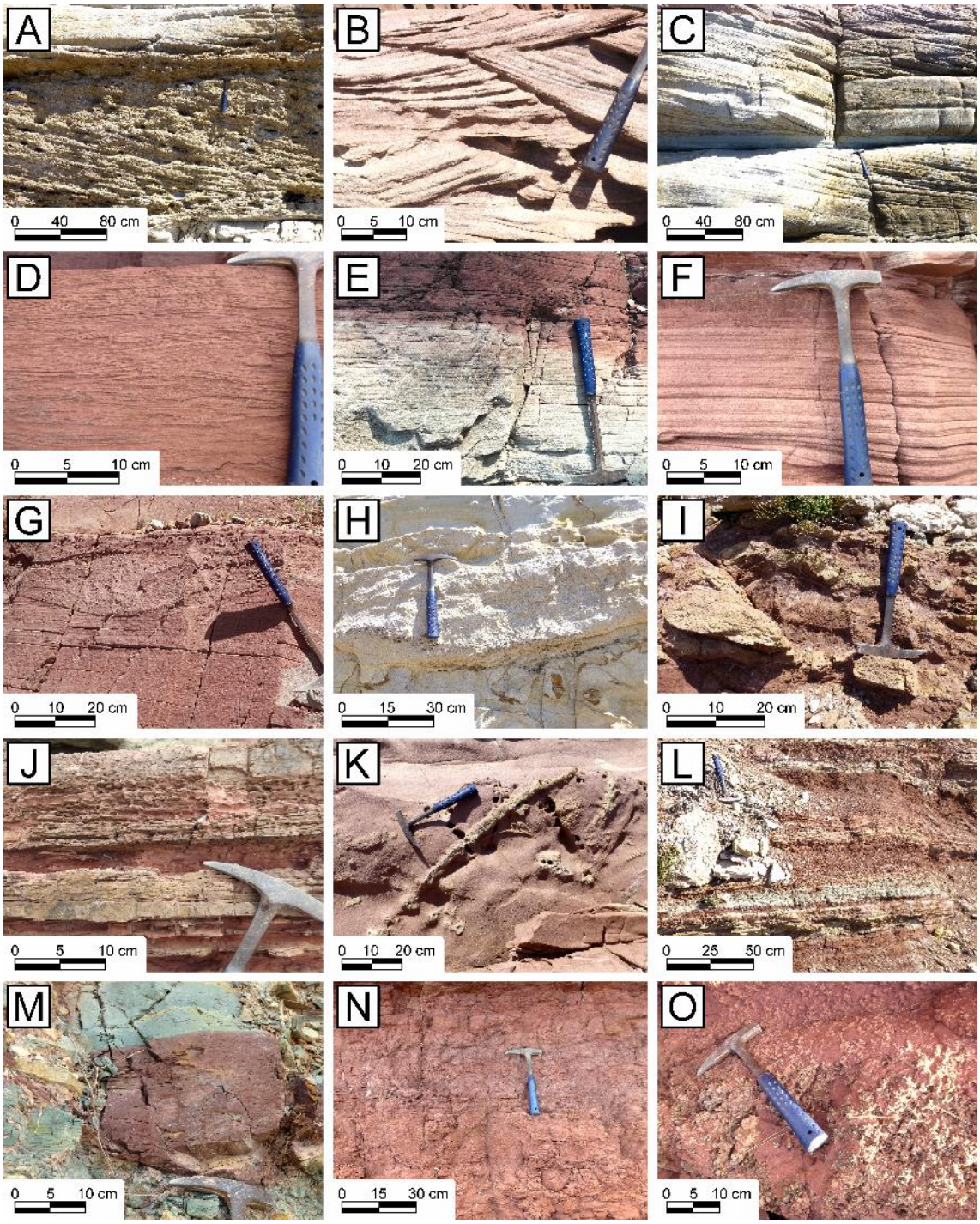

Figure 3. Photographic examples of each of the recognised lithofacies. **A:** Breccias with trough cross-bedding (*Gt*), Pedra Alta Formation. **B:** Sandstone with trough cross-bedding (*St*), Punta Roja Formation. **C:** Sandstone with planar cross-bedding (*Sp*), Pedra Alta Formation. **D:** Sandstone with ripple cross-lamination (*Sr*), Estellencs Formation. **E:** Sandstone with horizontal bedding (*Sh*), Estellencs Formation. **F:** Sandstone with low angle cross-bedding (*Sl*), Pedra Alta Formation. **G:** Sandstone infilling a scour (*Ss*), Estellencs Formation. **H:** Massive sandstone (*Sm*), Pedra Alta Formation. **I:** Massive yellowish and irregular sandstone (*Sm*), Son Serralta Formation. **J:** Sandstone with burrows (*Sb*), Estellencs Formation. **K:** Sandstone with root

traces (*Sb*), Pedra Alta Formation. **L:** Sandstones with interbedded lutites (*Si*), Son Serralta Formation. **M:** Laminated lutites (*Fl*), Estellencs Formation. **N:** Massive lutites (*Fm*), Estellencs Formation. **O:** Palaeosols (*P*), in this case a Calcisol, Estellencs Formation.

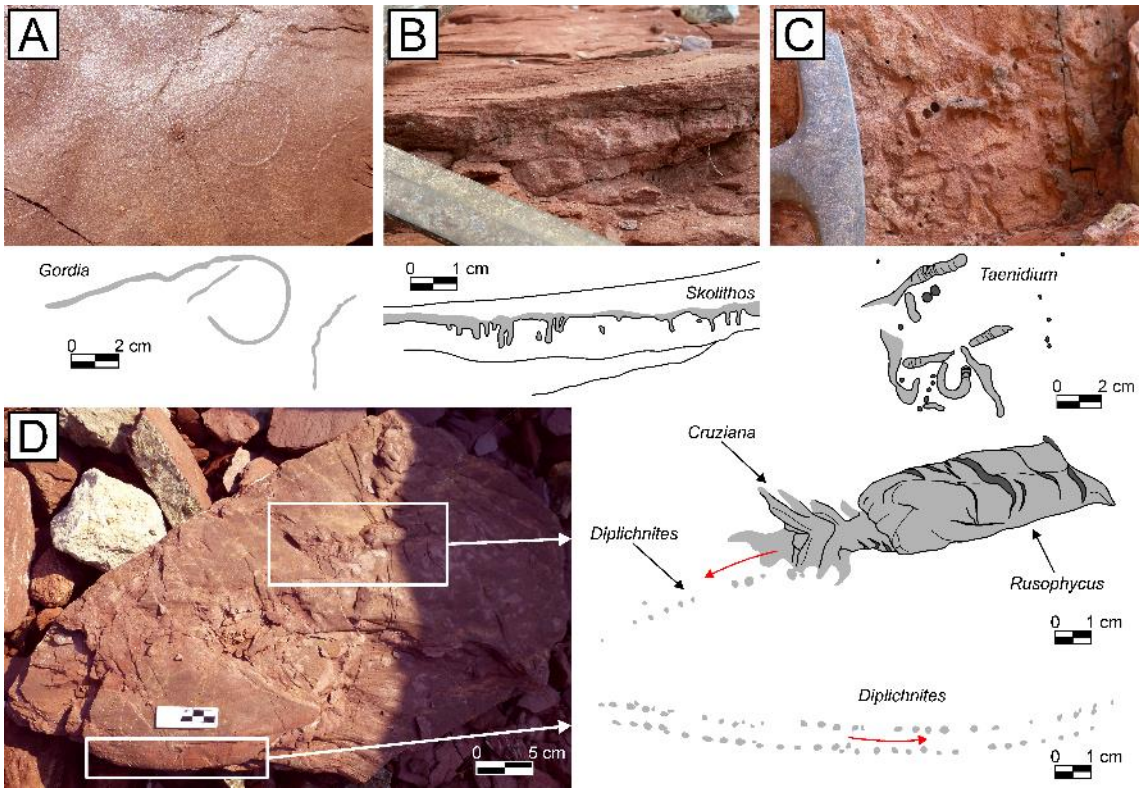

Figure 4. Field photographs and schematic drawings of the studied invertebrate trace fossils from Punta Negra and Punta Roja sections, middle part of Estellencs Formation, Aegean. **A:** *Gordia* isp., Punta Negra. **B:** *Skolithos* isp., Punta Negra. **C:** *Taenidium* isp. cf. *T. barretti*, Punta Roja. **D:** *Rusophycus* isp. - *Cruziana* isp. - *Diplichnites* isp. cf. *D. gouldi*, Punta Negra. Red arrows in D represent direction of movement.

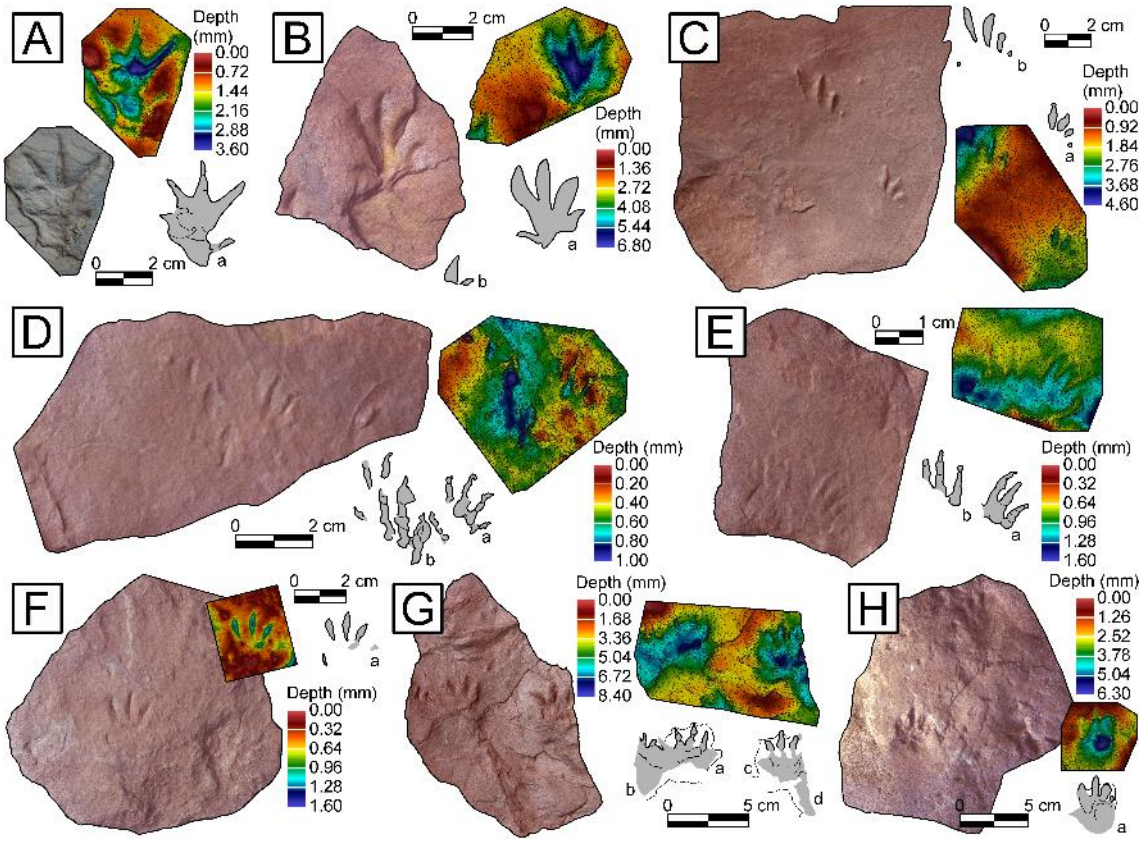

Figure 5. Textured 3D models, false colour-coded depth maps and schematic drawings of the studied ichnites from Punta Negra section and its lateral equivalent at Platja de sa Marina, middle part of Estellencs Formation, Aegean. **A:** *Rhynchosauroides* isp. 1, PN-7.6?-01, Punta Negra. **B:** *Rhynchosauroides* isp. 1, PN-14.7-01, Platja de sa Marina. **C:** *Rhynchosauroides* isp. 2, PN-7.6?-03, Punta Negra. **D:** *Prorotodactylus mesaxonichnus*, PN-14.6-02, Platja de sa Marina. **E:** cf. *Prorotodactylus mesaxonichnus*, PN-14.6-03, Platja de sa Marina. **F:** cf. *Prorotodactylus mesaxonichnus*, PN-14.6-01, Platja de sa Marina. **G:** Indeterminate morphotype, PN-7.6-01, Punta Negra. **H:** Indeterminate morphotype, PN-7.6?-02, Punta Negra. See Supplementary Table 2 for measurements.

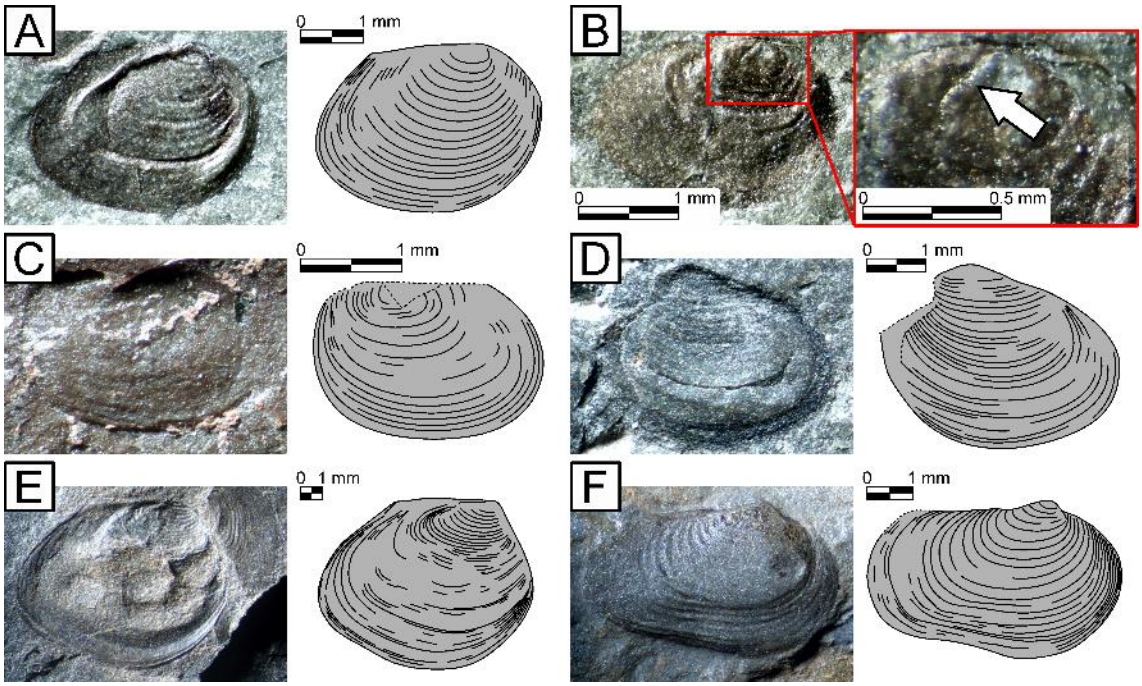

Figure 6. Photographs and schematic drawings of the different forms of studied clam shrimp ("conchostracan") carapace valves. **A:** *Hornestheria* sp. aff. *Ho. sollingensis*, DA21/03-02-58, Aegean, Pedra Alta. **B:** *Hornestheria* sp. aff. *Ho. sollingensis*, DA21/03-02-81, Aegean, Pedra Alta. **C:** "Conchostraca" indet., DA21/03-01-01a, Aegean, Punta Roja. **D:** "Conchostraca" indet., DA21/03-03-02, Aegean, ravine between Pedra Alta and Punta Negra. **E:** *Hornestheria*? sp. indet. morphotype 1, DA21/03-04-11, lower–middle? Anisian, ravine between Pedra Alta and Punta Negra. **F:** *Hornestheria*? sp. indet. morphotype 2, DA21/03-04-07-1b, lower–middle? Anisian, ravine between Pedra Alta and Punta Negra. White arrow in **B** indicates sculpture on the larval carapace valve.

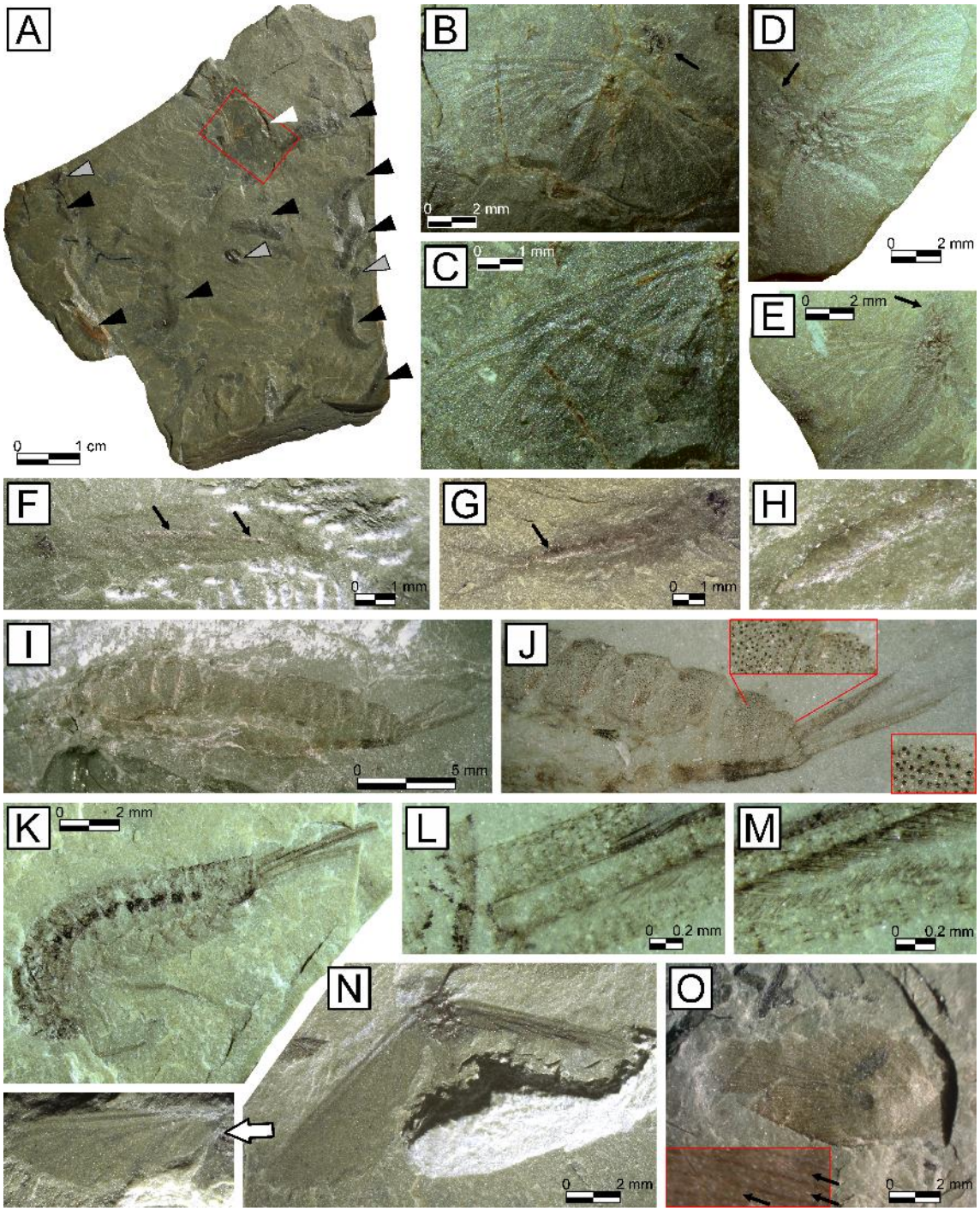

Figure 7. Insects from Pedra Alta section, upper part of Estellencs Formation, Aegean. **A:** Slab TS-D, showing mayflies (white arrowhead indicates an adult specimen, and black arrowheads indicate nymphs) and clam shrimps (some of them marked with grey arrowheads). **B–C:** *Hammephemera* sp. cf. *Ha. pulchra* (Sharephemeridae), TS-D-1, complete adult mayfly (white arrowhead and red square in A), and detail of its left forewing. **D–E:** *Hammephemera* sp. cf. *Ha. pulchra*, TS-A-1 and TS-F-1 respectively, adult specimens. **F–H:** Detritivore mayfly nymph type, DA21/03-02-87a and DA21/03-02-90a respectively, very abundant form that appears in the same slabs having *Hammephemera* adults, and that commonly show 3D cololites

(arrows in F and G, and H detail of cololite in G). **I–J:** *Triassoephemera punctata* (Triassoephemeridae), MBCN23697a, nymph specimen (insets in J are details of its cuticle punctuations). **K–M:** *Triassonurus doliiformis* (Siphlonuridae), TS-C-1, nymph specimen (details of chaetotaxy in cerci and paracercus; L base of the cerci and paracercus). **N:** *Hammephemera* sp. cf. *Ha. pulchra*, DA21/03-02-88, adult specimen (photograph on the right with forewing showing venation). **O:** Blattodea indet., DA21/03-02-85, forewing of an indeterminate cockroach, possibly of the species *Voltziablatta intercalata* (note the intercalary veins marked by the arrows in the inset). Photographs J and L–M taken with the specimens wet with alcohol.

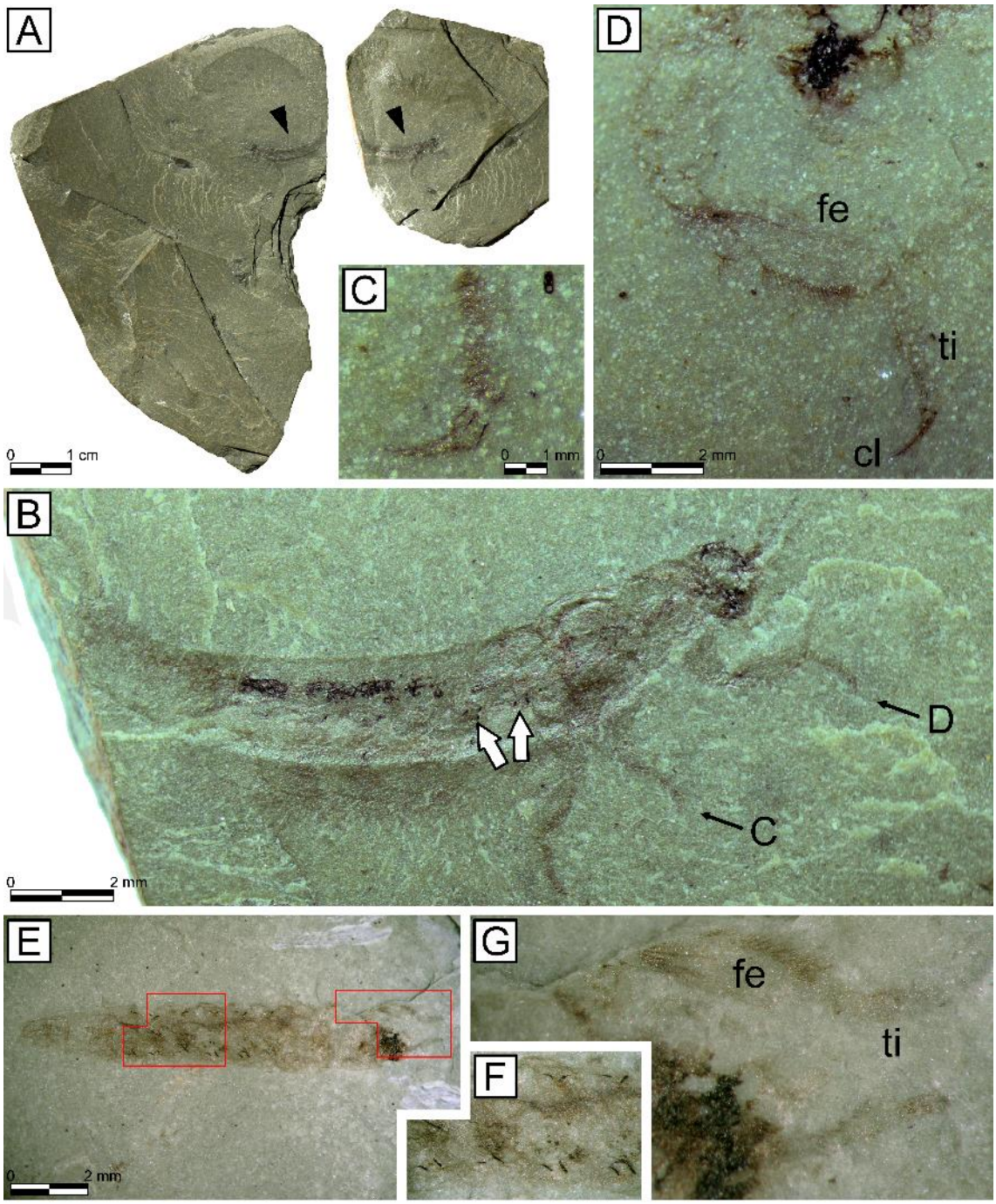

Figure 8. cf. *Voltziaephemera fossoria* (Voltziaephemeridae) from Pedra Alta section, upper part of the Estellencs Formation, Aegean. **A:** Counterpart (left) and part of the slab TS-J having the virtually complete nymph figured by Calafat (1988) (black arrowheads indicate the nymph). **B:** TS-J-1a, habitus of specimen (white arrows indicate some of the abdominal "black-coloured comma-shaped sclerified structures" sensu Sinitshenkova *et al.*, 2005). **C–D:** Detail of the distal mid leg showing distal setae in the tibia (C) and detail of the fore leg of burrowing type (D), both showing a simple claw each. **E–G:** DA/21/03/02/38a, exuvium and details of its abdominal "black-coloured comma-shaped sclerified structures" in F, and fore leg of burrowing type and head in G. Photographs C–D and E–G taken with the specimens wet with alcohol. Scale of F and G referred to graphic scale in E. Abbreviations: cl = claw, fe = femur, ti = tibia.

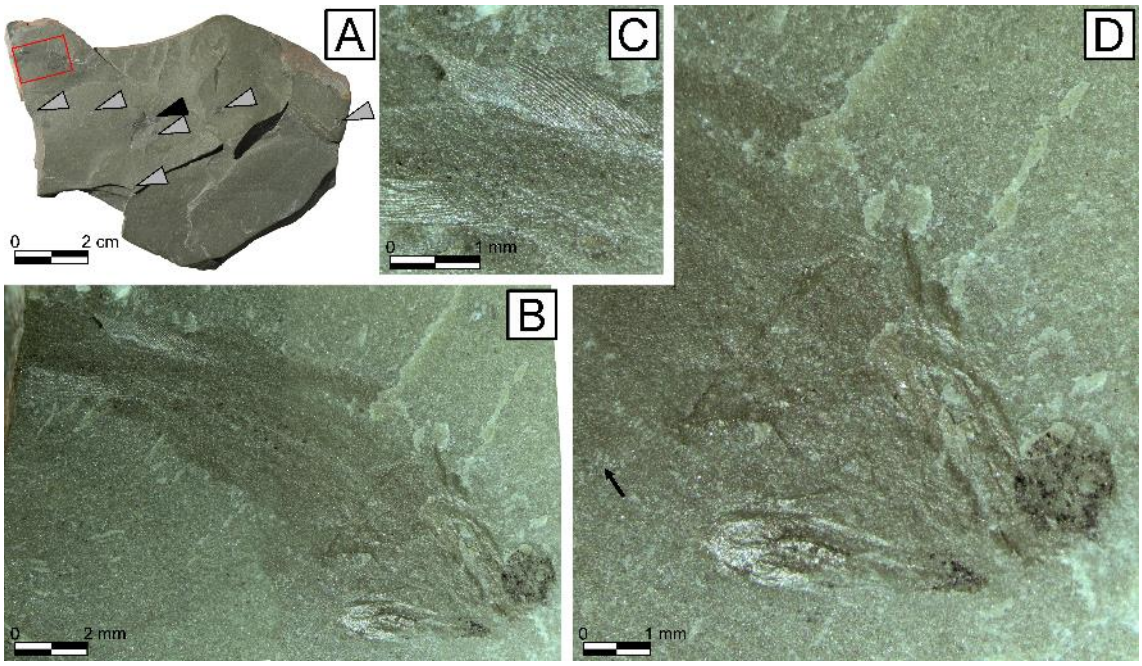

Figure 9. Indeterminate juvenile osteichthyan. From Pedra Alta section, upper part of Estellencs Formation, Aegean. **A:** Complete view of the slab TS-E, black arrowhead indicates the remain of a mayfly adult (TS-E-2), grey arrowheads indicate clam shrimp specimens (TS-E-3 to TS-E-8) and the red rectangle indicates the area corresponding to picture B. **B:** Complete view of the fish (TS-E-1). **C:** Detail of the anal fin (upper in the photograph) and dorsal fin (possible second dorsal fin); note that the fin radii are well marked in this compression fossil. **D:** Detail of the head (arrow indicates the right pectoral fin).

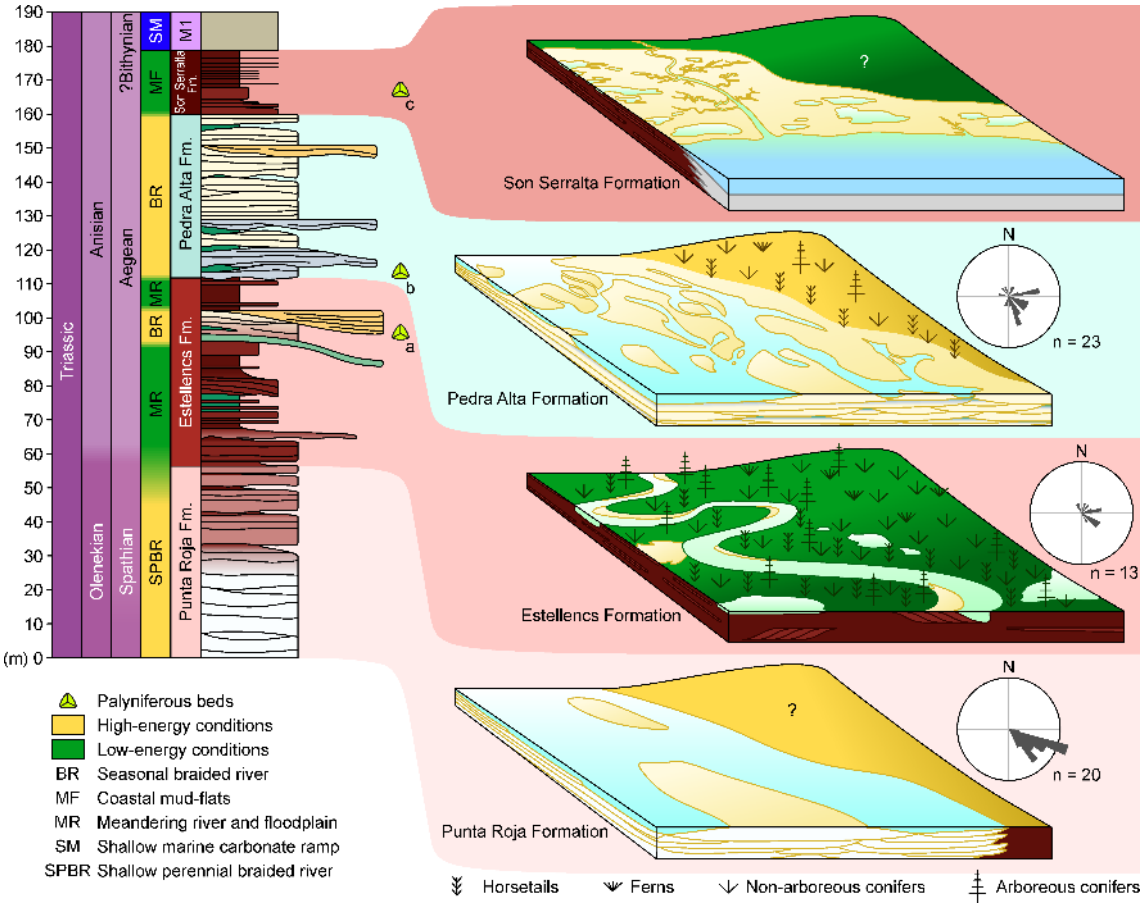

Figure 10. Synthetic stratigraphic log for the four formations of the Triassic *Buntsandstein* facies of Mallorca defined herein and their respective palaeoenvironmental interpretation, with indication of the three beds that have been dated with spores and pollen: [a, sample 4481 of Calafat (1988) and conifer cones of Grauvogel-Stamm & Álvarez-Ramis (1996)], dated as indeterminate lower Anisian (Grauvogel-Stamm & Álvarez-Ramis, 1996; Diez *et al.*, 2010), here inferred as lower? Aegean (Supplementary Table 3); [b, samples ME0 to ME7 of Diez (2000)], dated as upper? Aegean (Diez, 2000; Diez *et al.*, 2010; Supplementary Table 3); [c, sample 4389 of Calafat (1988)], dated as indeterminate lower Anisian (Diez *et al.*, 2010), here inferred as uppermost Aegean, perhaps even stretching into the Bithynian (Supplementary Table 3).

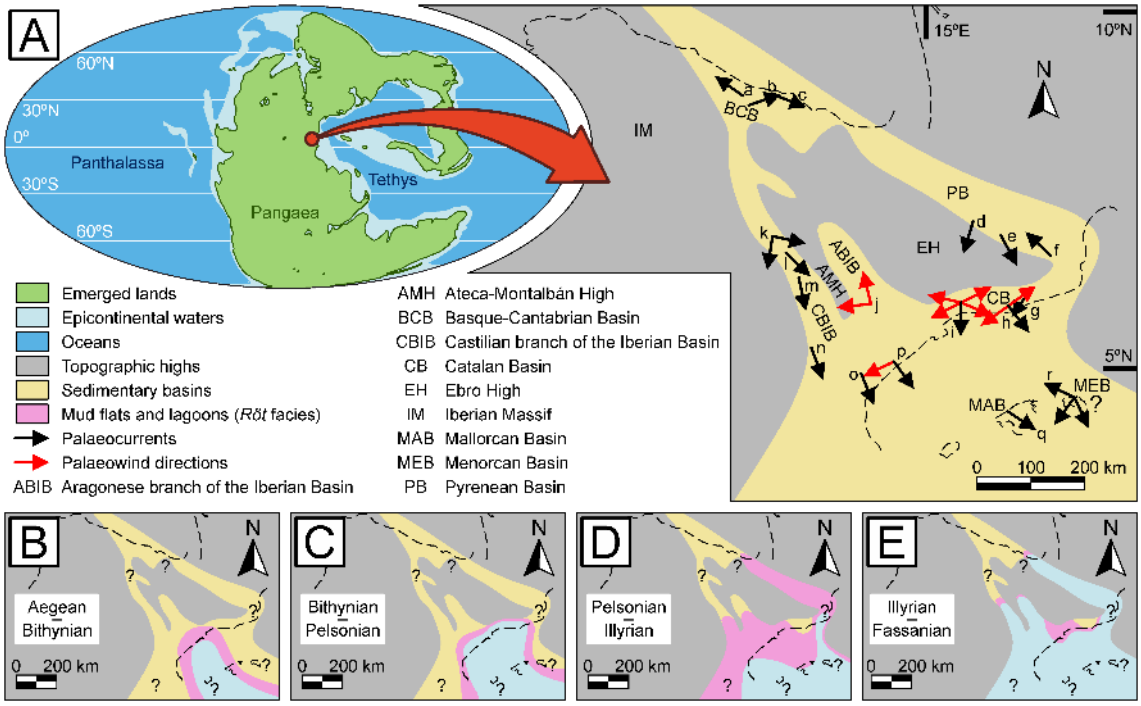

Figure 11. Palaeogeographic evolution of the western peri-Tethys during the Anisian. Dashed lines correspond to present-day coastline. **A:** Map of the Iberian area during the Anisian, with indication of the main basins and palaeocurrent directions. Base map modified from Edel *et al.* (2018), basin margins modified from Lago *et al.* (2012) and palaeocurrent/palaeowind direction data from the following works: [a, Cicera] [b, Peña Sagra–Cohilla] [c, Riocorvo] from López-Gómez *et al.* (2019b); [d, Peranera] from Nagtegaal (1969); [e, Segre] from Robles & Llompart (1987); [f, Castellar de n'Hug] from Borruel-Abadía *et al.* (2015); [g, carretera Figueró–Montmany] from Marzo (1980); [h, Eramprunyà] from Marzo (1986); [i, Sant Gregori–l'Albiol] from Galán-Abellán *et al.* (2013a); [j, Peñarroyas–Torre de las Arcas] from Soria *et al.* (2011); [k, Ayllón–Castro] from Matesanz-Yagüe (1987); [l, Riba de Santiuste] from Franzel *et al.* (2021); [m, Rillo de Gallo] from Ramos (1979); [n, Landete] from López-Gómez (1985); [o, Gàtova] from Borruel-Abadía *et al.* (2015); [p, Benicàssim] from López-Gómez *et al.* (2012); [q, Mallorca] from the present work; [r, Menorca] from Linol *et al.* (2009). Palaeocurrents and palaeowind directions have been corrected for both the counterclockwise rotation of Iberia in the Alpine orogeny and for the clockwise rotation of the Balearic Islands due to the opening of the València trough during the Miocene (Parés *et al.*, 1992; Roca, 1992). **B:** Extension of the carbonate ramps in the upper Aegean–lower Bithynian (mostly based on biostratigraphic data of Diez *et al.*, 2010). **C:** Extension of the carbonate ramps in the Bithynian–Pelsonian (mostly based on biostratigraphic data of Diez *et al.*, 2010 and Ortí *et al.*, 2020). **D:** Extension of the carbonate ramps in the Pelsonian–Illyrian (mostly based on biostratigraphic data of Diez *et al.*, 2010 and Ortí *et al.*, 2018, 2020). **E:** Extension of the carbonate ramps in the Illyrian–Fassanian (mostly based on biostratigraphic data of Diez *et al.*, 2010 and Ortí *et al.*, 2018, 2020). Note that

Mallorca, together with the southwestern Catalan Basin and the southeastern Iberian Basin, were the first areas to be reached by the sea.

Figure 12. Reconstruction of the palaeoecosystem of the Aegean (Anisian, Middle Triassic) Estellencs Formation of Mallorca. In the foreground, bottom left-hand corner, a specimen of the mayfly nymph *Triassoephemera punctata* emerging from the water on a stem of the horsetail plant *Equisetites mougeotii*. In the water, several specimens of the clam shrimp *Hornestheria* sp. aff. *Ho. sollingensis*. Behind, three "detritivore type" mayfly nymphs resting on the base of a stem of *Equisetites mougeotii*. Outside the water, several *Hammephemera* sp. cf. *Ha. pulchra* adult mayflies fluttering around. In the background, there are some more stems of *Equisetites mougeotii* and different species of conifers: on the left, specimens of the conifer *Aethophyllum stipulare*; in the centre, arboreal conifers of the genus *Voltzia*; and on the right, the conifer *Pelourdea vogesiaca*. Among the vegetation, there is a diapsid reptile (*Macrocnemus*-like, one of the possible producers of tracks here identified as *Rhynchosauroides* isp.) that has catched a small fish, and several more *Hammephemera* sp. cf. *Ha. pulchra* specimens. Created by Henry Sutherland Sharpe. © 2021 Henry Sutherland Sharpe. Used under license.

Table 1. Sedimentary lithofacies recognised in the outcrops of the Triassic red-beds of Mallorca.

Code	Lithofacies	Sedimentary structures, processes and fossil content	Geometry and structures
Gt	Stratified, matrix to clast-supported, gravel to pebble-sized breccia of reworked lutite, sandstone or calcrete (intraformational) clasts.	Crude trough stratification. Positive granoselection has been observed in some beds. It corresponds to 3D megaripples that rework the floodplains, or scour fills of major channels (Miall, 1977; Gómez-Gras & Alonso-Zarza, 2003). Tree logs are common.	
St	Stratified, very fine to very coarse-grained sandstone.	Trough cross stratification. It corresponds to sinuous or linguoid 3D megaripples of lower flow regime (Miall, 1985, 2006). No fossils have been found.	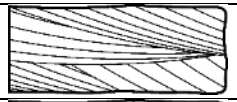
Sp	Stratified, very fine to fine-grained sandstone.	Planar cross stratification. It corresponds to transverse or linguoid 2D bars of lower flow regime (Miall, 1977, 1985, 2006). No fossils have been found.	
Sr	Stratified, very fine to medium-grained sandstone.	Ripple-marks, mostly climbing and wave ripples. Sometimes convolute lamination. It corresponds to ripples formed during low regime and waning flows, at the top of channel sequences or at crevasse splays (Miall, 1985). Rarely with rhizocretions, burrows, invertebrate traces and/or tetrapod ichnites.	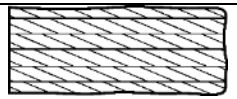
Sh	Stratified, very fine to fine-grained sandstone.	Horizontal stratification and lamination. It corresponds to deposition under planar bed flow of lower flow regime or traction carpets in upper flow regime (Miall, 1977, 1985, Postma, 1990). Plant remains appear frequently.	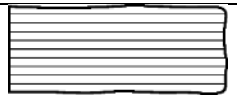
Sl	Stratified, very fine to medium-grained sandstone.	Low-angle cross stratification. Sometimes convolute lamination. It corresponds to deposition during low regime and waning flows, at the top of channel sequences or at crevasse splays (Miall, 2006). Rarely with rhizocretions, burrows, invertebrate traces and/or tetrapod ichnites.	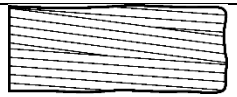
Ss	Stratified to massive, fine- to coarse-grained sandstone.	Clear to crude trough cross stratification. Usually with soft pebbles. It corresponds to scour fills (Miall, 2006). No fossils have been found.	
Sm	Massive, very fine to medium-grained sandstone.	Massive (in macroscopic view). It corresponds to sediment gravity flows (Miall, 2006) or to beds with lamination obliterated by bioturbation.	
Sb	Massive, fine-grained sandstone.	Abundant invertebrate burrows and/or root traces. It corresponds to the biotic reworking of overbank deposits (Miall, 1985).	
Si	Very fine to fine-grained sandstones interbedded with lutites.	Alternation of thin layers of sand and lutite, usually irregular or deformed, sometimes even brechified. Often with retraction cracks. It corresponds to sands deposited under upper flow regime and lutites deposited under low flow regime because of tidal influence (Shanley *et al*., 1992; Shiers *et al*., 2018). No fossils have been found.	
Fl	Laminated lutites.	Fine lamination, mostly horizontal, but can also be low angle cross lamination or ripple lamination. It corresponds to abandoned channel or pool, overbank or waning flood deposits (Miall, 1977, 2006). Plant remains and arthropods are very abundant in some horizons.	
Fm	Massive lutites.	Massive, sometimes bioturbated with root traces and burrows. It corresponds to overbank, abandoned channel or drape deposits (Postma, 1990; Miall, 2006).	
P	Lutites or sandstones without clear lamination.	Massive to crudely laminated. Very abundant carbonate nodules; root traces and gleyed patches are common. It represents palaeosols, corresponding to either vertic Calcisols or to Calcisols (Mack *et al*., 1993).	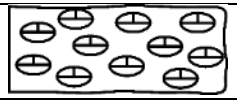

Table 2. Architectural elements recognised in the outcrops of the Triassic red-beds of Mallorca. Arrows (→) indicate the usual succession. Lithofacies in brackets are often missing in the "ideal" succession. Formations in brackets only present that architectural element rarely. Diagrams not to the same scale.

Code	Element	Principal lithofacies assemblages	Features and interpretation	Diagrams	Formation
SB	Sandy bedforms	(*Gt*)→*Sp*→(*Sr*) (*Gt*)→(*Sm*)→*St*→*Sl*→*Sr* *Sr*→*Fl*→(*Fm*)	Shallow channel-fill assemblages, channel-floor dune fields, and bar-top assemblages, respectively (all in the sense of Miall, 2006). Metric thickness.	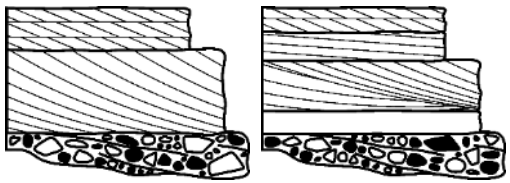	Pedra Alta Formation Punta Roja Formation
LA	Lateral accretion deposits	*St*→(*Sm*)→*Sr*→*Fm* *Sm*	Point bars of meandering rivers (Miall, 2006) or tidally influenced point bars (*e.g.*, Ghinassi, 2021). Metric and metric–centimetric thickness.	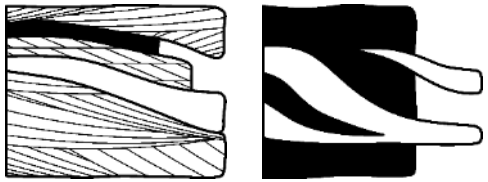	Son Serralta Formation Estellencs Formation
LS	Laminated sand sheets	*Sh* *Sl*	Upper flow-regime plane bed conditions (Miall, 2006). Metric–centimetric thickness.	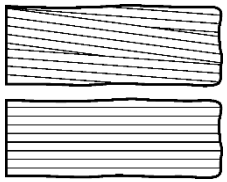	Pedra Alta Formation (upper Punta Roja Formation)
LV + *CS*	Levees and Crevasse splays	(*Gt*)→(*St*)→(*Sl*)→*Sr* *Ss* *Sb* *P*	Overbank flooding (Miall, 2006). May be affected by pedogenesis. Given the limited lateral extension of the studied deposits, it cannot be established whether the observed deposits belong to one architectural element or to the other. Centimetric thickness.	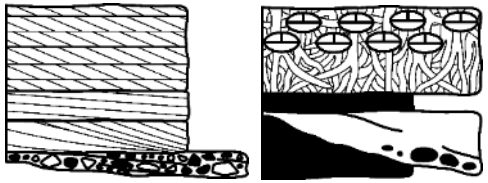	Son Serralta Formation Estellencs Formation
FF	Floodplain fines	(*Fl*)→*Fm*→(*P*) *Si*	Deposits of overbank low-energy flows or sedimentation in pools and playa-lakes (Miall, 2006). May be affected by pedogenesis. The lithofacies *Si* indicates deposits under tidal influence. Metric–centimetric thickness.	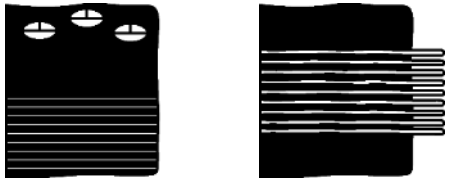	Son Serralta Formation Estellencs Formation (upper Punta Roja Formation)